Book of abstracts

Rivers in an uncertain future

NCR days 2021| Enschede, February 11-12

Jord J. Warmink, Anouk Bomers, Vasileios Kitsikoudis, R. Pepijn van Denderen & Fredrik Huthoff (eds.)

NCR publication: 46-2021

Netherlands Centre for River studies NCR

NCR Days 2021

Rivers in an uncertain future

Jord J. Warmink, Anouk Bomers, Vasileios Kitsikoudis, R. Pepijn van Denderen & Fredrik Huthoff (eds.)

Organising partner:

UNIVERSITY OF TWENTE.

Co-sponsored by:

NWO
Nederlandse Organisatie voor Wetenschappelijk Onderzoek

J.M. Burgerscentrum

Organising partner

University of Twente
P.O. 217
7500 AE Enschede
The Netherlands

telephone: +31 53 489 35 46
e-mail: secretariat-mfs-et@utwente.nl
www: https://www.utwente.nl

Contact NCR

dr. ir. K.D. Berends (programme Secretary)
Netherlands Centre for River Studies
c/o Deltares
P.O. 177
2600 MH Delft
The Netherlands

telephone: +31 6 21 28 74 61
e-mail: secretary@ncr-web.org
www: https://www.ncr-web.org

Cite as: Warmink, J.J., Bomers, A., Kitsikoudis, V., van Denderen, R.P., Huthoff, F. (2021), *Rivers in an uncertain future: NCR Days proceedings*. Netherlands Centre for River Studies, publication 46-2021

Photo credits cover: IJssel river from Bureau Beeldtaal Filmmakers (2018)

Contents

Introduction

Welcome to the 23rd edition of the NCR Days, the annual meeting of the Netherlands Centre for River studies (NCR), this year organized by the University of Twente on 11 and 12 February 2021. For the first time in its history the NCR Days are held online.

Currently, we live in uncertain times. The global Covid-19 pandemic puts stress on society and our personal lives and forces the NCR Days to be held online. At the same time, the effects of climate change are increasingly felt by society and pose serious concerns for the future. Not only may we face increasingly high discharges, but also more intense periods of droughts, which can create stress on various river functions. This puts scientists and river managers in front of the challenge to deal with both the inherent complex behaviour of rivers and the climate change uncertainty, now and even more so in the future. Therefore, the theme of the NCR Days is this year: Rivers in an uncertain future.

We present to you an exciting program with three excellent keynote speakers. Koen Blanckaert (Vienna University of Technology) will speak about riverine inflows in lakes, which are sources of nutrients, organic matter, oxygen, contaminants and sediment. Tatiana Filatova (University of Twente) will talk about the role of individual decisions in shaping patterns of risk and in adapting to climate change. Finally, Matthijs Kok (Delft University of Technology) will focus on flood risk along rivers and measures to reduce flood risk in an effective way.

In the program, we have 20 oral presentations organized around the 6 themes of the NCR Days 2021: Advances in river modelling, Ecological sustainability in rivers and estuaries, Threats for river functions, Sediment management and measures, Small-scale river dynamics, and Long-term river behaviour and morphology. Additionally, we have 14 poster presentations with a variety of topics organized randomly in 2 poster sessions. All keynote lectures, oral presentations (prerecorded and live) and 1-minute poster pitches will be available on the NCR-Vimeo channel after the conference. In between the oral and poster sessions, we have two social sessions where you can meet colleagues in an informal way and maybe even discover some hidden talents of yourself, or of others.

The organisation of the NCR Days is grateful for the financial support of the Dutch Research Council (NWO) and the J.M. Burgerscentrum – Research School for Fluid Mechanics. Additionally, we thank Koen Berends and Anna Kosters, secretary and interim secretary of the NCR programme committee, and Anke Wigger, Dorette Olthof, Lieke Lokin, Matthijs Gensen and Luuk van Laar for their great help and support in setting up and running a smooth online conference.

We hope you will enjoy the presentations, discussions and interaction during the NCR Days 2021. All the best and stay safe and healthy.

Jord Warmink
Anouk Bomers
Vasileios Kitsikoudis
Pepijn van Denderen
Fredrik Huthoff

Conference organisation

Organising partner

The NCR Days 2021 is organised by the Marine and Fluvial Systems (MFS) group of the University of Twente. The aim of the MFS group is to increase our understanding of the natural and socio-economic processes affecting water systems. Furthermore, we focus on developing tools that can effectively be used to support the management of rivers, river basins, seas and coastal zones.

Venue

This edition of the NCR Days will be held online. ZOOM is used as communication platform. Below you find a description of the various sessions during these NCR Days and how they are organised.

Plenary keynote sessions: these sessions are typical Zoom meetings with live presentations by the keynote speakers and a short Q&A afterwards.

Poster sessions: following the keynotes, 1-minute prerecorded poster pitch movies are played to enable the audience to choose which posters to visit in the following poster session. In the very special poster sessions every poster presenter is assigned her/his own Zoom breakout room. The audience can move from poster to poster by selecting the appropriate breakout room. The program is displayed on a slide on the plenary room. In every breakout room, the presenter displays one Powerpoint slide showing an outline of his or her work. The audience can ask questions to the poster presenter by un-muting or via the chat. The poster pitch movies shown after the keynote lecture will be posted on the NCR-Vimeo channel after consent of the authors. The poster sessions themselves are not recorded.

Social sessions: the two social sessions are dedicated to meet new people and stimulate interaction. Each session has a slightly different outline. The session on Thursday will resemble a blind-speed-date session where you can meet colleagues in an informal way. The session on Friday will have a more game-like set-up, but the rest it is still a surprise. The social session starts in the plenary room at the indicated time. Key to success is a high attendance of all conference participants.

Parallel sessions: these sessions resemble typical oral presentations. Earlier experiences have shown that giving a live presentation helps a lot in conveying your message. Therefore, we prefer live presentations (using screen sharing), but if you are more comfortable with presenting a prerecorded movie that is also possible. Presentations are 12 minutes, with 3 minutes for questions afterwards. All presentations (prerecorded and live) will be posted on the NCR-Vimeo channel after consent of the authors.

Zoom instructions for participants

NB: We highly recommend you to use the Zoom Desktop Client to join the conference. This will enable you to smoothly switch rooms and raise your hand button to ask a question. It is also possible to join using the web browser, but Zoom is only supported by the Chrome and Firefox browsers.

Preparation. Before you join the Zoom meeting it is convenient to be well prepared. This only takes a few minutes.

What do you need? For the Zoom meeting you only need a laptop, desktop, tablet or phone with a good internet connection, camera and microphone. A headphone is recommended to avoid ambient sound.

What to do before the NCR Days start? Download and install *the latest version* of the ZOOM Desktop Client here: https://zoom.us/support/download
Test your computer by joining a test meeting at any time here: https://zoom.us/test

Register for the conference. Registration for the conference is still possible:
https://www.aanmelder.nl/121344/subscribe.

Joining the conference. Click on the link that will be send to all registered participants. In case you did not receive the link on February 10, please contact us at ncrdays2021@utwente.nl. Type in your name and organisation. In this way all participants know who you are when speaking or using the chat function.

Important! During the conference, all participants are muted and are not allowed to unmute themselves. When needed (for example during the Q&A), the hosts of the conference will enable you to unmute.
Please keep your camera off during the presentations. All presentations are recorded and published afterwards. The recordings look nicer with only the presenter in view.
Please turn on your camera when asking a question, or during the poster and social sessions.
During the conference the chief technical host (Luuk van Laar) is present in the plenary room (the main room when you enter the ZOOM meeting). You can contact (private chat) him in case of questions.

Need more information? An extensive manual on using Zoom is available here:
https://support.zoom.us/hc/en-us/articles/201362193-Joining-a-Meeting
In case of questions, please contact ncrdays2021@utwente.nl or call 053-4893546.

Program

Online Icebreaker Party. Wednesday February 10, 2021

15.45-16.00	Digital walk-in
16.00-18.00	Icebreaker party featuring: **The famous NCR-days pub quiz**

Block 1. Thursday morning February 11, 2021

9.15-9.30	Digital walk-in	
9.30-9.40	Opening and announcements	
9.40-9.50	Welcome by Suzanne Hulscher (Chair MFS department, University of Twente)	
9.50-10.35	**Keynote** Koen Blanckaert (Vienna University of Technology) Title: Hydro- and morphodynamics of dense river inflows into lakes	
10.35-10.45	Introduction Young-NCR	
10.45-11.00	Break	
11:00-11:30	Social session 1 Speed dates	
11.30-11.45	Break	
	Parallel sessions (11:45-12:40)	
	1A: **Advances in river modelling** Session leader:Gertjan Geerling (Deltares)	1B: **Ecological sustainability in rivers and estuaries** Session leader: Rob Lenders (RU)
11:50-12:05	Burhan Yildiz (Deltares) A satellite-image-based method to overcome data scarcity for river morphodynamic modelling	Natasha Flores (RU) Upstream passability assessment of the LTD shore channel inflows by migratory fish species
12:05-12:20	Rutger Pasman, (TUD) Damping of ship-induced primary waves in groyne fields	Kshitiz Gautam (IHE, Deltares) Assessing morphological changes and impact on ecology in Koshi River using remote sensing and cloud computing
12:20-12:35	Daan Kampherbeek (UT) Modelling ship waves for the purpose of overtopping	Frank Collas (RU) Macro- and mesoplastic abundance and composition in the water column of the river Waal

Block 2. Thursday afternoon February 11, 2021

<table>
<tr><td>14.00-14.10</td><td colspan="2">Opening and announcements</td></tr>
<tr><td>14.10-14.55</td><td colspan="2">Keynote
Matthijs Kok (Delft University of Technology)
Title: Probabilistic flood risk approaches along rivers</td></tr>
<tr><td>14.55-15.05</td><td colspan="2">Pitches for poster session 1</td></tr>
<tr><td>15.05-15.20</td><td colspan="2">Break</td></tr>
<tr><td>15.20-15.50</td><td colspan="2">Poster session 1
7 parallel poster presentations
1. Eline Sieben (UU) A multi-criteria analysis for sediment management strategies
2. Roline Montijn (Deltares) Numerical study on the transition between river bar regimes due to varying discharge
3. Johan Harms (TUD) Numerical and physical modelling of the effect of groynes lowering
4. Stijn Overmeen (UT) Determining the wind drag coefficient for shallow, fetch-limited water systems: A case study in Fryslân, The Netherlands
5. Anna Kosters (Deltares) Short-term morphological effects of the pilot ‘Xstream-bloc groynes’ in the Ijssel
6. Fateme Ebrahimierami (UT) Salt accumulation at floodgates and salt-water intrusion in rivers
7. Amin Shakya (IHE) Approaches to predict bedform states, associated flow resistance and depth: physics-based to machine learning</td></tr>
<tr><td>15:50-16:00</td><td colspan="2">Break</td></tr>
<tr><td></td><td colspan="2">Parallel sessions (16:00-17:10)</td></tr>
<tr><td></td><td>2A: Threats for river functions

Session leader: Francesco Bregoli (RU)</td><td>2B: Sediment management and measures
Session leader: Marcel van der Perk (UU)</td></tr>
<tr><td>16:05-16:20</td><td>Vera van Bergeijk, (UT)
What is the effect of dike cover damages on the failure probability of wave overtopping?</td><td>Meghan Irving (TUD)
Morphological Impacts of Porcupine River Training Structures</td></tr>
<tr><td>16:20-16:35</td><td>Kees Sloff (TUD)
Long-term bed level change in the Dutch Rhine branches and its impacts to water availability</td><td>Jana Cox (UU)
Future sediment budget and distribution for the Rhine-Meuse delta</td></tr>
<tr><td>16:35-16:50</td><td>Matthijs Gensen (UT)
Compensating human interventions at a river bifurcation</td><td>Patricia Buffon (IHE, TUD)
Water injection for dredging sediment in reservoirs – insights from preliminary experiments</td></tr>
<tr><td>16:50-17:05</td><td>Matthew Czapiga (TUD)
Impact of Weir Location on Discharge Partitioning in Longitudinal Training Walls</td><td>Pepijn van Denderen (UT, HKV)
Insight into the local bed-level dynamics to assist management of multi-functional rivers</td></tr>
</table>

Block 3. Friday afternoon February 12, 2021

<table>
<tr><td>12.45-13.00</td><td colspan="2">Digital walk-in</td></tr>
<tr><td>13.00-13.10</td><td colspan="2">Opening and announcements</td></tr>
<tr><td>13.10-13.55</td><td colspan="2">Keynote
Tatiana Filatova (University of Twente)
Title: Computational models of adaptive human behaviour in face of environmental hazards</td></tr>
<tr><td>13.55-14.05</td><td colspan="2">Pitches for poster session 2</td></tr>
<tr><td>14.05-14.20</td><td colspan="2">Break</td></tr>
<tr><td>14.20-14.50</td><td colspan="2">Poster session 2
7 parallel poster presentations
1. Eray Bilgili (UT) The influence of mesh structure on simulated water levels and flow velocities in meander rivers
2. Victor Chavarrias (Deltares) Modelling morphodynamic changes over fixed layers
3. Marcel van der Perk (UU) Impact of Chelicorophium curvispinum on the concentration-discharge response of suspended sediment in the Rhine River
4. Judith Zomer (WUR) Multiscale bedform migration and interaction in the Waal river, the Netherlands
5. Huck de Haas (TUD) Dynamic morphology of the Sittaung estuary, Myanmar: A detailed investigation and modeling of rapid bank erosion
6. Kifayath Chowdhury (TUD) Flow Structure at the Pannerdense Kop Bifurcation
7. Iris Niesten (WUR) Flow and sediment transport in a stratified estuary: first insights from field data</td></tr>
<tr><td>14:50-15:20</td><td colspan="2">Social session 2
Interactive game</td></tr>
<tr><td>15.20-15.35</td><td colspan="2">Break</td></tr>
<tr><td rowspan="4"></td><td colspan="2">Parallel sessions (15:35-16:20)</td></tr>
<tr><td>3A: Small-scale river dynamics

Session leader: Suleyman Naqshband (WUR)</td><td>3B: Long-term river behaviour and morphology
Session leader: Astrid Blom (TUD)</td></tr>
<tr><td>15:35-15:50</td><td>Lieke Lokin (UT)
The evolution of primary dunes during low flows on the Waal river</td><td>Claudia Ylla Arbós (TUD)
Scenarios for Controls of River Response to Climate Change in the Lower Rhine River</td></tr>
<tr><td>15:50-16:05</td><td>Sjoukje de Lange (WUR)
Quantifying hydraulic roughness from field data: can bed morphology tell the whole story?</td><td>Hermjan Barneveld (WUR, HKV)
Efficient long-term one-dimensional morphodynamic modelling in alluvial rivers using simplified models – theory and validation</td></tr>
<tr><td>16:05-16:20</td><td>Francesco Bregoli (IHE/RU)
Sand-bed river response to drier and wetter climate: the case of Pilcomayo</td><td>Freek Huthoff (UT, HKV)
Laying bare systemic river bed changes in the river Rhine</td></tr>
<tr><td>16.20-16.35</td><td colspan="2">Break</td></tr>
<tr><td>16.35-16.55</td><td colspan="2">Plenary wrap-up (Suzanne Hulscher)</td></tr>
<tr><td>16.55-17.15</td><td colspan="2">Poster and Presentation award ceremony/Closing</td></tr>
</table>

Keynote speakers

Koen Blanckaert (Professor of Hydraulic Engineering, TU Wien)
Hydro- and morphodynamics of dense river inflows in lakes

Koen has a degree in Civil Engineering from Ghent University and a PhD from EPFL. Before his appointment at TU Wien in 2017, he was a senior scientist at EPFL, Visiting Professor at the Research Center for Eco-Environmental Sciences of the Chinese Academy of Sciences and Associate Professor at the Hong Kong University of Science and Technology. In parallel, he has worked as consultant in Switzerland. His research has focussed on flow processes and their interactions with sediment transport and biota.

Koen will speak about dense (negatively buoyant) rivers flowing into lakes. These riverine inflows are sources of nutrients, organic matter, oxygen, contaminants (e.g., mercury, microplastics), heat and sediment particles. Koen will illustrate some hydro- and morphodynamic processes with field measurements from the inflow of the Rhône River into Lake Geneva (France/Switzerland), and discuss the broader relevance of these observations.

Matthijs Kok (Professor of Flood Risk, Delft University of Technology & HKV)
Probabilistic flood risk approaches along rivers

Matthijs Kok (1956) is professor of Flood Risk at the faculty of Civil Engineering at the Delft University of Technology and expert in Risk Management (flood protection and fresh water supply). He covers almost all areas in Uncertainty, Decision, Risk Analysis and Flood Risk assessment. In his approach, supporting decisions is the ultimate aim of his analytical research. He is one of the founders of HKV, and since 1995 this company has grown to an organisation with 70 employees which combines consultancy with scientific research on water and risk related issues. He is chairman of the Expertise Network for Flood Protection (ENW) working group on Flood Risk, which is the leading authority on the development of technical design and maintenance guidelines in the Netherlands, based on the risk approach.

His presentation focuses on flood risk issues along rivers. In the presentation, attention will be given to flooding probabilities and consequences of flooding. Much attention will be given to measures which will reduce flood risk in an efficient way, using a river system perspective.

Tatiana Filatova (Professor of Computational Economics, University of Twente)
Computational models of adaptive human behaviour in face of environmental hazards

As a computational social scientist, Tatiana has been working on water-related challenges and climate change adaptation for the past 15 years. Between 2009-2015 she joined Deltares as a water economist. Her research focuses on agent-based modeling to study individual choices, behavioral change and evolution of social institutions in relation to water and climate risk assessments (e.g. NWO VENI & VIDI projects). Most of Tatiana's current work centers around her ERC project that links individual adaptation to climate-driven flood risks in cities with macro damage assessments in climate-economy models. Prof. Filatova leads the Dutch 4TU.Federation Strategic Research Program on Resilience of social-technical-environmental systems 'DeSIRE'.

Tatiana will talk about the role of individual decisions (of households, farmers, firms) in shaping patterns of risks and in adapting to changing climate. She will discuss the essence and added value of computational agent-based modeling (ABM) in assessing risks and resilience, and will present examples of such complex adaptive systems models in applications to floods and droughts. ABM enables behaviorally-rich representation of human agency, learning, social interactions and institutions (like markets or social norms) in formal models. It is the primary method to integrate environmental & natural systems models with social and behavioral factors that shape environmental risks.

Keynote papers

Hydro- and morphodynamics of dense river inflows into lakes

Koen Blanckaert[a*], David Andrew Barry[b]
[a]*Technische Universität Wien, Institute of Hydraulic Engineering and Water Resources Management, Vienna, Austria.*
[b]*Ecole Polytechnique Fédérale de Lausanne (EPFL), Faculty of Architecture, Civil and Environmental Engineering (ENAC), Environmental Engineering Institute (IIE), Ecological Engineering Laboratory (ECOL), Lausanne, Switzerland*

Keywords — Turbidity current, density current, field measurements

Introduction

Dense inflows plunge under the lighter surface waters of the receiving water body (Fig. 1) (Fisher et al., 1979). This plunging process is accompanied by intense mixing, and conditions the pathway of the subsequent underflow along the bottom of the receiving water body. The density of the underflow changes during its propagation due to mixing with the ambient water and exchanges of sediment with the bottom.

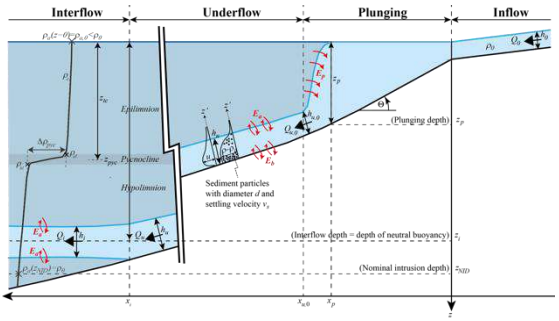

Figure 1. Conceptual representation of the flow processes of dense river inflow into a lake.

Open-channel inflows into lakes are vectors of momentum, sediments and contaminants. The inflow of sediments leads to reservoir sedimentation and can generate turbidity currents (underwater avalanches) that threaten infrastructure. The spreading and mixing of the introduced quantities control the water quality.
Knowledge on the relevant hydro-and morphodynamic processes is still largely based on laboratory experiments in simplified configurations (Alavian et al. 1992). The main simplifications are typically a constrained narrow-width geometry, a lack of sediment, a lack of stratification, and a smooth bottom.
A field investigation on the geometrically unconstrained inflow of the sediment-laden Rhône River into the stratified Lake Geneva (France/Switzerland) is reported. The principal research questions are: (i) what are the hydro- and morphodynamic processes in the plunging region; (ii) how can the mixing in the plunging region be parameterized; (iii) what are the hydro-and morphodynamic processes related to the turbidity currents; can the observations be explained with commonly used models ?

Methods

A unique feature of the investigated configuration is that the properties of the riverine inflow, the lake stratification and the lake bathymetry are all known from publicly available data (Fig. 2).
An intricate morphological feature is the delta-canyon-fan system that is cut by the inflowing Rhône River into the bottom of Lake Geneva (Fig. 2) (Forel, 1892).

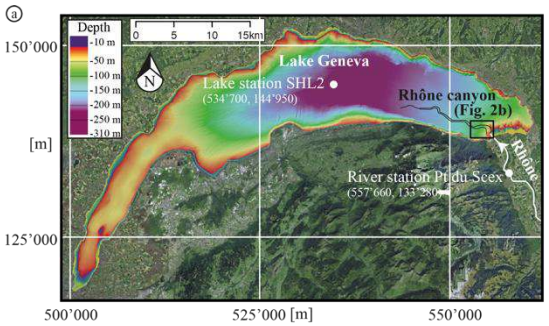

Figure 2. Lake Geneva, the Rhône River inflow, the Rhône River submarine canyon and the measuring stations on the river and in the lake.

Continuous flow measurements were performed with ADCP's moored at three locations in the canyon, where the depths are 130m, 150m and 190 m, resp. The ADCPs provide the vertical profiles of the velocity. Continuous monitoring of the surface patterns in the plunging area was performed with an autonomous remote sensing system, equipped with RGB and IR cameras, installed on a viewpoint overlooking the river mouth.
Additional event-wise measurements were made in the plunging region. A balloon equipped with RGB and IR cameras observed the surface patterns with higher spatial and temporal resolution, and the 3-D velocity pattern were measured with a boat-towed ADCP. This ADCP provided in addition the elevation of the lake bottom.

* Corresponding author
Email address: koen.blanckaert@tuwien.ac.at

Results

Plunging

The images form the remote-sensing cameras revealed beautiful and quite surprising surface patterns in the plunging region (Fig. 3). The riverine inflow converges when entering the lake, and vortical stabilities at multiple spatial scales occur at the interface between the river and lake waters. The triangular plunge line and vortical instabilities do not occur in laterally constrained geometries, such as found in typical laboratory flumes.

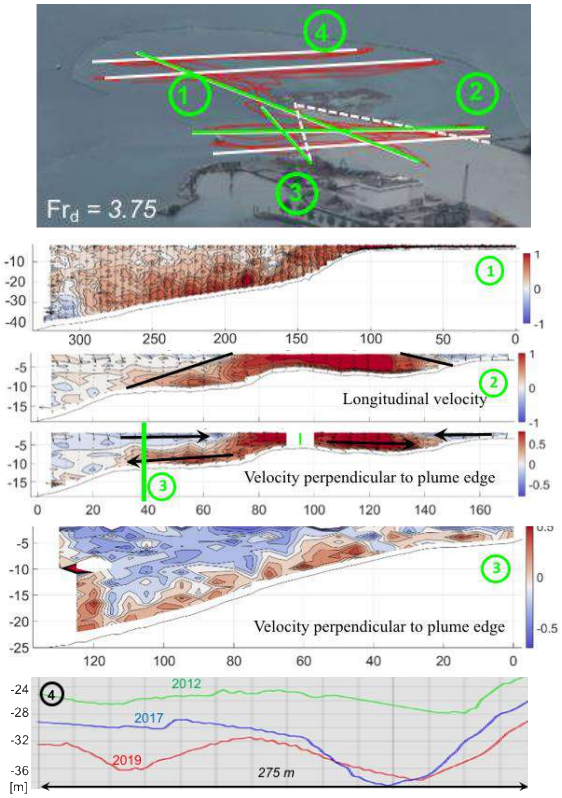

Figure 3. From top to bottom. Surface pattern revealed by remote sensing and boat trajectories; Velocity along longitudinal transect 1; longitudinal velocity across cross-section 2; Velocity perpendicular to the plume edge in cross-section 2; Velocity perpendicular to the plume edge along transect 3.; Bathymetric changes along cross-section 4.

The boat-towed ADCP measurements clearly reveal the corresponding 3-D flow structure (Fig. 3). A “classical” plunging flow structure is visible in the longitudinal-vertical transect no 1 along the axis of the riverine inflow. The measurements in the cross-section no 2 and transect no 3 reveal that the riverine inflow collapses laterally. This is different from the plunging in laterally constrained geometries, where the lateral collapse is suppressed, leading to significant amplification of plunging mixing.

Surprisingly large bathymetric changes of the order of 10 m per year were observed in the plunging area.

Turbidity currents

In general, the Rhône inflow is captured in the thermocline of the lake. Storm-events in the Rhône watershed, however, temporarily lead to high suspended sediment concentrations in the Rhône and an increased density excess that induces turbidity currents in the lake that break through the thermocline and reach the fan of system at a depth of 280 m.

The maximum velocity in these turbidity currents is about 5 m s^{-1}, which is significantly higher than the velocity of the river inflow (Fig. 4).

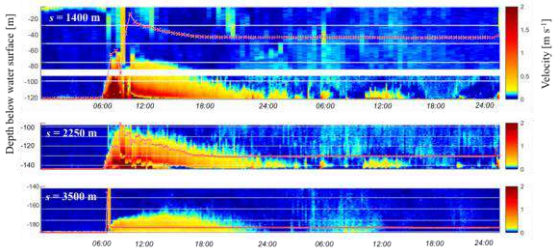

Figure 4. ADCP measurements of a turbidity current on July 3th,2018 at locations in the canyon where the lake depth is 130m, 150m, and 190 m, resp.

The peak discharge in the turbidity current is about 15’000 m^3 s^{-1}, which is about 30 times higher than the peak discharge in the river. A tentative explanation is that the turbidity current is fuelled by massively picking up sediment from the bottom in the plunging area, which increases its excess density. This pronounced interaction with the bottom is confirmed by a 6m thick layer of deposited sediment after the passage of the event.

References

Alavian, V., Jirka, G.H., Denton, R.A., Johnson, M.C., Stefan, H.G. (1992) Density currents entering lakes and reservoirs, Journal of Hydraulic Engineering, 118(11): 1464-1489

Fisher, H.B., List, E.J., Koh, R.C.Y., Imberger, J., Brooks, N.H. (1979) Mixing in inland and coastal waters, Academic Press. Chapter 6: Mixing in reservoirs, 148-228.

Forel, F.A. (1892) Le Léman : Monographie limnologique, Vol. 1, F. Rouge Ed., Lausanne, Switzerland, 543 p.

Probabilistic flood risk approaches along rivers

Matthijs Kok,
Delft University of Technology, Faculty of Civil Engineering and Geosciences
Postal Address: Postbus 5048, 2600 GA Delft
Matthijs.Kok@TUDelft.nl

Keywords — Flood protection, Flood Risk

Introduction

Probabilistic risk analysis is an international well known research area. The standard handbook of this approach is written by (Bedford and Cooke, 2001). In this book it is made clear that "probabilistic risk analysis differs from other areas of applied science because it attempts to model events that (almost) never occur. When such an event does occur then the underlying systems and organizations are often changed so that the event cannot occur in the same way again". The risk methodology are applied to assess risk in many sectors, for example the chemical and nuclear sector. However, the assessment of risk in flood protection systems differ from other technological systems, because these risks are partly driven by extreme natural events, like for example extreme storms, hurricanes or rainfall. Also, infrastructure is made of natural materials like clay and sand (think of levees and dunes), which means often a high variability and therefore larger uncertainties compared with man-made materials like concrete or steel.
In this keynote lecture I will handle the approaches which are followed to deal with these uncertainties.

Uncertainties

There are 2 interpretations of uncertainty: the frequentist and the Bayesian. According to the frequentist interpretation, a probability is the average number of times that a certain result is obtained in a long series of identical independent experiments. In this view, a probability is thus a relative frequency. According to the Bayesian interpretation, the probability of flooding is a measure of the likelihood that a flood will occur, given the knowledge at our disposal. The difference between *inherent* and *knowledge* uncertainty is irrelevant in the Bayesian interpretation, according to which the probability that a flood will occur is not uncertain; the probability is a measure of uncertainty. The probability is no longer, therefore, a physical property (which could be measured) but a subjective 'degree of belief'.

Flood Risk

A risk analysis tries to answer the flowing questions:

a. What can happen?
b. How likely is it to happen?
c. Give that it occurs, what are the consequences?

Often, risk is defined by a set of scenarios s_i, with probability p_i and consequences d_i.
There are, however, many different definitions of risk. In hydraulic engineering, flood risk is a concept that concerns both the possible impact of flooding and the probability that it will occur. It indicates the consequences, and also the probability of these consequences. Risk is often expressed as probability x economic damage. Risk is more than that, however. Flood risk can also be expressed in terms of other risk measures, such as societal risk (the probability that a large group of people will lose their lives) and individual risk (the probability that an individual will die). Which risk measure is preferable depends on the factors that determine how serious an imminent event is perceived to be. The Dutch policy towards flood risk considers three measures of risk: the annual expected damage, the individual risk and the societal risk, see Kok et al (2017).

Flood risk Reduction

A clear idea of flood risks and the extent to which measures can be taken to reduce them can support decision-making on flood risk management. Levee reinforcements, providing extra room for rivers, spatial interventions and crisis management and public readiness measures all impact on flood risk, albeit in different ways. By showing the impact of such diverse measures on the flood risk, it is possible to make consistent and comparable decisions. Which individual measures or combinations of measures are ultimately the most appropriate will not only depend on the effect on the flood risk, but also on the costs, and any benefits apart from flood risk management.
Flood risk can help with decisions as to whether the level of safety provided is adequate: whether it is an *acceptable* risk, in other words. The first Delta Commission assessed the acceptability of flood risks on the basis of cost-benefit analysis (economic risk).

Some decisions may reduce the risk only marginal, but some decisions may reduce the risk a lot. If the (societal) costs of these risk are equal, than it would be rational to implement only measures which reduce risk a lot. This is the challenge of the probabilistic flood risk approach, since measures may not only reduce the probability, but may also reduce the consequences. From a flood risk point a view, both type of measures can be efficient. However, we often seen that it is relatively easy to reduce the probability with a factor 10, but it is often quite difficult to reduce the consequences with 10%. This means that we also have to take into count the economic, ecological and other cost when discussing about decisions. For example, evacuation plans can reduce the risk, and might be very cheap.
In figure 1 the possible measures are shown which can be taken in Room for the River programs.

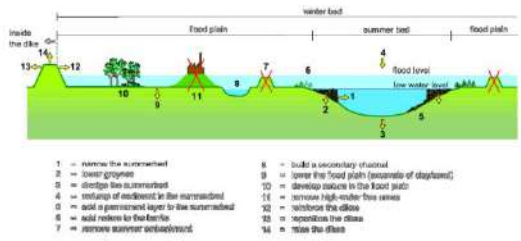

Figure 1 Room for the River measures (Kok et al, 2017)

Also other type of measures can be taken into account, for example strengthening of flood defences. Because flood defences might fail because of multiple failure mechanisms, we all have to take into account. In figure 2, a design to handle three different failure mechanism of river levees are shown.

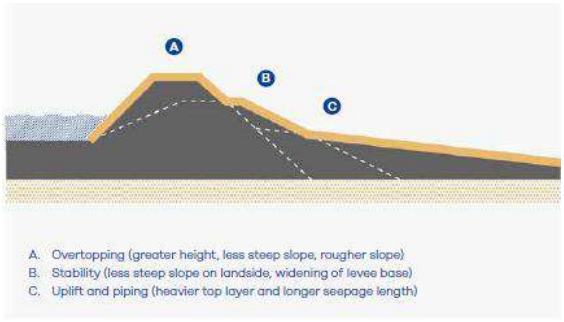

Figure 2. Example of the design of the levee profile based on three failure mechanisms. The thick orange line envelopes the solutions to the three failure mechanisms, and shows the design profile.(Kok et al, 2017)

Systems approach

Often, risk is assessed for only one part of the river system, a 'dijkring' or a dijktraject'. However, risk does not limit itself to these boundaries. In my opinion, we have to look at the interactions within the river system, and the uncertainties associated with it. In a recent thesis (Curran, 2020) the systems approach was followed. It was shown the flood risk of an area can be assessed taking account possible overflow and breaches of flood defences upstream this area. In the thesis, so called fragility curves are used to assess the flooding probability. These curves represent the conditional probability of failure, given the hydraulic load, for example the waterlevel. In figure 3 an example is given.

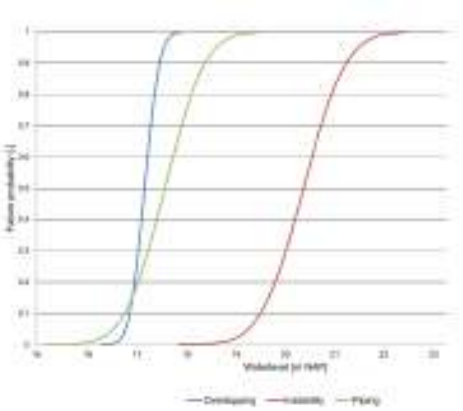

Figure 3 Example of a fragility curve.

Together with the probability density function of water levels, the flood probability can be relatively easy assessed. However, it is still relatively difficult to predict breaches at specific locations, so the systems approach in rivers still needs further development. Predicting overtopping seems more easy, and that is why in the Grade system for the river Rhine upstream Lobith, only possible breaches due to overtopping are included (Hegnauer et al, 2014).

Conclusion

The probabilistic flood risk approach is capable to include uncertainties which can be identified within river systems. However, a full probabilistic systems approach including all failure mechanisms of levees needs data which are not yet available.

References

Bedford, Tim and Roger Cooke (2001) Probabilistic Risk Analysis: Foundations and Methods., Cambridge Press, 414 p

Curran, A. (2020). Flood risk analysis of embanked river systems. Probabilistic systems approaches for the Rhine and Po river. Deft University of Technology.

Hegnauer, M. J.J. Beersma, H.F.P. van den Boogaard, T.A. Buishand, and R.H. Passchier (2014). Generator of Rainfall and Discharge Extremes (GRADE) for the Rhine and Meuse basins - Final report of GRADE 2.0

Kok, M., R. Jongejan, M. Nieuwjaar and I. Tanczos (2017). Fundamentals of Flood Protection, Expertise Network of Flood Protection.

Session 1A
Advances in river modelling

A satellite-image-based method to overcome data scarcity for river morphodynamic modelling

Amgad Omer[a], Mohamed Yossef[a], Erik Mosselman[a,b], Burhan Yildiz[a,b,c*]
[a]*Deltares Boussinesqweg 1, 2629 HZ, Delft, The Netherlands*
[b]*Delft University of Technology, Department of Hydraulic Engineering, Faculty of Civil Engineering and Geosciences, P.O. Box 5048, 2600 GA, Delft, the Netherlands*
[c]*Mugla Sitki Kocman University, Department of Civil Engineering, 48000, Mugla, Turkey*

Keywords — Morphological modelling, Bangladesh, data scarcity

Introduction

Data scarcity poses a big challenge to morphodynamic modelling of large fast-changing rivers. Modellers need to rely on field measurements to construct their models, but dynamic changes may limit the validity of survey data to a few months only. Moreover, even field surveys using echosounders or acoustic Doppler velocity profilers add uncertainties to the system (Czuba et. al., 2011). That leads to our main question: What if field measurements are missing or incomplete? Then, modellers need to develop some engineering analysis to overcome data limitations and create alternative paths. In this study, we present a method to generate river bed levels, and sediment erosion-and-deposition maps from satellite images of a large braided-anabranched river. The method provides a solid data production way to compensate for frequent surveys. The resulting data can be used as a sole source of bed topography input, but also as an intelligent interpolator in case of scarce measurement data, or as a basis for validation of field survey data. We applied the method to the morphological modelling of the Jamuna River in Bangladesh.

Case Study

The Jamuna River in Bangladesh is one of the most dynamic and braided rivers in the world. Bank erosion causes portions of the bank-line to retreat hundreds of metres annually; affecting millions of people (Mosselman, 2006). We carried out morphological modelling of the Jamuna River to develop suitable interventions to increase flood safety, preserve the stability of the banks, and to improve flow conditions into the Old Brahmaputra offtake (Fig. 1). We developed the model in Delft3D by using a 2D depth-averaged model with a structured mesh.

* Corresponding author
Email address: burhan.yildiz@deltares.com (B. Yildiz)

Despite the availability of hydrological and sediment grain size data in the project region, the lack of bathymetric survey data was found to be a critical hurdle for the model setup and validation. Therefore, additional engineering approaches were sought to overcome this situation.

Figure 1: Map of the project region

Method

We use two satellite images; in this case from the years 2017 and 2018 (Fig. 2). First, we mark the positions of the bars in each image (Fig. 3a). The comparison with the previous year's image reveals the movement of bars in one year. It also indicates the locations where sediment eroded or deposited within that year; if the bars were captured dry when the image was taken (Fig. 3b). A combination of ArcGIS, Open Earth Tools, and the QuickIn tool of Delft3D software were used to process the data, and project it on the model grid.

Results

The result of the applied method for the 2017-2018 period is given in Fig. 4. The erosion and deposition locations can be observed from the resulting map. The observed pattern can be

used to calibrate and validate the model in the absence of survey data. In this study, we used these maps in the model calibration step, viz. in identifying the suitable sediment transport formula and morphological model parameter settings. Once the model retrodicted the erosion and deposition patterns observed on the 2017-2018 map, we could validate the model by using another year, for instance, the 2018-2020 erosion-and-deposition map.

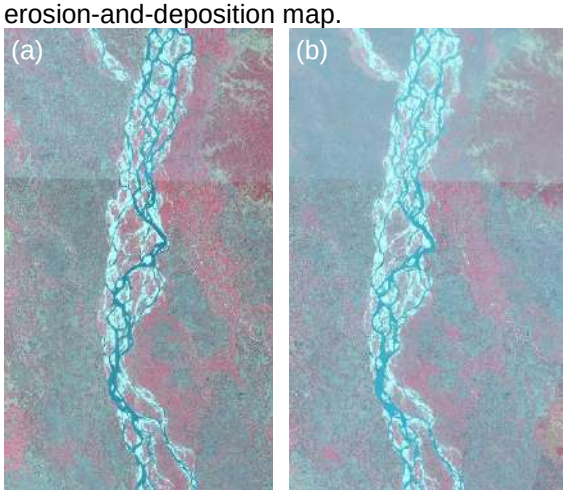

Figure 2: Satellite images of the Jamuna river (a) at 2017 and (b) at 2018

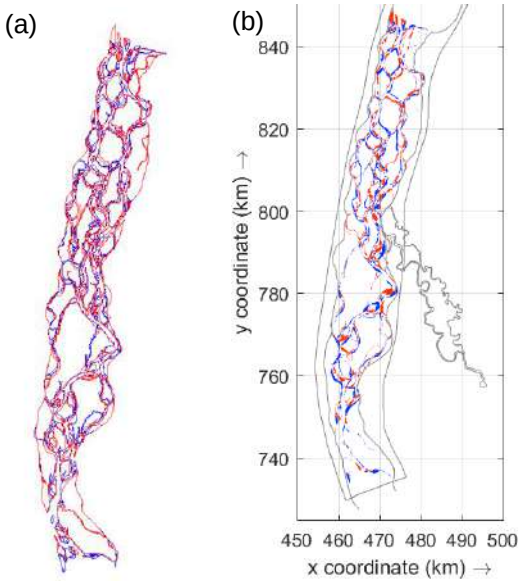

Figure 3: (a) Bar locations in 2017 (blue) and in 2018 (red) (b) interpolated sediment erosion-and-deposition map (erosion locations: blue, deposition locations: red)

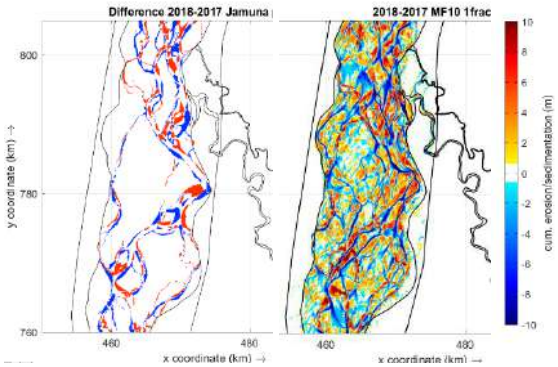

Figure 4: Comparison of model results with the validation data

Conclusion and Discussion

A modeller needs to cope with several uncertainties in a project. Maybe the most important tackle comes when the region lacks reliable data. Especially in river morphology modelling projects, where one generally cannot see the practical results in a near future, validation methods need to be reliable. The method presented here can be used to overcome data scarcity in terms of bathymetric surveys. It can be used safely to generate sediment erosion and deposition maps for the major bars, using only the satellite images. Although these maps do not provide an idea about the magnitude of erosion or deposition in full, they indicate the locations of the deposition and erosion, which can be used for calibration and validation of the model. Moreover, from the satellite images of preceding years several maps can be obtained to have more insight into the system dynamics. Nonetheless, the application of the method is limited to the parts of the river, which are dry during low flows, such that they are visible on the images. Perennially submerged locations cannot be distinguished using the satellite images.

Acknowledgements

This study is part of the Joint Cooperation Programme between Bangladesh and the Netherlands. The fourth author of this study (B.Y.) is granted a scholarship for his Post Doc study funded by TUBITAK from Turkey.

References

Czuba, J.A., Best, J.L, Oberg, K.A., Parsons, D.R., Jackson, P.R., Garcia, M.H., and Ashmore, Peter, 2011, Bed morphology, flow structure, and sediment transport at the outlet of Lake Huron and in the Upper Saint Clair River: Journal of Great Lakes Research, v. 37, no. 3, p. 480–493.

Mosselman, E. (2006). Bank Protection and River Training Along the Braided Brahmaputra–Jamuna River, Bangladesh. In Braided Rivers (eds I. Jarvis, G.H. Sambrook Smith, J.L. Best, C.S. Bristow and G.E. Petts). https://doi.org/10.1002/9781444304374.ch13

Damping of ship-induced primary waves in groyne fields

Rutger Pasman[a], Ralph Schielen[a], Jeremy Bricker[a], Arne van der Hout[a], Erik Mosselman[a], Wim Uijttewaal[a], Frank Collas[b] & Freek Huthoff[c,d]
[a]*Delft University of Technology, Delft, the Netherlands*
[b]*Radboud University, Nijmegen, the Netherlands*
[c]*HKV, Delft, the Netherlands*
[d]*University of Twente, Enschede, the Netherlands*

Keywords — ship-induced waves, groyne field, ecological preservation

Introduction

Recent ecological studies (Collas et al., 2018) show that ship-induced waves can reduce suitability of fish habitats along the river banks between groynes. Specifically eggs and young fish are vulnerable to these waves (Wolter & Arlinghaus, 2003). For the river Waal in the Netherlands the breeding and growing season of this fauna is from April to September, which generally corresponds to flow conditions where the groynes in the river are not completely submerged. The preferred habitat of fish is in the shallow zones close to the bank, which experience a high degree of hydrodynamic variability due to ship-induced waves. The goal of this research is to explore whether fish habitat during the growing and breeding season can be improved by reducing the flow impact of passing ships through structural modifications ("notching") of groynes.

Method

The 2D hydrodynamic model XBeach is used to simulate ship-induced wave dynamics (Roelvink et al., 2015). The model consists of a straight river channel with groynes along the banks. In the main channel, a steady flow is imposed. Passing ships are included in the model by defining a moving pressure field. Various groyne geometries are considered to study the flow properties in the groyne field. Two hydro-ecologic parameters are defined for the assessment of habitat suitability in-between the groynes:

1. Water level range: the difference between the highest water level and the lowest water level when a ship is passing.
2. Flow velocity range: the maximum change of the velocity vector during a ship is passing.

Both parameters are calculated for a 60-second time interval centred around the passing of a ship. The 'Flow velocity range' takes into account the magnitude as well as the direction of the flow field, as illustrated in Figure 1.

The figure shows the two horizontal components of the velocity vector (u and v-velocity), for a specific fixed location in the groyne field during the 60 second time interval. A circle is fitted around these velocity points, of which the diameter is the 'Flow velocity range'. This calculation is carried out for each location in the groyne field.

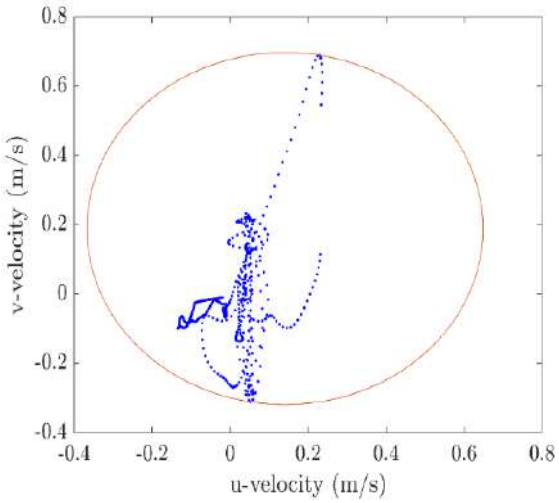

Figure 1. plot of the u- and v- directed velocity values during ship passing to determine the maximum velocity range.

Results

Figure 2 shows the results of the 'Flow velocity range' for two different groyne-configurations. The top plot shows the velocity range for a sequence of traditional impervious groynes. The middle plot shows the velocity range when the groynes are "notched", i.e. when a 10 m opening is created in the groynes. The bottom plot shows the difference in 'Flow velocity range' between the two situations. Herein, a negative value (blue) indicates regions where the notching has reduced the flow velocity range, and, hence, where fauna habitability has improved. In general, the velocity range has improved near the tips of the groynes, the center of the groyne field and close to the river banks, which is the area of interest for fauna habitat. When a ship passes the modified groyne field, the largest flow velocities occur within the notches (see

* Corresponding author
Email address: huthoff@hkv.nl (Freek Huthoff)

middle plot). Immediately next to the notch, the velocity range improves the most. Additional simulation runs with changes in notch location and notch size have shown that shallow wide notches close to the river bank appear to be most effective in reducing the 'Flow velocity range' in the groynes field (see Pasman 2020, results not shown here).

Conclusions

Results from the modelling study show that a notched groyne can have a positive influence on the fish habitat in rivers. Close to the notch, the fish habitat may locally become less suitable because of the higher flow velocities associated with flow through the notch. However, in large parts of the groyne field the flow variability is reduced, because of the inter-connection between neighbouring groyne fields. This makes most of the areas in the groyne fields more suitable for fish habitats. An optimal location of the notch for creating hospitable fish habitat appears to be close to the bank with a wide but shallow notch shape. This suggests that with relatively simple modifications the ecological value in the groyne fields can be improved significantly.

References

Collas, F. P. L., Buijse, A. D., van den Heuvel, L., van Kessel, N., Schoor, M. M., Eerden, H., & Leuven, R. S. E. W. (2018). Longitudinal training dams mitigate effects of shipping on environmental conditions and fish density in the littoral zones of the river Rhine. *Science of the Total Environment*, *619–620*.

Pasman, R. (2020). *Damping of ship-induced primary waves: Damping ship-induced primary waves in rivers by modifying groynes with the aim of increasing fauna habitat quality*. MSc Thesis. Delft University of Technology.

Roelvink, D., van Dongeren, A., Mccall, R., Hoonhout, B., van Rooijen, A., van Geer, P., de Vet, L., & Nederhoff, K. (2015). *Xbeach Manual*. 138.

Wolter, C., & Arlinghaus, R. (2003). Navigation impacts on freshwater fish assemblages: The ecological relevance of swimming performance. *Reviews in Fish Biology and Fisheries*, *13*(1), 63–89.

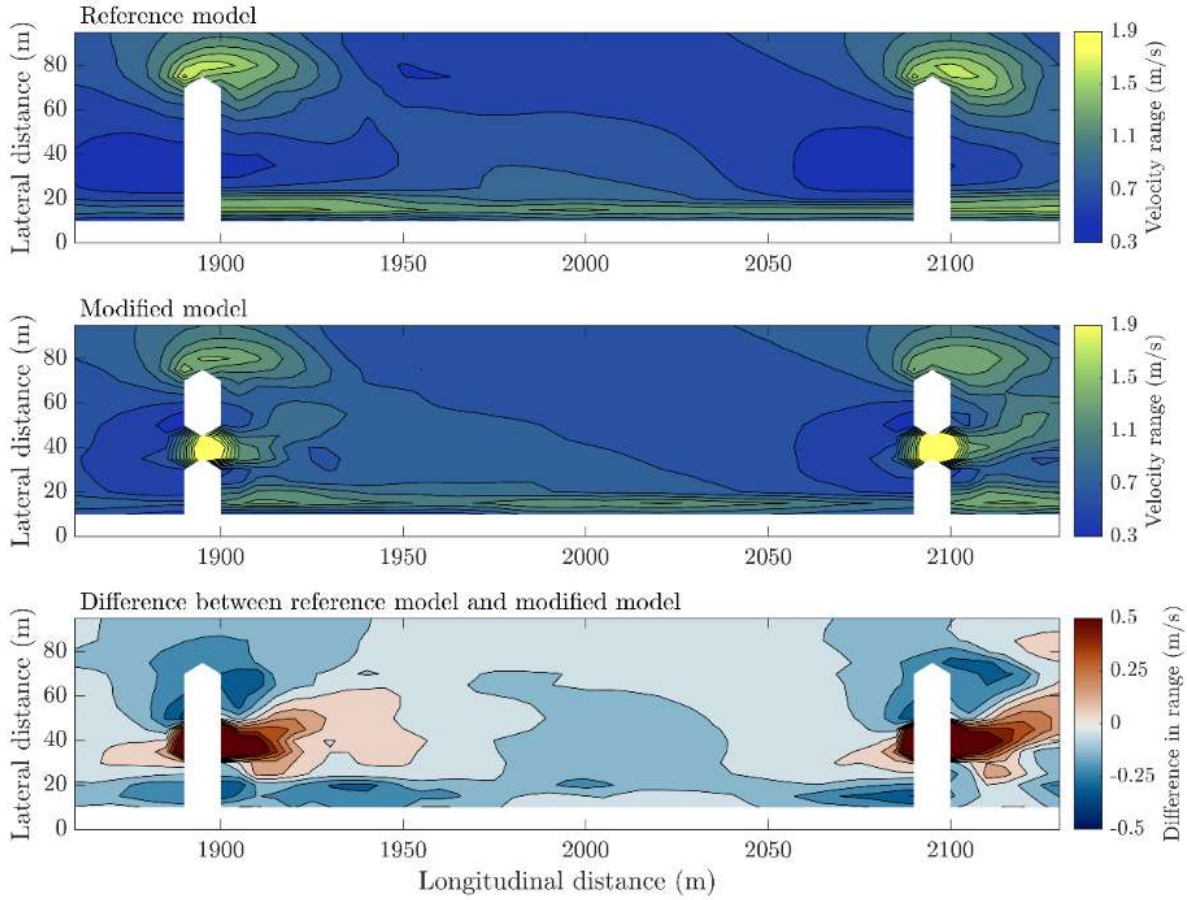

Figure 2. Flow velocity range during passing of a ship (travelling upstream). The base flow in the main channel is from left to right.

Modelling ship waves for the purpose of overtopping

Daan Kampherbeek[1*], Matthijs P. Benit[2], Geert H.P. Campmans[1], Jord J. Warmink[1]
[1]University of Twente, daan.kamp@hotmail.com, g.h.p.campmans@utwente.nl, j.j.warmink@utwente.nl
[2]Arcadis Nederland B.V., matthijs.benit@arcadis.com

Keywords — ship waves, SWASH, pressure field method, secondary ship waves, numerical modelling

Introduction

In the Netherlands, inland waterways are an important part of the transport infrastructure. On the Waal alone, 120-140 million tonnes of freight gets transported annually. Every ship sailing on these waterways causes ship-induced waves, which have an impact on quays and dikes. Along low-lying quays and dikes, specifically overtopping by ship waves can pose hazards for pedestrians and vehicles and hamper operations. Overtopping is caused by both the long, primary ship waves as well as the shorter secondary ship waves.

Although a lot of effort has been spent on quantifying the effects of ship waves, there are no widely applicable, reliable methods for assessing ship-wave induced overtopping in engineering practice. Currently, the most used methods for estimating ship-wave effects are analytical methods (ENW, 2007). Analytical methods that are available for this purpose are too limited in accuracy and validity (Verheij and Van Prooijen, 2007) for general application. Modelling methods such as potential flow models (Pinkster et al. 2004, Pinkster et al. 2014) or shallow water flow models like Delft3D or XBeach (Zhou et. al., 2013) cannot sufficiently represent the short, secondary ship waves. Based on earlier research, there are strong indications that SWASH should be able to model both primary and secondary components of the ship wave, due to it having a higher dispersion accuracy than other models. SWASH is a three dimensional transient model for simulating non-hydrostatic, free- surface and rotational flow (Zijlema et al., 2011). It has frequently been applied for the assessment of wave overtopping (Vanneste et. al. 2014), (Suzuki et. al. 2017). This research aims to clarify whether SWASH is a suitable tool for modelling ship-induced wave conditions at the bank for the purpose of overtopping.

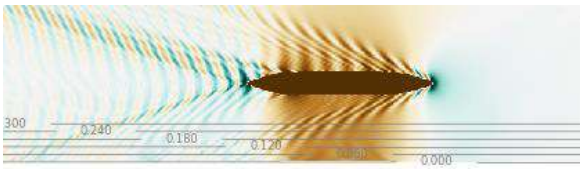

Figure 1: Top view of a simulation showing both primary and secondary ship waves as generated when simulating a towing tank experiment from Lataire et. al. (2009). The colors represent the water level with brown a water level below the reference level and green above it.

* Corresponding author
Email address: daan.kamp@hotmail.com
(Daan Kampherbeek)

Approach

To test our hypothesis, three main steps are undertaken to find out how SWASH performs when modelling ship-induced waves for overtopping. In the first step, the pressure field method is implemented in SWASH for the generation of ship-waves. This method has demonstrated good results for the primary waves in Delft3D and XBeach. In the pressure field method, a ship is represented as a space- and time-varying pressure field at the water surface. The sensitivity of the model to various settings is tested as well as several alternative spin-up procedures. The second step is the validation of the model with measurements. We have done this using measurements in the Port of Rotterdam, at the Nauw van Bath in the Scheldt river (Schroevers et. al., 2011) and with towing-tank measurements (Lataire et. al. (2009). The third step is a comparison of the performance of SWASH to available analytical methods: DIPRO+ which is prescribed in the Netherlands, and BAW guidelines used for the design of waterways in Germany.

Results

Implementing the pressure field method in SWASH proved to be feasible. First tests showed that the proposed methodology can be used to generate both primary and secondary ship waves, see Figures 1 and 2. An important aspect is the numerical stability which was shown to be wavering for typical situations (such as a the application of a surface piercing, sloped bank or bluntly shaped vessels). The notable persistent spin-up effects could be separated from the physical primary and secondary waves by a spin up procedure with included launching the ship first, and subsequently accelerating it. The resulting wave signal proved to be sensitive to the horizontal resolution of the computational grid. Model parameters which

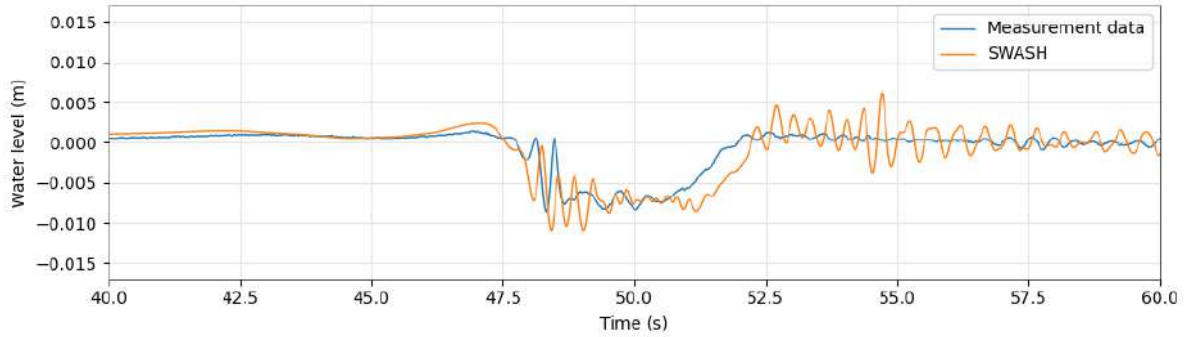

Figure 2: The water levels as measured by the top wave gauge in Figure 1. Both the long, primary wave as well as the shorter secondary waves are clearly visible.

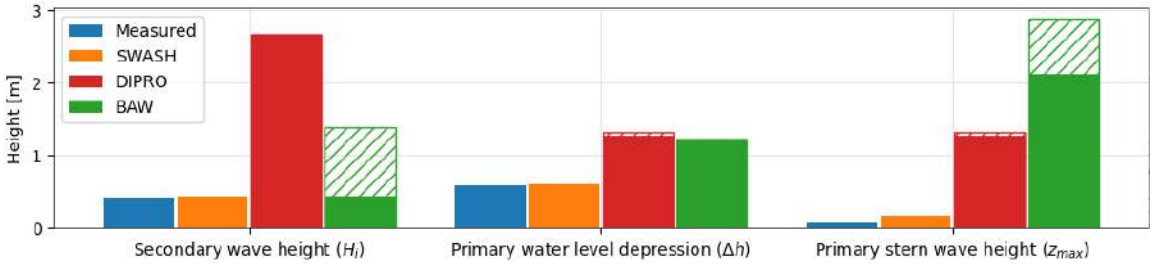

Figure 3: Wave characteristics as measured, simulated by SWASH and calculated using two analytical methods (DIPRO+ and BAW) for the simulation in Figure 1. The shading represents the uncertainty range in the analytical methods originating from the schematisation and assumptions.

are important for wave overtopping , such as bottom roughness and turbulence, have a small influence on the generated ship wave signal. The computational time for the each test was roughly one week on a conventional desktop system. Simulations of observed passages in the Port of Rotterdam and the Nauw van Bath demonstrate that our methodology can represent the wave signal accurately in complex geometries. Figure 3 shows wave characteristics in SWASH compared to measurements and guidelines used in the Netherlands (DIPRO) and Germany (BAW). SWASH clearly and consistently outperforms both Dutch and German guidelines.

Conclusions

Overall, it was demonstrated that SWASH is a valuable tool for estimating ship-induced wave conditions. The model has proven to be able to accurately represent both primary and secondary ship waves. Wave signals and components can be estimated more accurately than with any other existing method. For the purpose of overtopping, SWASH can be used to generate both primary and secondary waves to serve as input for an overtopping model. To use SWASH in a standardized engineering methodology for ship-wave generation, further study on the accuracy and sensitivity of the wave signals modelled by SWASH is necessary. For this kind of study, measurements on the ship-induced surface excursion and flow velocities at the banks would be a useful addition.

References

ENW (2007). Ontwerpbelastingen voor het rivierengebied. Technical report, Ministerie van Verkeer en Waterstaat Expertise Netwerk Waterkeren.

Verheij, H. and van Prooijen, B. (2007). Verbetering DIPRO Q4264.01. Technical Report July.

Vanneste, D., Altomare, C., Suzuki, T., Troch, P., and Verwaest, T. (2014). Comparison of numerical models for wave overtopping and impact on a sea wall. In Proceedings of the Coastal Engineering Conference, volume 2014Janua, pages 1–14.

Lataire, E., Vantorre, M., Eloot, K., 'Systematic Model Tests on Ship-Bank Interaction Effects', Proceedings International Conference on Ship Manoeuvring in Shallow and Confined Water: Bank Effects, Antwerp 2009, pp. 9-22.

Schroevers, M., Huisman, B. J., Van Der Wal, M., and Terwindt, J. (2011). Measuring ship induced waves and currents on a tidal flat in the Western Scheldt Estuary. 2011 IEEE/OES/CWTM 10th Working Conference on Current, Waves and Turbulence Measurement, CWTM 2011, pages 123–129.

Zhou, M., Roelvink, D.J.A., Verheij, H., and Ligteringen, H. (2013). Study of Passing Ship Effects along a Bank by Delft3D-FLOW and XBeach. International Workshop on Next Generation Nautical Traffic Models, (1998):71–80.

Zijlema, M., Stelling, G. and Smit, P., 2011. SWASH: An operational public domain code for simulating wave fields and rapidly varied flows in coastal waters. Coast. Engng., 58, 992-1012.

Pinkster, J.A. and Ruijter, M.N. (2004), The Influence of Passing Ships on Ships moored in Restricted Waters. In Offshore Technology Conference, pages 1–10, Houston, Texas, U.S.A, 2004. ISBN 9781615679713..

Pinkster, J.A. and Pinkster, H.M.J. (2014), A fast, user-friendly, 3-D potential flow program for the prediction of passing vessel forces. In PIANC World Congress, page 12, San Francisco, USA, 2014.

Session 1B
Ecological sustainability in rivers and estuaries

Upstream passability assessment of the LTD shore channel inflows by migratory fish species

N.Y. Flores[a*], F.P.L. Collas[a, b]
[a]Department of Animal Ecology and Physiology, Institute for Water and Wetland Research, Radboud University, Nijmegen, The Netherlands
[b]Netherlands Centre of Expertise on Exotic Species (NEC-E), Nijmegen, The Netherlands

Keywords — European eel, flow velocity, high discharge, River Rhine, spawning

Introduction

Higher fish densities have been observed in the shore channels behind the longitudinal training dams (LTDs) compared to nearby groyne fields in the river Waal (Collas et al., 2018). Though, no thorough assessment has been made of the passability of migratory fish species several of which have been red listed by the IUCN (e.g. the European eel – *Anguilla anguilla*). Many of these species have complex diadromous life cycles that require them to migrate upstream in order to spawn or mature. Their migration may be limited by extreme flow velocities near infrastructure.

Upstream migration potential is mainly determined by the swimming performance of fish. Several swimming performance endpoints exists, amongst them: 1) the critical swimming speed (U_{crit}) and 2) the burst swimming speed (U_{burst}). The U_{crit} is a prolonged speed maintained for up to 60 minutes. The U_{burst} is the highest speed maintained for fewer than 20 seconds. These two swimming speeds used in conjunction may serve as indicators of the passability of a river section by migratory fish species (Wolter & Arlinghaus, 2003; 2004). Additionally, the maximum flow velocity (V_{max}), described as the maximum ambient flow velocity at which a fish species has been observed in the field may be used to assess if ambient flow velocities are within a range that would not limit the occurrence of a species (Del Signore et al., 2014).

Extensive flow velocity monitoring in the shore channels has shown that the inflows of the shore channels have the highest recorded flow velocities and as such are potentially the main bottleneck for upstream migration. This study aims to assess the passability of the shore channel inflows for native diadromous fish species during upstream migration. The shore channels along the LTDs are expected to serve as refuge for fish species, therefore it was hypothesized that the shore channel inflows provide pathways with ambient flow velocities below the critical and burst swimming speeds of fish species.

Methods

Fish Species

A list of diadromous fish species occurring in the Waal was compiled. The total length (TL) or standard length (SL) for adult males and juveniles were obtained from www.fishbase-.org and a European fish species handbook (Kottelat & Freyhof, 2007), respectively. The length-length equations from www.fishbase-.org were used to convert SL to TL. Male length was used since this information was available for the majority of the relevant fish species.

To assess the passibility during upstream migration of fish species, V_{max} of the adult fish life stages were used to rule out any datasets with flow velocities within the ambient flow velocities of fish species (Del Signore et al., 2014).

For each fish species the TL was used to derive the U_{crit} and U_{burst} swimming speed by using available linear regressions between the swimming speeds and TL (Wolter and Arlinghaus, 2003; 2004). The maximum distance in meters that could be covered based on the U_{burst} swimming speed was determined assuming a 19.99 sec burst swimming speed performance time. This maximum distance was then used to visually assess the passability of the inflows when the U_{crit} was found to be insufficient to pass.

Flow Velocity

ADCP measurement datasets from RWS surveys were obtained for the highest discharges surveyed at the inflows of the three LTDs and including the years 2017, 2018 and 2019. An additional dataset from a 2016 survey consisting of ADCP measurements collected in the main channel near the LTDs was obtained as a reference dataset.

The ADCP datasets were imported into Voxler 4 software (Golden Software LLC.) for 3D visualization and analysis. The flow velocity magnitudes of the point datasets were gridded into 3D lattices by using the inverse distance isotropic method. The resolution was set to 200 nodes per axis. The lattices were corrected for the river bottom by using interpolated bottom heights from the datasets.

* Corresponding author
Email address: nflores@science.ru.nl (N.Y. Flores)

Then the U_{crit} and U_{burst} of each species were subtracted from the flow velocity lattices to create new lattices showing the final swimming speed of the species ($U_{fish}=U_{crit}-V_{water}$ and $U_{fish}=U_{burst}-V_{water}$) An isosurface was used to determine the volumes of the lattice where forward motion could be expected to occur (≥ 0.00001 m/s).

A number of conditions were used to visually assess the lattices for the passability of each fish species (Fig. 1). For each lattice, the fish species were assigned a pass, unlikely to pass, or a does not pass.

Figure 1. Decision tree for the passability analysis by diadromous fish species of the shore channel inflows.

Results and discussion

Larger juveniles (TL = 70 mm; Fig. 2) were able to pass some of the study sites, including the Wamel inflow in February of 2018 and all of the inflows in March of 2019, corresponding with the lowest monthly average discharge assessed (1.862 m^3/s) among the high discharge datasets. For example, the European eel juveniles have been observed in the North Sea in the winter starting their upstream migration (Kottelat & Freyhof, 2007), hence according to this assessment their swimming performance in this river section may be highly impacted by high discharges, which decreased their passability to 0% in 2017. During more average discharge conditions (1430 m^3/s in June 2018) the juveniles were able to pass in Dreumel and Ophemert based on their U_{crit}.

Adults did not have problems passing in the inflows with the exception of the Three-spined stickleback (*Gasterosteus aculeatus aculeatus*), which was unable to pass the high flow velocities due to a low TL. However, it was able to pass the Dreumel inflow in June 2018, which coincided with the spawning migration period for the species (Kottelat & Freyhof, 2007).

The Wamel inflow in February 2018 was the most passable of the study sites (100% passability), during the second lowest discharge assessed (2.229 m^3/s). The Ophemert inflow was the least passable of the inflows. Fish species were able to pass all of the 10 3D lattices produced once they reached a minimum TL of about 165 mm.

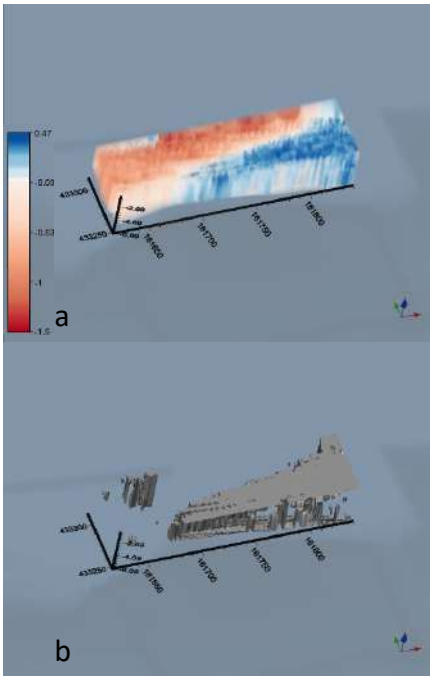

Figure 2. Images of the Wamel inflow December 2017 (a) 3D lattices showing the final swimming speed of juvenile European eel and (b) the isosurface of passable lattice when using U_{crit}.

Acknowledgements

Rijkswaterstaat financially supported this study (RWS 31153573, Habitatgeschiktheid Langsdammen). We would like to express sincere gratitude to Henk Eerden and Margriet Schoor for their input during the study.

References

Collas, F.P.L., Buijse, A.D., van den Heuvel, L., van Kessel, N., Schoor, M.M., Eerden, H., Leuven, R.S.E.W. (2018). Longitudinal training dams mitigate effects of shipping on environmental conditions and fish density in the littoral zones of the river Rhine. Science of the Total Environment, 619-620, 1183-1193.

Kottelat, M., & Freyhof, J. (2007). Handbook of European Freshwater Fishes. Berlin, Germany: Publications Kollelat, Cornol, and Freyhof.

Del Signore, A., Lenders, H., Hendriks, J., Vonk, J., Mulder, C., & Leuven, R. S. E. W. (2016). Size-Mediated Effects of Water-Flow Velocity on Riverine Fish Species. River Research and Applications, 32, 390–398. doi:10.1002/rra.2847

Wolter, C., & Arlinghaus, R. (2003). Navigation impacts on freshwater fish assemblages: the ecological relevance of swimming performance. Reviews in Fish Biology and Fisheries, 13(1), 63-89. doi:10.1023/A:1026350223459

Wolter, C., & Arlinghaus, R. (2004). Burst and critical swimming speed of fish and their ecological relevance in waterways. Leibniz-Institut für Gewässerökologie und Binnenfischerei (IGB), 77-93.

Assessing morphological changes and impact on ecology in Koshi River using remote sensing and cloud computing

Kshitiz Gautam[a,b], Sanjay Giri[b], Gennadii Donchyts[b], Biswa Bhattacharya[a]
[a]*IHE Delft Institute for Water Education, Department of Hydroinformatics and Socio-Technical Innovation*
P.O. Box 3015, 2601 DA, Delft, the Netherlands
[b]*Deltares*
P.O. Box 177, 2600 MH, Delft, the Netherlands

Keywords — River Morphology, Ecology, Koshi Tappu, Google Earth Engine, Water Occurrence Probability

Introduction

The rivers emerging to lowlands from the mountainous terrain in the Himalayan region partially release their sediment as their gradient changes from high to low forming braided patterns and alluvial fan. Multiple channels of such braiding rivers provide the river with the flexibility of moving over a large span of width. The large width and dynamics of multiple channels pose a greater challenge to river management efforts. River management measures and interventions in such rivers may lead to adverse impacts affecting not only flow passage and morphology, but also ecology and habitats.

The morphological study of such large and dynamic rivers has become much easier and effective with the support of remote sensing techniques. The remotely sensed data from multiple satellite missions, such as Landsat and Sentinel, over a wide spatial and temporal range are now freely available. However, using these imageries and working out with them may require large storage and computational capacities. Using freely available cloud computing platforms could decrease the cost of computation for processing such a large amount of data.

Koshi River in Nepal, a highly sediment-laden river (Sinha et al., 2019), is among such rivers that lie in the transition zone at Chatara where it converts into a braided channel within a reach of about 150 km to India after which it becomes a meandering channel. The river is the origin and lifeline to the oldest and one of the most diverse Ramsar sites of Nepal, the Koshi Tappu Wildlife Reserve (KTWR). The changing planform of the river over time has brought changes in the land use and land cover of the area (Chaudhary et al., 2016; Chettri et al., 2013; Devkota et al., 2018) which might have an effect on the ecology and habitat of the area. This change in morphology may have been caused by the natural processes as well as by the manmade structures in and along the river. The objective of this study is to analyse and quantify the morphological changes of the Koshi River due to the Koshi barrage and identify its relationship with vegetation dynamics and ecology affecting the wildlife of KTWR using freely available satellite images and cloud computing.

Method

An algorithm developed by Donchyts (2018) in Google Earth Engine (GEE) to identify the surface water occurrence is used as the basis for quantifying the change in the area of erosion and sedimentation within the selected reach of the river. The algorithm uses multiple images of the area over a selected time frame to create a single floating-point image of the area. The images from one monsoon season to another are used in order to capture the driest and wettest periods and generate the floating-point image. Normalized Difference Water Index (NDWI) is calculated and used for analysing the water occurrence probability in the image. Changes in the area are calculated by taking the difference in the area of such occurrence probability over the desired time period and presented as a resulting image. This image is used to analyse the morphological changes in the planform of the river. The change in vegetation in the reach is also calculated in conjunction with morphological changes. Possible correlation of reach-scale morphological processes and changes with human intervention, vegetation dynamics and wildlife of KTWR is deduced. In this paper, we present the quantification of morphological changes in a selected reach with a barrage (near KTWR).

Effect of the barrage

The upper reach of Koshi is controlled by Koshi Barrage and embankments along both sides. Change in planform at the area of the barrage at different times are shown in Fig.1. It is obtained by subtracting the water occurrence pixels of one year from its preceding year. The result shows that the river was flowing through the western part of the barrage along the embankment at the downstream reach during 2000-2001. While the western part accreted during 2001-2002, the river was shifting towards the central part. The river continued to erode

and flow through the central part during 2002-2003. However, the channel shifted towards the east during 2003-2004 channelizing along the east embankment as the accreted area was large on the western side. The changes occurred upstream of the barrage as well during the same period when the channel shifted away from the eastern embankment and channelizing towards the central part.

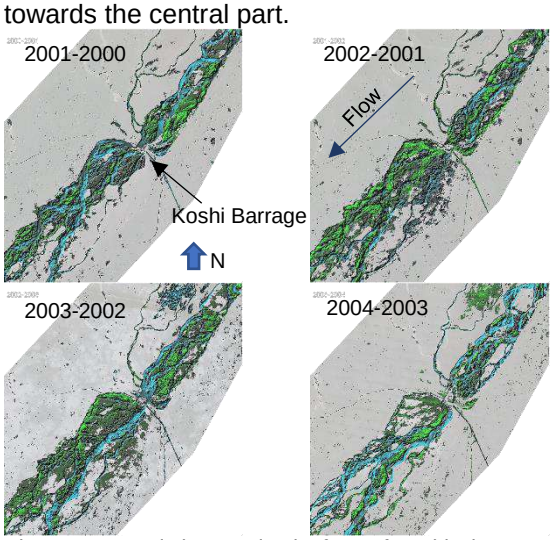

Figure 1. Annual changes in planform of Koshi River reach stretching about 13 km upstream and 15 km downstream of the Koshi Barrage during 2000 – 2004 (green = accreted area, light blue = eroded area).

This continually shifting behaviour of the river can be attributed to the operation of the gates (56 in total) of the barrage. The gate operation appears to be altered considering the intakes of the irrigation canals as well as to shift the deep channels away from the embankment. The narrowing of the upstream reach due to the barrage was reported in previous studies as well (Giri et al., 2019). The changes are quantified in terms of eroded and accreted areas as well, based on water occurrence probability, shown in Fig.2.

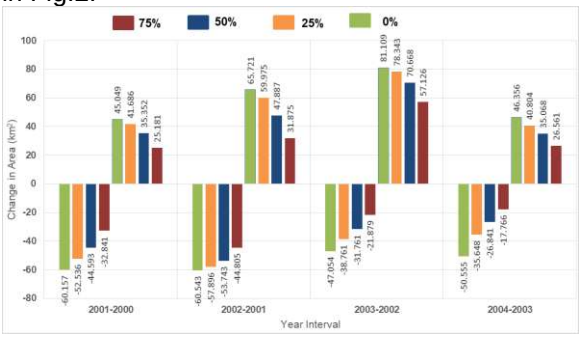

Figure 2. Erosion (-ve) and accretion (+ve) areas based on water occurrence probability within the stretch shown in images of Fig.1. The numbers 0, 25, 50 and 75 denotes the upper limit of water occurrence probability.

The result shows how the areas of erosion and accretion change when the upper limit of the water occurrence is altered. For example, 0% of the upper limit implies the changes in area within maximum and minimum water levels.

The changing planform of the river has led to the changes in the vegetation cover of the upstream area which belongs to KTWR and serves as important biodiversity to its habitats. The study on the interrelation between morphological and vegetation changes and their impact on habitats of KTWR is in progress.

Conclusion

Based on the initial findings of the study, which is still ongoing, the following conclusions can be drawn:

1. Freely available satellite images contain much information that can be used to study and interpret the river morphological changes, their impacts and interaction with other processes.
2. Use of GEE saves a lot of computational time, memory and cost to analyse a large amount of satellite data to obtain useful information about water bodies and lands.
3. Morphological changes of rivers can be studied using the water occurrence probability, though quantification of such changes in a more accurate manner still needs further research.
4. Human interventions in dynamic river systems have a large impact on changing planform and morphology.

References

Chaudhary S, Chettri N, Uddin K, Khatri TB, Dhakal M, Bajracharya B, Ning W (2016) Implications of land cover change on ecosystems services and people's dependency: A case study from the Koshi Tappu Wildlife Reserve, Nepal. Ecological Complexity 28: 200-211 DOI 10.1016/j.ecocom.2016.04.002

Chettri N, Uddin K, Chaudhary S, Sharma E (2013) Linking Spatio-temporal land cover change to biodiversity conservation in the koshi tappu wildlife reserve, Nepal. Diversity 5: 335-351 DOI 10.3390/d5020335

Devkota L, Giri S, Crosato A (2018) Impact of the Koshi barrage and embankments on river morphology and dynamics

Donchyts, G. (2018) Planetary-scale surface water detection from space. PhD Doctoral Thesis. Delft University of Technology DOI 10.4233/uuid:510bd39f-407d-4bb6-958e-dea363c5e2a8

Giri, S., Thompson A., Mosselman, E., Donchyts, G. (2019). Deep-Channel Dynamics: A Challenge for Erosion Management in Large Rivers. 14th International Symposium on River Sedimentation, September 16-19, Chengdu, China

Sinha R, Gupta A, Mishra K, Tripathi S, Nepal S, Wahid SM, Swarnkar S (2019) Basin-scale hydrology and sediment dynamics of the Kosi river in the Himalayan foreland. Journal of Hydrology 570: 156-166 DOI https://doi.org/10.1016/j.jhydrol.2018.12.051

* Corresponding author
Email address: kga002@un-ihe.org (Kshitiz Gautam)

Macro- and mesoplastic abundance and composition in the water column of the river Waal

Stephanie B. Oswald[a], Margriet M. Schoor[b], Frans Buschman[c], Frank P.L. Collas[a*]
[a]Department of Animal Ecology and Physiology, Institute for Water and Wetland Research, Radboud University, Nijmegen, The Netherlands
[b]*Rijkswaterstaat Oost Nederland, Arnhem, The Netherlands*
[c]*Department of River Dynamics and Inland Water Transport, Deltares, Delft, The Netherlands*

Keywords — freshwater systems, stow net fishing, 'ankerkuil visserij', River OSPAR, river Rhine

Introduction

Plastic pollution has become one of the most eminent environmental challenges (Winton et al., 2020). Until recently studies on plastic presence mainly focussed on the marine environment. However, the potential role of rivers as a main transport pathway and source of plastics to the ocean urges extensive monitoring of riverine plastics since about 80% of the plastic litter found in the oceans are transported by rivers (Jambeck et al., 2015).

Based on the size of plastic different groups of plastics can be differentiated. Macroplastics are pieces larger than 25 mm in size, mesoplastics have sizes between 5 and 25 mm and microplastics range between 100 nm and 5 mm. Depending on plastic size the adverse effects can be ingestion (leading to reduced growth), entanglement, strangulation and lacerations.

The majority of studies that assess plastic concentrations in rivers is limited to the water surface, mainly analysing floating material. Plastic concentration studies in the Dutch part of the river Rhine also focus on the upper water layer (Mani et al., 2016, Vriend et al. 2020).

Therefore, this study aims to assess the quantity and quality of macro- and mesoplastic in the entire water column of the river Waal. Additionally, a comparison will be made between plastic composition from the water column and the local riverbanks. Postulated research questions are: 1) what is the composition and origin of macro- and mesoplastic in the water column of the river Waal, 2) does the composition differ between river bank and water column and 3) what is the quantity of macro- and mesoplastics in the entire water column of the river Waal?

Methods

Sampling

Water column monitoring was performed using a stow net connected to an anchor (Figure 1). It uses a static stow net thereby passively monitoring plastic pieces. The Net is positioned from the bottom to the surface and samples the entire water column (floating plastics + suspended plastics + bed-load plastics). The net was placed in the water for at least half an hour after which it was retrieved and all plastics in the fine mesh were collected.

Monitoring was performed on the edge of a groyne field and the main channel near IJzendoorn and in a shore channel behind the longitudinal training dam near Tiel. Sampling was performed in 2018, 2019 and 2020 during various discharges. All samples were subsequently washed to remove organic matter from the plastic material. Thereafter the plastic material was grouped into macro- and mesoplastic based on their size and identified to plastic category using the river OSPAR classification categories (Schone Rivieren, 2017)

Figure 1. Vessel equipped with a stow net attached to an anchor used for macro- and mesoplastic sampling in the current study.

Net efficiency

Due to the larger mesh size, the catching efficiency of the net was reduced resulting in an underestimation of plastic concentration. An efficiency test was performed by introducing plastics of different sizes corresponding to macro- and mesoplastic of both hard and soft plastic in the water column in front of the net. The subsequent retrieval rate was used to determine net efficiency.

* Corresponding author
Email address: f.collas@science.ru.nl (F.P.L. Collas)

Figure 2. Example of collected macroplastics during stow net fishing in the river Waal.

Plastic abundance

Abundance of plastic was expressed in several endpoints: 1) particles per sampled volume (particles.m^{-3}) and 2) particles per hour (particles.h^{-1}). All results were calculated for the sum of macro- and mesoplastics, but also individually for each size range in the two different locations. The endpoint particles per hour were used to derive the total amount of plastics pieces that go through the Waal River a year using a bootstrapping procedure.

Results and discussion

Undefined soft plastics (2.5 – 50 cm (soft plastic)) and undefined plastics film (0 – 2.5 cm (soft plastic) were the dominant plastic items recorded. Also candy- snack and chips packaging, string and cord (diameter < 1 cm) and tampons and tampons packages were found often. Of all string and cords with diameter < 1 cm 29% originated from geotextile material.

The majority of plastic could no longer be identified to country of origin. A total of 19 source countries were identified of which only 5 belonged to the river Rhine basin. Most plastics were from Germany (71%) with only 9% originating from the Netherlands. A multitude of plastics from eastern European countries were found potentially linked to commercial navigation from these countries. Some plastics originated from the USA indicative of potential plastic input through tourism.

Composition of plastic in the water column was found to be consistent in time and between the two sampling locations. Though the plastic composition differed between the local river banks and the water column.

The plastic concentration (particles.m^{-3}) was highest on the 2nd of September 2019 at 0.018 particles.m^{-3}. Variation between sampling dates was limited. Based on the derived plastic concentration per hour for sampling in 2018 and 2019 a median amount of 352 million macro- and mesoplastic particles were going through the river Waal yearly. This yearly total is limited to low discharge conditions since monitoring was limited to discharges of less than 1200 m^3.s^{-1} at gauging station Tiel. During high discharges additional plastic particles could enter further increasing the yearly number of plastics going through the river Waal even further.

Future research should focus on determining the plastic composition and concentration during higher discharges.

Acknowledgements

The stow net fishery was performed by Sportvisserij Nederland as part of the INTERREG VA programme Germany-Netherlands ‘Green Blue Rhine Alliance’. Part of the plastic counting and identification was financially supported by Rijkswaterstaat (RWS 31162321, Methodiekontwikkeling en analyse plastic in de IJssel, Waal en Niederrhein, najaar 2020).

References

Jambeck, J.R., Geyer. R., Wilcox, C., Siegler, T.R., Perryman, M., Andrady, A., Narayan, R., Law, K.L. (2015). Marine Pollution. Plastic Waste Inputs from Land into the Ocean. Science, 347, 768–771.

Mani, T., Hauk, A., Walter, U. and Burkhardt-Holm, P. (2016). Microplastics profile along the Rhine River. Scientific Reports, 5, 17988.

Schone Rivieren. (2017). Handleiding voor monitoring. Available on: https://schonerivieren.org/images/Onderzoek/DEF_Handleiding_monitoring__Schone_Rivieren_2018-2019.pdf

Winton, D.J., Anderson, L.G., Rocliffe, S., Loiselle, S. (2020). Macroplastic pollution in freshwater environments: focussing public and poly action. Science of the Total Environment, 704, 135242.

Vriend, P, Van Calcar, C., Kooi, M., Landman, H., Pikaar, R. and Van Emmerik, T. (2020). Rapid Assessment of Floating Macroplastic Transport in the Rhine. Frontiers in Marine Science, 7, paper 10..

Session 2A
Threats for river functions

What is the effect of dike cover damages on the failure probability of wave overtopping?

Vera M. van Bergeijk[a*], Jord J. Warmink[a], Suzanne J.M.H. Hulscher[a]
[a] *University of Twente, Department of Water Engineering and Management, Faculty of Engineering Technology, P.O. Box 217, 7500 AE, Enschede, the Netherlands*

Keywords — Failure probability, Erosion, Grass

Introduction

Climate change increases the vulnerability of grass-covered river dikes due to increasing river discharges in the winter and weaking of the dike cover during droughts in the summer. Wave overtopping is one of the main failure mechanisms of grass-covered dikes. Large waves during a storm overtop the dike, flow over the crest and flow down along the landward slopes. The high flow velocities in combination with turbulence result in erosion of the grass cover (Figure 1).

According to the WBI, the dike fails when an erosion depth of 20 cm is reached. Damages in the dike cover as the result of animal borrowings are weak spots that are vulnerable for wave overtopping erosion. In this study, we calculate the effect of these damages on the failure probability of wave overtopping to determine the vulnerability of these damages.

Figure 1: Erosion of the grass cover by overtopping waves results in the formation of a small cliff (Peeters et al., 2012).

Dike cover damages

Damages in the dike cover are more vulnerable for wave overtopping erosion due to (1) an increase in the hydraulic load and (2) the weaking of the dike cover. Firstly, a damage of the dike results in the formation of a vertical cliff (Figures 1 and 2). When the water flows over this cliff, a jet forms that impacts in the jet impact zone leasing to an increase in the hydraulic load. Secondly, the grass cover is often damaged resulting is a decrease in the cover strength.

In this study, we investigate the vulnerability of small damages resulting in a maximum cliff height of 20 cm. These damages can be the result of animal burrowing, small slope instabilities and erosion holes as the result of wave overtopping.

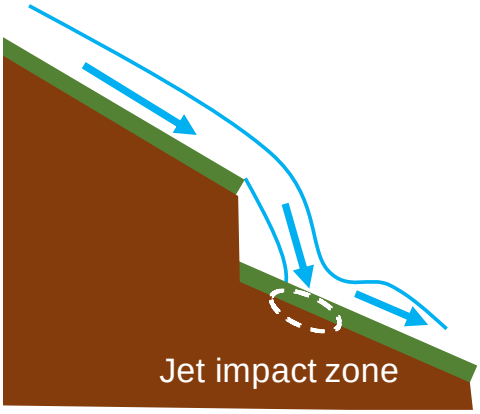

Figure 2: Flow over a vertical cliff at a damage results in the formation of a jet that impacts in the jet impact zone (white dashed circle).

Method

The failure probability is calculated using the framework of Van Bergeijk et al. (2021) using the water level, wind speed and critical velocity as stochastic variables. The erosion depth along the dike profile is computed using the analytical grass-erosion model (Warmink et al., 2020) where the cover strength is modelled using the critical velocity and the hydraulic load is simulated using the flow velocity and the turbulence parameter ω. The failure probabilities are calculated for a grass-covered river dike near Millingen a/d Rijn (Van Bergeijk et al., 2021).

Firstly, the failure probability of a regular dike profile with a good grass cover is calculated. A regular grass-covered dike profile is most likely to fail at the landward toe where the flow velocity is high and the slope change results in an increase in the load on the dike cover. The increase in the hydraulic load is modelled using a turbulence parameter $\omega_{toe} = 2.75$ (Warmink et al., 2020).

Next, the failure probability for a damage $P_{f,damage}$ on the landward slope is computed. The failure probability depends on the location of the damage - because the flow velocity increases along the slope - and

* Corresponding author
Email address: v.m.vanbergeijk@utwente.nl (V.M. van Bergeijk)
URL: people.utwente.nl/v.m.vanbergeijk (V.M. van Bergeijk)

the type of cover at the damaged location. The $P_{f,damage}$ is calculated along the landward slope for four cover types with different critical velocities U_C (Table 1). The additional load due to jet impact is simulated using the relation found by Van Bergeijk et al. (2021)

$$\omega_{damage} = 0.074\, U_C + 2.1 \qquad (1)$$

where the turbulence parameter ω_{damage} depends on the cover quality.

Table 1: The critical velocity for four cover types (Verheij et al. 1995).

Cover type	Critical velocity [m/s]
Good grass	6.5
Poor grass	2.5
Good clay	1.0
Poor clay	0.4

Results

The failure probability at the inner toe $P_{f,toe}$ of a regular dike profile is $4.8 \cdot 10^{-5}$. The failure probability for a damage $P_{f,damage}$ increases along the landward slope (Figure 3) related to the increase in flow velocity along the slope. In case of a good grass cover at the damage, the failure probability at the inner toe is larger compared to the failure probability of the damage. This is because the additional load due to the slope change at the inner toe ω_{toe} is larger than the additional load near the damage ω_{damage}. For the other three qualities, the damage has a higher failure probability. A damage is 12, 60 and 120 times more likely to fail compared to the inner toe for a poor grass, good clay and poor clay cover, respectively.

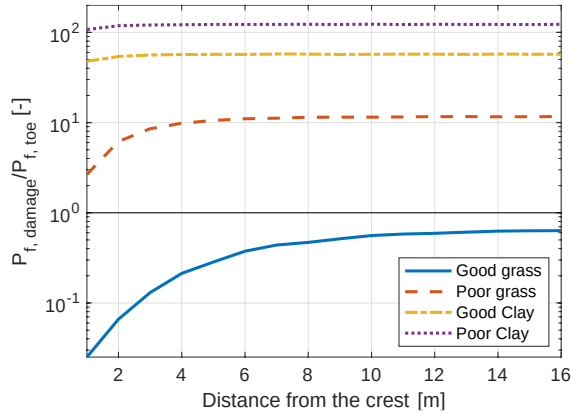

Figure 3: The ratio between the failure probability of a damage on the landward slope $P_{f,damage}$ and the inner toe $P_{f,toe}$ for four cover types.

Application

According to the current failure definition, a grass-covered dike fails once the erosion depth exceeds 20 cm. However, river dikes often consist of a clay core with a cover that is able to resist overtopping flows. The residual dike strength of the cover and core is not considered in the current failure definition. Design and assessment methods will become more cost-effective when the residual dike strength is taken into account.

The results of this study can be used as a first step for methods that include the residual dike strength. For example, the relation for the additional load near a cliff can be used in case the failure definition is extended to larger erosion depths where cliffs of 20 cm can form at multiple locations. The results are also applicable to small slope instabilities. A small slope instability does not lead to flooding but makes the dike more vulnerable for wave overtopping. Therefore, it is important to consider the interaction between macro-stability and wave overtopping in studies on progressive slope instabilities.

Conclusions

Damages in grass-covered slopes affect the failure probability by increasing the hydraulic load on the dike cover due to wave impact and decreasing the cover strength. When the grass cover is damaged, the damaged location is between 12 and 120 times more likely to fail compared to a regular dike profile depending on the cover quality. Damages on the upper slope are less vulnerable compared to damages on the lower slope due to the high flow velocity at the end of the slope. The results of this study can be used for methods that aim at taking the residual dike strength into account and thus improve dike assessment methods in general.

Acknowledgements

This research was funded by the Netherlands Organisation for Scientific Research (NWO), research programme All-Risk with project number P15-21.

References

Peeters, P., De Vos, L., Vandevoorde, B., Taverniers, E., Mostaert, F. (2012). Stabiliteit van de grasmat bij golfoverslag: golfoverslagproeven Tielrodebroek. Waterbouwkundig Laboratorium (WL), report 713_15b. Antwerp, Belgium

Van Bergeijk, V.M., Verdonk, V.A., Warmink, J.J., Hulscher, S.J.M.H. (2021) Spatially distributed failure probabilities of wave overtopping over grass-covered and damaged dikes. Submitted to Water.

Warmink, J., van Bergeijk, V., Frankena, M., van Steeg, P., Hulscher, S. (2020). QUANTIFYING THE INFLUENCE OF TRANSITIONS ON GRASS COVER EROSION BY OVERTOPPING WAVES. *Coastal Engineering Proceedings*, (36v), 39-39.

Verheij, H. J., Meijer, D. G., Kruse, G. A. M., Smith, G. M., Vesseur, M. (1995). Investigation of the strength of a grass cover upon river dikes. Deltares, *Report Q1878, Delft, The Netherlands*

Long-term bed level change in the Dutch Rhine branches and its impacts to water availability

Kees Sloff[a,b], Thomas van Walsem[c]
[a]*Deltares, Boussinesqweg 1, 2629 HV Delft*
[b]*Delft University of Technology, Faculty of Civil Engineering and Geosciences, Stevinweg 1, 2628 CN Delft*
[c]*Rijkswaterstaat, Water, Transport and Environment, Zuiderwagenplein 2, 8224 AD Lelystad*

Keywords — Morphology, flow-distribution, bed degradation

Background

Large-scale erosion of the river bed of the Dutch Rhine branches threatens (and sometimes encourages) several river functions (Visser, 2000, Ylla Arbos et al., 2020). However, the Delta-scenarios for 2050 and 2100 do not consider the impacts of further bed-level degradation. Although bed degradation is a slow process, it indirectly influences water levels, and moreover it modifies the distribution of discharges at the Pannerdense Kop and IJsselkop bifurcations (due to uneven rates of degradation of the downstream branches). The new strategic program "Integral River Management" (IRM) has adopted bed-degradation as a central theme and urges to implement approaches to stabilize the river bed. Still, the indirect impacts on river functions have only be estimated very roughly (quick-scans), without using models and most recent forecast of bed-level change.

As part of the project "Klimaatbestendige Netwerken", Rijkswaterstaat and Deltares have studied the sensitivity of water-availability (fresh-water distribution) to a refined version of the most recent forecasts of bed-level degradation. The main research questions are:

- What will be the possible future erosion of the river bed along the branches that is relevant for hydraulic response?
- What will be the impact on the long-term availability of water and the navigability during low-flow conditions.

Method

The use of a 1D hydrodynamic model allows a much better estimate than previous analytical and data-driven estimates. The approach in this study consists of 2 parts:

1. Forecast of bed-level degradation along the branches, based on observations.
2. Make use of the "Nationaal Water Model" (using a 1D hydraulic SOBEK model) to simulate the impacts on flow distribution.

* Corresponding author
Email address: kees.sloff@deltares.nl (Kees Sloff)
URL: www.deltares.nl/nl/experts/kees-sloff/

Results

Prediction of large-scale bed-level degradation of the Rhine is highly uncertain. The degradation process is not a linear trend, but irregular in time and space. It reacts on floods (acceleration), on decaying impacts of past river-training, sediment extraction, and Room for the River works (deceleration). Ten Brinke (2019) and Ylla-Arbos et al. (2019) presented section-average forecasts based on extrapolation of observed historic trends. This represents the business-as-usual-scenario, reference for IRM studies. However, as these are step-wise averages of long sections, they cannot be applied to the 1D model.

In our study (Sloff, 2019) we re-assessed the historic trends with consideration of gradual variation along the branches, and accounting for observed deceleration of the trends (confirmed by model simulations). For consistency with other programs (IRM) our prognosis does not significantly differ from the previous ones. Note that the prognosis cannot be based solely on results of morphological models. The existing models provide understanding in the processes and responses to ongoing developpments, but the models have not yet been well validated for long-term (>30 yrs) autonomic evolution of the river bed due lack of data and resources.

Figure 1 shows examples of the resulting estimated annual bed-level change until 2050, and the comparison to observed trends of the last 20 years (from processed multibeam measurements, P-Map data). For hydraulic response the scale of backwater curves, order of tenths of kilometres, allows us to use the smoothened lines presented in the figures. Important is that the Waal will continue to erode faster than the Pannerdensch Kanaal, and erosion in the Waal decreases downstream (hence slope will decrease). Figure 1 shows large variations in trends along the river. The smooth line is a representation to be used only for hydraulic impacts. The real complexity of erosion is for instance illustrated in Figure 2: the erosion in the upper Waal has only occurred in four inner bends. It is unknown how the fixed layers in outer bends at Erlecom and Nijmegen have contributed to this spatial variation.

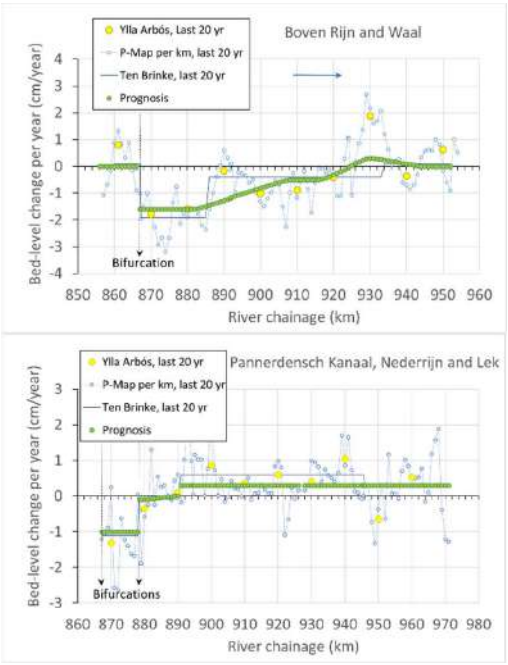

Figure 1. Prognosis for large-scale degradation (Sloff, 2019)

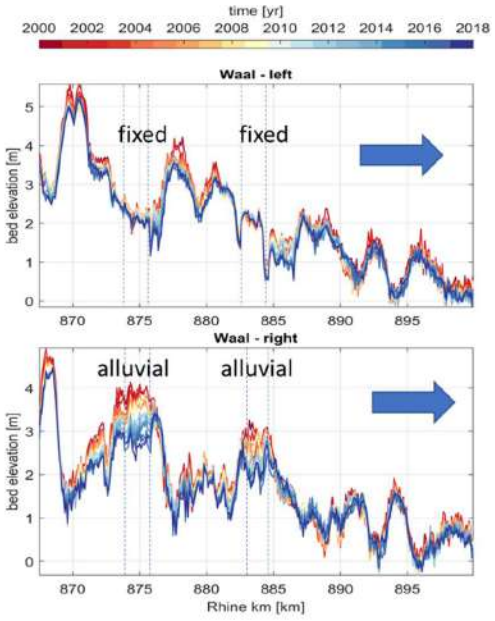

Figure 2. Erosion in alluvial inner bends in upper-part of the Waal. Dashed lines indicate the fixed layers

The 1D hydraulic simulations with adjusted bed show that the discharge to the Waal will have increased in 2050 with 20 to 30 m^3/s for the low flows and 40 to 120 m^3/s for high flows. See Figure 3. This is caused by the asymmetric development of branches downstream of the bifurcations. All scenario's show a significant reduction of water levels in the upper reaches, with several decimeters, maximal at low flows.

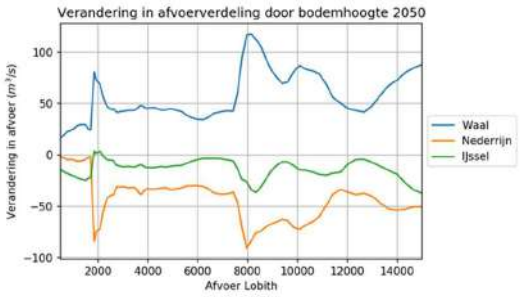

Figure 3. Change in discharge in 2050 compared to present

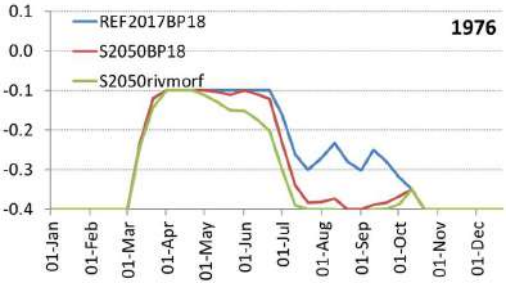

Figure 4. Computed level of IJsselmeer for dry year 1976, with reference scenario (REF2017BP18), climate change 'stoom' (S2050BP18) and climate change with bed-level degradation (S2050rivmorf), Source: Marjolein Mens

Figure 4 shows the impact on lake levels in Ijsselmeer for the extremely dry year 1976. The climate-change impact is dominant, but for return periods > 10 year the effect of bed-degradation becomes quite relevant.

Conclusions

Forecast of bed-level degradation shows that a shift in discharge distribution at bifurcations, and further decrease of water levels can be inferred. The computations show that impact on water availability in extreme dry years (T>10 year) is significant. There are still a lot of unknowns in the causes of bed degradation to make more accurate (model) predictions.

Acknowledgement

The study was carried out as part of KPP funding at Deltares. The hydraulic and water-availability analyses were carried out by Jurjen de Jong and Marjolein Mens, for which they are greatly acknowledged.

References

Brinke, W. ten (2019) Effecten morfologische ontwikkelingen op functies Rijn en Maas. Blueland Consultancy BV. Rapport B19.01, Okt. 2019.

Sloff, C.J. (2019) Prognose bodemligging Rijntakken 2020-2050. Deltares 11203738-005-8GS-0008. Dec. 2019.

Visser, P.J. (2000) Bodemontwikkeling Rijnsysteem. TU-Delft, Fac. CiTG, Oct. 2000.

Ylla Arbós, C., A. Blom, S. van Vuren, R.M.J. Schielen (2019) Bed level change in the upper Rhine Delta since 1926 and rough extrapolation to 2050. Delft University, Nov 2019.

Compensating human interventions at a river bifurcation

Matthijs R.A. Gensen[a*], Jord J. Warmink[a], Fredrik Huthoff[a,b], Suzanne J.M.H. Hulscher[a]
[a]*University of Twente, Department of Water Engineering and Management, Faculty of Engineering Technology, 7500AE Enschede, Netherlands*
[b]*HKV Consultants, 8203AC Lelystad, Netherlands*

Keywords — River intervention, River bifurcation, Discharge distribution, River engineering, Uncertainty analysis

Introduction

Human interventions in a bifurcating river system can disturb the discharge distribution at the river bifurcation. This causes unwanted water level increases in the branch which receives additional discharge. To avoid this, a set of compensating interventions can be designed such that they counteract each other's effect at the bifurcation. However, this may be challenging due to inherent uncertainties around discharges and hydraulic roughnesses. Therefore, in this study we assess the impact of compensating interventions on system-wide water levels considering a range of discharges and roughness conditions.

Methodology

An idealized 1D model is set up in the SOBEK environment with a schematization that is roughly based on the dimensions of the Dutch Rhine branches (Fig. 1). The branches have a uniform compound cross-section. The upstream boundary condition is a constant discharge ranging from 1000 to 18,000 m^3/s. The hydraulic roughness of the main channel and floodplain are set as stochastic, normally distributed variables with independent values for each of the branches.

Several configurations of the model schematization are used: 1 without any intervention and 3 with various combinations of compensating interventions implemented in the Waal and Pannerdensch Kanaal (Table 1). Interventions are either a dike set-back or a floodplain excavation, which are both typical 'Room for the River' type interventions. The compensating interventions are designed such that for a discharge of 16,000 m^3/s the effects of the interventions exactly offset each other at the bifurcation.

We run a quasi-random Monte Carlo Simulation to estimate the water level distributions for each model configuration and under each discharge condition. The effect of the intervention is quantified by subtracting the water levels in the non-intervened configuration from the water levels in the intervened configuration for each sample in the Monte Carlo Simulation. This results in a distribution of water level effects from which a mean effect and a 90% confidence interval of the effect is derived. We specifically look at downstream locations in the Waal and Nederrijn branch, where water level effects are fully determined by changes in the discharge distribution.

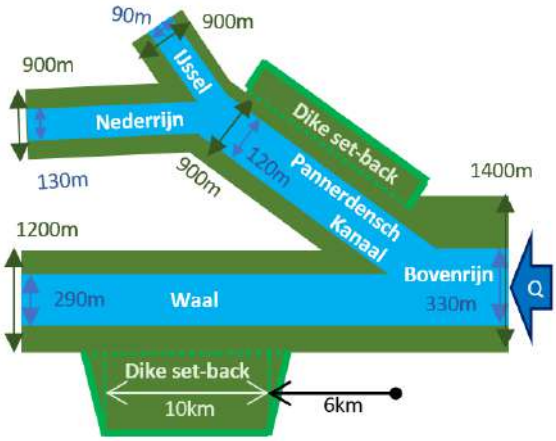

Figure 1. Model schematization, in the configuration in which two dike set-backs are implemented (see Table 1). The Waal, Nederrijn and IJssel are 93km, 107km and 113 km long, respectively.

Table 1. Model configurations, which include combinations of compensating interventions. Interventions types are a dike set-back (DS) and a floodplain excavation (FE)

Configuration	Waal intervention	Pannerdensch Kanaal intervention
No interventions	-	-
Compensation 1	500m DS	120m DS
Compensation 2	500m DS	0.39 FE
Compensation 3	1.46m FE	120m DS

Finally, we link the discharges to their corresponding return periods from GRADE (Prinsen et al., 2015). Then, for each configuration, we quantify design water levels with return periods of 100 years and 1250 years at downstream locations in the Waal and Nederrijn branch. This is done using Bayesian model averaging, whereby accounting explicitly for all discharge and roughness conditions.

* Corresponding author
Email address: m.r.a.gensen@utwente.nl (M.R.A. Gensen)
URL: https://people.utwente.nl/m.r.a.gensen (M.R.A. Gensen)

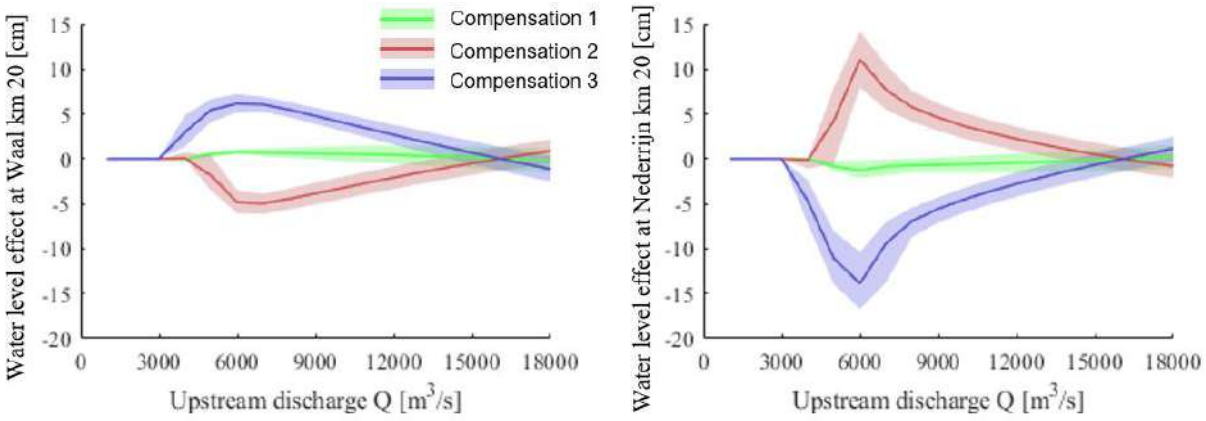

Figure 2: Effects on water levels at locations downstream of the interventions in the Waal (left) and Nederrijn (right) branch caused by the 3 variations of compensating interventions (see Table 1). The continuous line marks the mean effect and the shaded area marks the 90% confidence interval.

Results

Water level increases along downstream reaches in the system occur for various discharge conditions if the compensating interventions are not of the same type (Fig. 2). For moderately high discharges, a floodplain excavation is relatively more effective at reducing water levels than a dike set-back, therefore attracting additional discharge and increasing downstream water levels. Effects of the interventions on water levels along the smaller Nederrijn branch are higher in comparison to those along the Waal branch as Nederrijn water levels are more sensitive to discharge variations (Gensen et al., 2020). Consequently, the implementation of a floodplain excavation in the Pannerdensch Kanaal and a dike set-back in the Waal (i.e. compensation 2) leads to a significant increase in water levels in the Nederrijn for a discharge just over the bankfull level. Near perfect compensation is only achieved when two dike set-backs are used (i.e. compensation 1). Still, downstream water levels can be affected, even for the design condition of 16,000 m^3/s, because of uncertain roughness parameters.

Table 2 shows that the changes in water levels also impact design water levels (DWLs). These values are a good presentation for the changes further downstream along the branches. Interventions in the vicinity of the bifurcation point thus affect DWLs throughout the entire system. For both return periods, the DWLs are mainly affected by the water level changes at moderately high discharges. Thus, DWLs increase along the branch in which the floodplain excavation is implemented. Although the changes in DWLs seem small, Dutch regulations state that river interventions should not lead to water level increases of over 1mm under design conditions (Rijkswaterstaat, 2019).

Table 2. Changes in design water levels at locations downstream of the interventions in the Waal and Nederrijn (N.rijn) for return periods of 100 years and 1250 years.

	Change in design water level			
	100yrs		***1250yrs***	
Config.	$Waal_{km20}$	$N.rijn_{km20}$	$Waal_{km20}$	$N.rijn_{km20}$
Comp. 1	+0.4cm	–0.4cm	+0.2cm	–0.2cm
Comp. 2	–1.7cm	+1.7cm	–0.4cm	+0.4cm
Comp. 3	+2.2cm	–2.3cm	+0.6cm	–0.8cm

Conclusion

Compensating river interventions nearly always lead to unwanted water level increases along one of the downstream branches. This also impacts the design water levels. These negative effects can be minimized by implementing interventions of the same type. It is recommended to explicitly consider a range of discharge conditions and model uncertainties in the design of compensating interventions such that negative side-effects may be avoided.

Acknowledgements

This work is part of the Perspectief research programme All-Risk with project number P15-21, which is (partly) financed by NWO Domain Applied and Engineering Sciences, in collaboration with the following private and public partners: Rijkswaterstaat, Deltares, STOWA, HKV consultants, Natuurmonumenten and the regional water authorities Noorderzijlvest, Vechtstromen, it Fryske Gea, HHNK.

References

Gensen, M.R.A., Warmink, J.J., Huthoff, F., Hulscher, S.J.M.H. (2020) Feedback mechanism in bifurcating river systems: the effect on water-level sensitivity. Water 12(7), 1915.

Prinsen, G., Van den Boogaard, H., Hegnauer, M. (2015) Onzekerheidsanalyse hydraulica in GRADE. Deltares, Delft, Netherlands.

Rijkswaterstaat. (2019). Rivierkundig beoordelingskader voor ingrepen in de Grote Rivier

Impact of Weir Location on Discharge Partitioning in Longitudinal Training Walls

Matthew J. Czapiga[a,*], Astrid Blom[a], Enrica Viparelli[b]
[a] Delft University of Technology, Department of Hydraulic Engineering, Faculty of Civil Engineering and Geosciences, Delft, The Netherlands
[b] University of South Carolina, Department of Civil and Environmental Engineering, Columbia, South Carolina, USA

Keywords — Longitudinal Training Walls, Hydrodynamics

Introduction

A pilot project completed in 2015 replaced existing groynes with longitudinal training walls in the Dutch Waal River. The design seeks to mitigate river bed erosion and improve river function for navigation and ecology (*Havinga, et al.*, 2009). The change expanded the total flow width and separated the primary channel P_1 from three consecutive auxiliary channels A_1, A_2, and A_3 with longitudinal walls and fixed-elevation entrance side weirs. Figure 1a shows the field site spanning from Rhinekilometer (RK) 911 to 922, highlighting the location of channels, walls and entrance weirs. Water enters auxiliary channels via the weir at low flows and additionally via in-wall notches (broad-crested sections below the wall top), and wall over-topping at higher discharges.

This design seeks to increase low-flow depth and decrease both flood-flow depths and riverbed erosion in the primary channel. These factors relate to how discharge is partitioned between primary and auxiliary channels. Experimental results in a straight channel show that increasing discharge drives a larger proportion of flow into the auxiliary channel (*De Ruijsscher et al.*, 2019); a similar result is found at entrance A_3 in our field site (*De Ruijsscher et al.*, 2020). However, while discharge partitioning increases with depth over the weir at low flows, it is unaffected by weir design when the wall is inundated (*De Ruijsscher et al.*, 2019). We focus here on how discharge is partitioned to all three channels along a meandering river planform to determine how the position of the entrance weir affects discharge partitioning to auxiliary channels across a range of flow discharges.

Discharge Data

All weirs and walls were initially set relative to a reference water surface elevation, as to maintain equivalent relative elevations. In May 2018, weirs at A_1 and A_2 (Figure 1a) were raised by approximately 2 meters (*Sieben*, 2020). Discharge was measured at adjacent cross-sections along the primary channel and auxiliary channels over a range of flows from 632 m^3/s to 3482 m^3/s (approximately bankfull flow) during 2017 and 2018. The four largest discharge measurements (Q $\geq$ 1443 m^3/s) were collected before the weir change and the two lowest discharge measurements (Q $\leq$ 962 m^3/s) were collected after two weirs were raised. Flow in the auxiliary channel Q_A is normalized by the total discharge entering the domain Q_{tot} indicating the percentage of discharge shifted to auxiliary channels.

Results and Discussion

The discharge partitioning Q_A/Q_{tot} along the channel is plotted at six discrete total discharge values in Figure 1b. Line color shifts from red to blue as discharge increases and lines are segmented at the junction between walls. As total discharge increases, the percentage of flow shifted to auxiliary channel increases, but spatial trends vary among channels and at different discharge levels. The effect of weir height and position are entangled in our measurements at low-flow conditions, so this is omitted here.

At bankfull flow, all auxiliary channels convey about 25% of the total discharge on average (blue line in Figure 1b). However, the down-channel pattern in discharge varies among auxiliary channels and trends magnify as total discharge is increased. Channel A_2 gains discharge downstream, while A_3 loses discharge downstream, and A_1 shows a combination of these trends. Flows via the notches and wall over-topping, when active, tend to counterbalance weir flow as to maintain a common discharge value in all channels. As such, weir position does not affect the average discharge partitioning magnitude when the wall is over-topped, making the wall height a more relevant design parameter for these discharges.

These spatial patterns relate to how much flow can enter via the weir, so we consider the differences between weirs that leads to such opposite trends. Traditional factors controlling weir flow include the height, location, shape,

*Matthew J. Czapiga
Email address: M.J.Czapiga@tudelft.nl (Matthew J. Czapiga)

and length. Relative weir depth is not a factor, as the high-flow data was collected pre-2018 when relative weir submergence (versus a select reference profile) was equal in all channels. All weirs are broad-crested side weirs, while the weir to A_2 also bends to connect to the adjacent bank (Figure 1). Regardless, the weir is still parallel to flow due to deflection from an upstream ferry quay, suggesting shape difference is not significant. All weirs are approximately the same length. All channels lie along an inside bank, but A_3 is positioned just downstream of a curvature crossover and collects the most flow at all discharge levels (Figure 1b). Therefore, weir position is the only relevant variable to explain these trends.

Conclusions and Future Work

Our analysis of a field experiment illustrates that side weir position in meandering river planform affects how water enters into the auxiliary channels, but does not strongly affect the average magnitude of partitioned discharge when the wall is over-topped

The former result will be expanded in future work as it implies important morphodynamic consequences. The way water enters an auxiliary channel directly affects the grainsize, magnitude, and regime of sediment transport leaving the primary channel. Additionally, spatial patterns of erosion and sedimentation will vary depending on weir position, which can affect how engineers maintain these channels from common problems such as sedimentation.

Acknowledgments

This study is carried out as part of the Water2015 project 14508 "Long-term bed degradation in rivers: causes and mitigation", which is funded by the NWO Domain Applied and Engineering Sciences (AES, The Netherlands). There are no conflicts of interest.

References

De Ruijsscher, T. V., Hoitink, A. J. F., Naqshband, S., & Paarlberg, A. J. (2019). Bed morphodynamics at the intake of a side channel controlled by sill geometry. Advances in Water Resources, 134(February), 103452. https://doi.org/10.1016/j.advwatres.2019.103452

De Ruijsscher, T. V., Vermeulen, B., & Hoitink, A. J. F. (2020). Diversion of Flow and Sediment Toward a Side Channel Separated From a River by a Longitudinal Training Dam. Water Resources Research, 56(6). https://doi.org/10.1029/2019WR026750

Sieben, A. (2020). Overzicht afvoermetingen 2016-2019 project monitoring langsdammen, RWS–WVL, 7 February 2020.

Havinga, H., Schielen, R.M.J., & van Vuren, S. Tension between navigation, maintenace and safety calls for an integrated planning of flood protection measures River, Coastal and Estuarine Morphodynamics. RCEM2009, CRC Press (2009), pp. 137-143

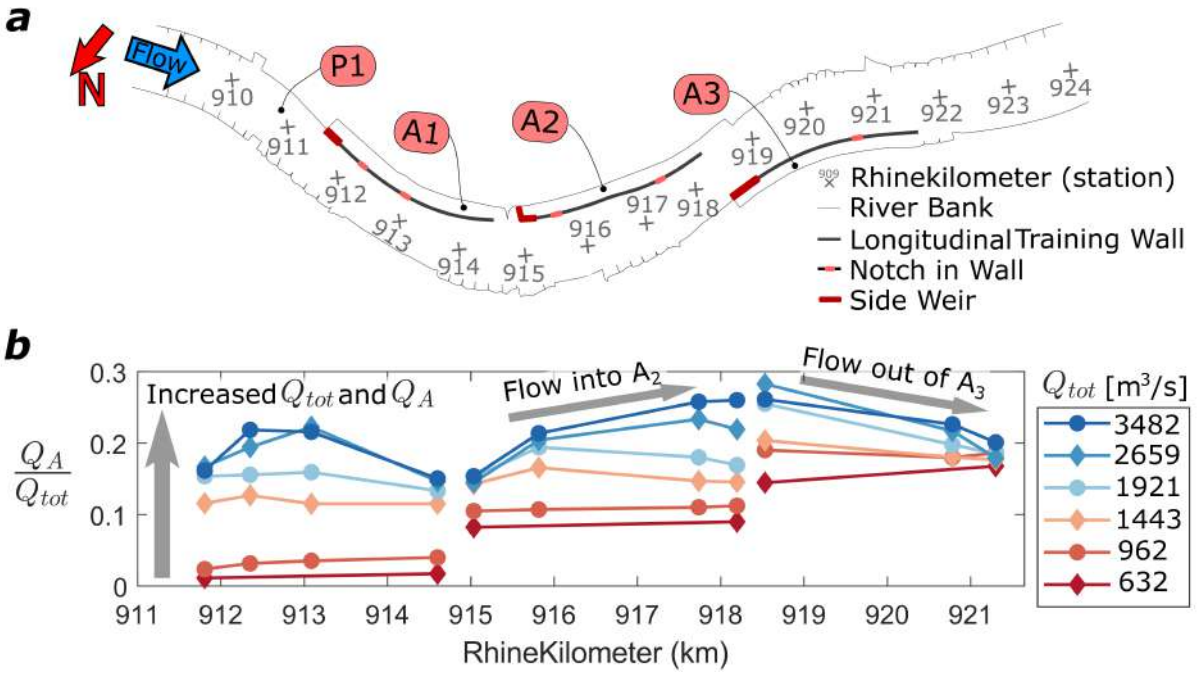

Figure 1: a) Plan view schematic of Longitudinal Training walls in the Waal River at Tiel, Netherlands. b) Proportion of measured discharge in the auxiliary channels Q_A relative to the total measured discharge upstream Q_{tot}.

Session 2B
Sediment management and measures

Morphological Impacts of Porcupine River Training Structures

Meghan Irving[a,*], Kees Sloff[a,b]
[a] TU Delft, Faculty of CEG, Building 23, Stevinweg 1, 2628 CN Delft, the Netherlands
[b] Deltares, P.O. Box 177, 2600 MH Delft, the Netherlands

Keywords — River Training, Porcupine, Morphology

Introduction

Flexible river training structures such as tetrahedron frames ('porcupines') can be attractive for control of braided river channel networks in regions where permanent control structures (e.g. groynes) are too expensive or potentially inefficient, such as areas with highly dynamic flow regimes and morphology. Porcupine fields (see Fig. 1) provide hydraulic resistance, generating energy loss through turbulence that may reduce velocities and promote sediment deposition (*Shang et al.*, 2013).

Porcupine systems can be used for bed or bank protection, and were implemented in a 2019 channel-control pilot project on the Ayeyarwady River in Myanmar. Incorporating porcupine resistance into numerical models has not been systematically evaluated. First, we must understand the processes that need to be captured for accurate predictions of impacts to flow and sediment transport, which is the focus of this work. Improved models can aid in future porcupine system design.

Figure 1: Porcupine field in secondary channel of Ayeyarwady River, Myanmar. Photo courtesy of H. Fredrikze, Royal HaskoningDHV.

Methods

Predicted impacts were examined using literature review and data from a 2018 porcupine flume experiment (*Nientker*, 2018), and then evaluated against pilot project observations. The pilot project was implemented in the Ayeyarwady River near Mandalay. In this location the river consists of a primary channel and four secondary channels (see Fig. 2).

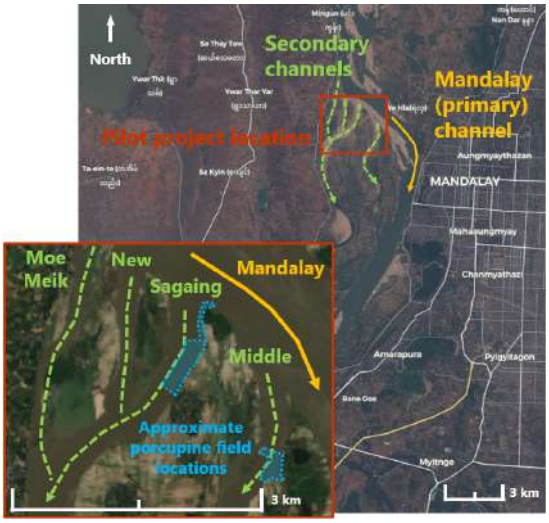

Figure 2: Ayeyarwady River pilot project location. Aerial imagery: Landsat 11/03/2020 (overview), 18/09/2020 (inset); (apps.sentinel-hub.com)

The main objective is to improve navigational stability by maintaining the current channel discharge distributions and hence a least available depth of 2 m in Mandalay channel. To encourage this, 2 m tall concrete porcupines were placed in a staggered configuration in secondary channels to increase local roughness (*Kreeke et al.*, 2018). Survey measurements were taken before and after the first wet season to examine morphological changes.

Results

Predicted Hydrodynamic and Morphological Impacts

The velocity and turbulence profiles through a field of resistance elements varies as density increases from 'sparse' to 'dense'. Dense fields generally reduce velocities and shear stresses inducing sedimentation. Sparse fields may experience erosion or deposition depending on the exact velocities and shear stresses. The leading, trailing and lateral field edges can have a different response than a central

*Corresponding author
Email address: meghan.irving@gmail.com (Meghan Irving)

(fully-developed) flow area for dense fields. Increased shear stresses and erosion may be observed at the leading or lateral edges, while deposition is likely in the center and trailing edge. This effect may be absent in sparse fields where edge velocity gradients are weak. In addition, channel placement dictates initial flow velocities in or along the field (e.g. higher velocities in an outer versus inner bend).

Pilot Study Observations

The pilot porcupines likely exhibit transitional or sparse behavior of the flow field, where significant scour at leading and lateral edges was not evident; however, porcupines located at the leading edge and especially in high-energy areas (e.g. outer bend) did show signs of scour and sinking into the bed (see Fig. 3). Porcupines were also partially buried through deposition, while largely maintaining their installation elevation.

Buried (shorter) porcupines offer less flow resistance and velocity reduction. Therefore upstream porcupines sinking can cause downstream porcupines to sink as they receive higher flow velocities. Loss of elevation may reduce the field's long-term effectiveness.

Fig. 3 also suggests that transverse resistance gradients from equi-height porcupines installed at varying cross-sectional elevations (generally higher at the inner bend) have helped push the flow (and thalweg) towards the outer bend.

Note that limited site data prevents us from entirely separating porcupine-induced changes from external influences.

Conclusion

Numerical modeling of porcupine systems must take into account changes in resistance due to porcupine burial over time, through sinking or deposition. They should accurately capture predicted behaviors according to field density including variations at leading and lateral edges to make informed design choices. In addition, estimating the strength of transverse gradients may be important if protecting the outer bend is a design goal. Further studies are needed to validate and expand these results for a wider range of field configurations and flow conditions.

Acknowledgements

This work was conducted as a Civil Engineering Masters thesis at TU Delft. Special thanks to my committee members A. Blom, J. Bricker and F. Schuurman, and to H. Fredrikze of Royal HaskoningDHV for providing the pilot data.

References

Shang, Q., Xu, H., Li, G. (2013) Overview of research on the influence of permeable structures. Applied Mechanics and Materials 405-408, pp. 2115–2122. issn: 16609336.

Nientker, G. (2018) Porcupines for river training: A study on the near-field effects of porcupines. Tech. rep. Delft University of Technology.

Kreeke, P. van de, Schuurman, F., Commandeur, A., Laboyrie, H., Kesteren, J. van, Nieuwenhuis, O. (2018) Report AIRBM - Component 3, Engineering, Design, Capacity Building and Construction Supervision for Sub-Project 1. Detailed Design Report.

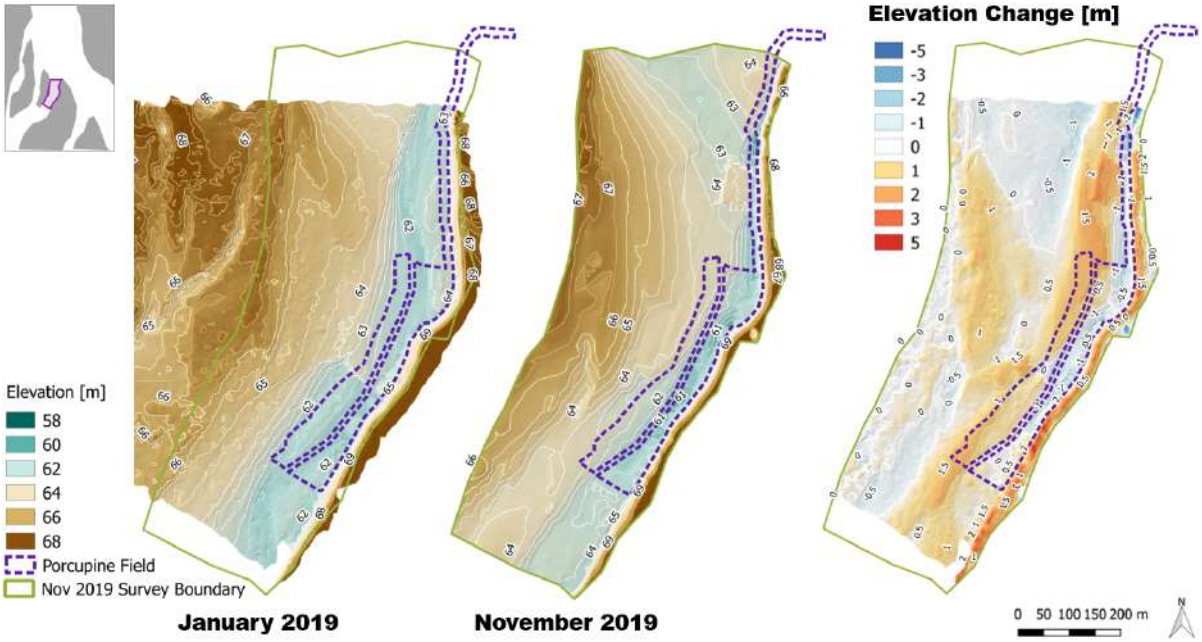

Figure 3: Morphological change in Sagaing Channel (November elevation minus January elevation).

Future sediment budget and distribution for the Rhine-Meuse delta

Jana R. Cox[a,*], Frances E. Dunn[a], Jaap H. Nienhuis[a], Marcel van der Perk[a], Maarten G. Kleinhans[a]
[a] *Faculty of Geosciences,Utrecht University, Utrecht, The Netherlands*

Keywords — Sediment budget, Dredging, Climate change

Introduction

Delta channels worldwide are undergoing natural and anthropogenic activities which change their sediment budget and sediment distribution. The Rhine-Meuse delta (see Figure 1 in the Netherlands has a negative sediment budget i.e. it annually looses sediment (Becker (2015); Frings et al. (2019); Cox et al. (submitted)). The primary cause of this loss is the extensive dredging undertaken in the RMD which maintains navigation to the network of offshore and inland ports which make up the Port of Rotterdam (Becker (2015); Cox et al. (submitted)). As sea levels rise and upstream sediment supply is predicted to decrease (Dunn et al. (2019)), knowledge of future sediment budgets and distribution is crucial to maintain delta elevation. Here we construct a sediment budget for two future scenarios 2050 and 2085 which incorporate both socio-economic change and climate scenarios for the region.

Constructing a sediment budget

To construct a budget for the region, we include the fluxes from the fluvial and coastal boundaries and the dredging Becker (2015):

$$SB = \Delta_{rivers} + \Delta_{coast} - \Delta_{dredging} \quad (1)$$

where SB is the calculated sediment budget (Mt/a), Δ_{rivers} is the flux of suspended sediment from the upstream rivers (Mt/a), Δ_{coast} is the flux of suspended sediment from the coast and $\Delta_{dredging}$ is the amount of dredged material removed from both the channels and ports of the RMD (Mt/a). Note that as the majority of sediment entering and distributed in the RMD is suspended sediment we neglect the bed load component from our budget. The upstream river flux is calculated using the BQART model (Dunn et al. (2019)) which incorporates future changes in the basin including future dam construction, land use change, socio-economic change and important climate factors (precipitation, temperature, glacier extent). At the coastal boundary, the predicted import of sediment due to changing sea level rise is calculated using a 1D model for the RMD.

Both the riverine and coastal fluxes incorporate the changes as indicated by the KNMI'14 climate predictions and scenarios of change for the RMD (KNMI (2015)). These scenarios give rates of sea level rise and predictions of upstream discharge for the RMD specifically. A dredging component is calculated by creating a simple forecast based on the last 30 years of dredging data for the region.

Partitioning and dispersal of sediment in the region and resulting bed level change was modelled by comparing the annual sediment loads of various measuring stations of suspended sediment in the system and using modelled discharge for the RMD from a SOBEK-RE model for normal conditions. We assume that suspended sediment follows discharge partitioning under normal flow conditions and resulting flow directions. This assumes wash load behaviour of the dominant suspended load term and for neglects nodal point relations for bed load partitioning. For future calculations we employ a linear relation between discharge (as predicted by the KNMI'14 scenarios) and suspended sediment, assuming discharge distribution and thus the resulting sediment distribution will remain the same over the bifurcations and confluences of the system in the future. We also incorporate overbank sedimentation at present and in the future in the Lek and Waal branches following from Middelkoop (2010).

A negative sediment budget

Regardless of climate scenario, the RMD will experience a negative budget in the future in both 2050 and 2085 (see Figure 2). Despite an increase in fluvial and coastal sediment supply, dredging completely overwhelms both these components. Moreover, the partitioning and dispersal of suspended sediment in the system will continue to be uneven. Most of the additional sediment will be deposited in the primary navigation channels: the Nieuwe Waterweg and Nieuwe Maas branches and this sediment will consequently be removed from the system entirely by dredging under current sediment management strategies. Meanwhile, the southern branches which contain several valuable ecological areas will not receive sufficient

*Corresponding author
Email address: j.r.cox@uu.nl (Jana R. Cox)

sediment to maintain their elevation in the face of sea level rise. The crosscut tidal channels will also have negative sediment budget which will exacerbate the current trends of bed erosion. The upstream rivers will have increased annual sediment flux which indicates that the Biesbosch wetlands should be supplied with sufficient sediment to maintain their elevation.

Implications for the RMD

A negative sediment budget comes with several management challenges for the RMD. The uneven distribution of sediment will lead to various issues:

1. The navigation channels will require more frequent and higher volumes of dredging to maintain their nautically guaranteed depth which will increase costs and will need to be considered.
2. The intertidal wetlands in the Haringvliet and Hollands Diep branches will receive insufficient sediment to maintain their elevation and thus will be under pressure to keep up with sea level rise.
3. Meanwhile in the cross cut tidal channels, insufficient sediment contributes to bed erosion, bank instability and increased flood risk

Future work & Acknowledgements

Further research will focus on testing the sensitivity of the suspended sediment fluxes to seasonal events. This research is a part of the research program Rivers2Morrow (2018-2023). Rivers2Morrow is focusing on the long-term development of the Dutch river system and its response to changing conditions such as river discharges, sea level rise and human interference. Universities, research institutes, NGOs, consultancy companies and government agencies that participate in this program are all working together on gaining knowledge in order to improve operations, maintenance and policies. Rivers2Morrow is financed by the Directorate-General for Water and Soil Affairs and Directorate-General for Public Works and Water Management (Rijkswaterstaat), both being a part of the Dutch Ministry of Infrastructure and Water Management. All measurement data was made available by Rijkswaterstaat and Port of Rotterdam. Our words of gratitude for collecting and sharing this data go out to technical staff of Rijkswaterstaat and Port of Rotterdam.

References

Becker, A, 2015. "Sediment in (be)weging".

Cox, J.R., Huismans, Y.H., Leuven, J.R.F.W, Vellinga, N.E., van der Vegt, M, Hoitink, A.F.J., Kleinhans, M.G., submitted. Anthropogenic effects on the contemporary sediment budget of the lower Rhine-Meuse Delta channel network.

Dunn, FE, Darby, SE, Nicholls, RJ, Cohen, S, Zarfl, C, Fekete, BM, 2019. Projections of declining fluvial sediment delivery to major deltas worldwide in response to climate change and anthropogenic stress. Environmental Research Letters 14 8 084034.

Frings, RM, Hillebrand, G, Gehres, N, Banhold, K, Schriever, S, Hoffmann, T, 2019, From source to mouth: Basin-scale morphodynamics of the Rhine River. Earth-Science Reviews 905-911.

KNMI, KNMI, 2015, '14-klimaatscenario's voor Nederland; Leidraad voor professionals in klimaatadaptatie De Bilt

Middelkoop, H, Erkens, G, van der Perk, M, 2010. The Rhine delta—a record of sediment trapping over time scales from millennia to decades. Journal of soils and sediments 10, 628–639. 4

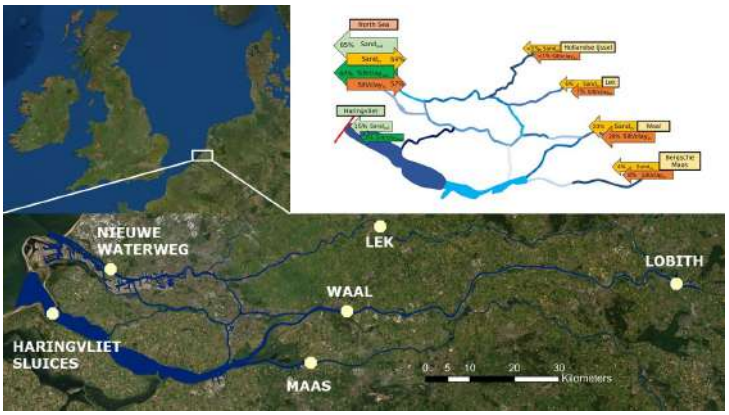

Figure 1: Map of the Rhine-Meuse delta, the relative sediment fluxes at the upstream and coastal boundaries and the location of the main suspended sediment measuring stations used in the study

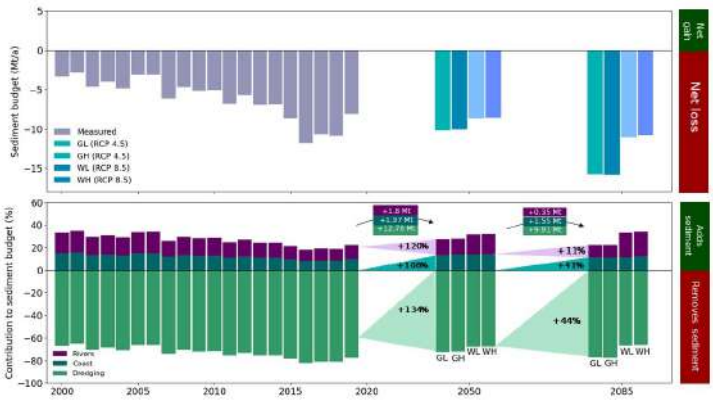

Figure 2: The predicted future sediment budget for the RMD under a range of scenarios (see KNMI (2015)) and the relative change of the river flux, coastal flux and dredging component of the budget through time.

Water injection for dredging sediment in reservoirs – insights from preliminary experiments

Patricia Buffon[a,b,*], Daniel Valero[a], Wim Uijttewaal[b], Mário Franca[a,b]
[a] IHE Delft, Water Resources and Ecosystems Department, P.O. Box 3015, 2601 DA, Delft, the Netherlands
[b] TU Delft, Department of Hydraulic Engineering, P.O. Box 5048, 2628 CN, Delft, the Netherlands

Keywords — Sediment dynamics, Turbidity currents, Sustainable infrastructure

Introduction

River dams have been largely implemented to store water for energy production, irrigation, flood control, and human and animal water supply; albeit some environmental implications. A negative consequence of damming rivers is the associated loss of connectivity. Several concerns can be raised in terms of sediment entrapment, among others: the continuous reduction of reservoirs' storage capacity, the altered morphodynamics and the impact on ecosystems of the river reach. Therefore, the ultimate goal of sediment management frameworks for river water reservoirs is granting sediment continuity through the dams. Nevertheless, choosing the most suitable strategy is complex, and a comprehensive knowledge about techniques and the environment is necessary to successfully achieve this goal.

This ongoing experimental research focuses on turbidity currents triggered by a water jet. The proposed experimental framework is an idealized conceptual model of Water Injection Dredging (WID), which can potentially be applied in water reservoirs as a sediment management technique. Other current sediment management techniques are described in *Annandale, Morris and Karki* (2016), and the history and application of WID is discussed by the World Association for Waterborne Transport Infrastructure (PIANC) in *PIANC Report nº 120* (2013).

Problem definition

Scouring may happen when injecting water into a partially compacted mobile bed. Particles can be suspended and finally transported downstream by a buoyancy-driven flow, which is commonly known as a turbidity current. Flow processes occurring during application of WID are presented in Figure 1.

In this study, these processes are spatially divided in water (i) injection, (ii) impact zone, (iii) near field, and (iv) far field. The inlet velocity of the water jet defines the initial input of energy that can trigger the aforementioned processes. The jet impact in the scouring hole will lead to a resuspension of sediment that may be conceptualised as the upstream boundary condition of the triggered turbidity currents (near field). These processes together will define the transport of mass, momentum, and turbulence into the far field. Ultimately, these will determine the feasibility of the technique in a specific site. An example of this modelling approach application is described in *Winterwerp et al* (2002). A set of preliminary experiments were performed to refine the experimental design, and are presented below.

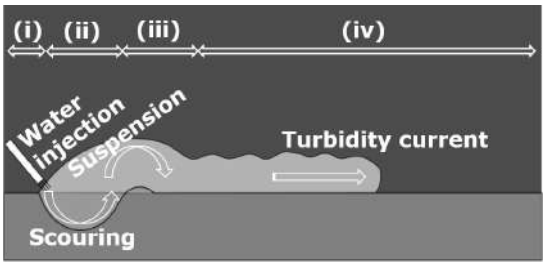

Figure 1: Sketch and problem definition. (i) injection, (ii) impact zone, (iii) near field, and (iv) far field.

Methodology

The experimental setup consisted of:

- A flume 4 m long, 2 m high, and 22 cm width equipped with a sediment damping tank;
- A 3D-printed diffuser device positioned at 45^o reproducing a 2D water jet, with the discharge recorded upstream by a flowmeter;
- A lighter-weighted sediment (D_{50} = 0.548 mm and ρ = 1243 kg/m^3) was used to build the mobile bed of – roughly horizontal – slope .

The flume before the beginning of the experiment, the diffuser, and sediment are shown in Figure 2.

*Corresponding author
Email address: p.buffon@tudelft.nl (Patricia Buffon)
URL: www.un-ihe.org/patricia-buffon (Patricia Buffon)

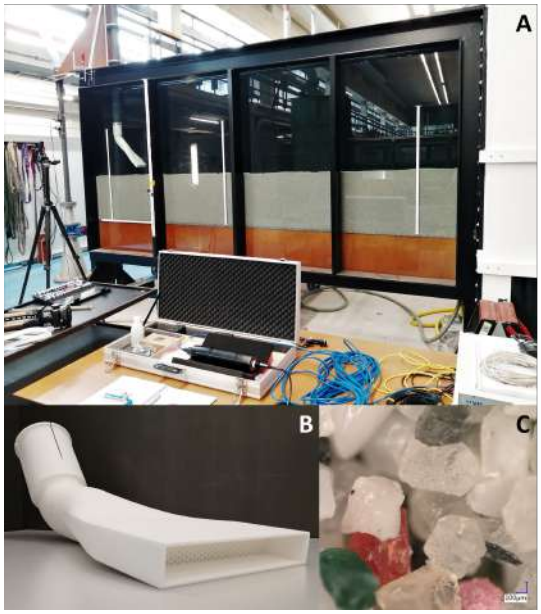

Figure 2: Experimental setup: (a), the 2D and 3D-printed water jet (b), and sediment (c).

Preliminary results

Three exploratory experiments are presented below (for a short video of these experiments, see *Buffon*, 2020).

- Experiment 1 (Figure 3a): in the first experiment, a pulse in the water discharge was released (approximately 9 l/s), triggering a non-desired situation in which a large quantity of sediment was abruptly suspended;
- Experiment 2 (Figure 3b): insufficient discharge was applied (approximately 2 l/s), also leading to a non-desired situation in which the sediment was suspended in a controlled way, but it was not efficiently transported in the downstream direction by the turbidity current;
- Experiment 3 (Figure 3c): in the third experiment, an intermediate discharge was achieved (approximately 4 l/s), triggering the desired situation that will be further investigated. In this case a cloud of sediment was suspended, and plunged in a turbidity current that transported sediment in the downstream direction.

Future work

Adaptations have been conducted in the flume, and a series of new experiments (similar to Figure 3c) will follow, attempting to quantify key hydrodynamic processes and optimum conditions to apply the technique.

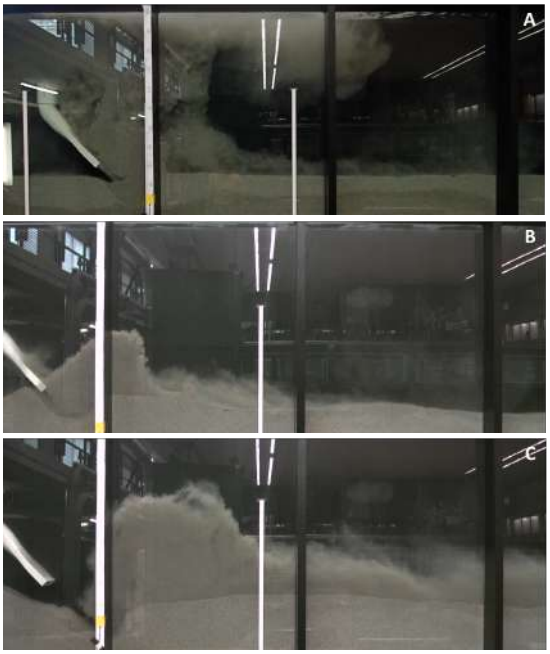

Figure 3: Set of preliminary experiments: (a) Experiment 1 - peak of discharge; (b) Experiment 2 - low discharge; (c) Experiment 3 - intermediate discharge.

Acknowledgements

The first author acknowledges CAPES (Coordenação de Aperfeiçoamento de Pessoal de Nível Superior, a Foundation within the Ministry of Education in Brazil) for funding her Ph.D. Program (grant number 88881.174820/2018-01), the Hydraulic Engineering laboratory of TU Delft, and the River Basin Development chair group of IHE Delft for providing additional resources to develop the experimental work.

References

Annandale, George W.; Morris, Gregory L.; and Karki, Pravin. 2016. Extending the Life of Reservoirs: Sustainable Sediment Management for Dams and Run-of-River Hydropower. Directions in Development. Washington, DC: World Bank. doi: 10.1596/978-1-4648-0838-8

Buffon, Patricia. 2020. Turbidity currents triggered by a water jet. Available at: https://www.youtube.com/watch?v=UeIzG7p43uU. Last access: 07/01/2021

Winterwerp, J. C.; Wang, Z. B.; van Kester, J. A. Th. M. and Verweij, J. F. 2002. Far-field impact of water injection dredging in the Crouch River. Proceedings of the Institution of Civil Engineers - Water and Maritime Engineering 2002 154:4, 285-296. doi.org/10.1680/wame.2002.154.4.285

World Association for Waterborne Transport Infrastructure (PIANC), Report n° 120, Maritime Navigation Commission. 2013. Injection Dredging. Bruxelles, BE: PIANC Secrétariat Général. ISBN: 978-2-87223-205-5

Insight into the local bed-level dynamics to assist management of multi-functional rivers

R. Pepijn van Denderen[a*], Andries J. Paarlberg[b], Denie C.M. Augustijn[a] and Ralph M.J. Schielen[c,d]
[a] *Faculty of Engineering Technology, University of Twente*
[b] *HKV Consultants*
[c] *Ministry of Infrastructure and Water Management-Rijkswaterstaat*
[d] *Faculty of Civil Engineering and Geosciences, Delft University of Technology*
Keywords — River morphology, bed level dynamics

Introduction

River discharge fluctuations cause bed-level variations at various scales, resulting from spatial gradients in the river's geometry (Bolla Pittaluga et al., 2014), local interventions (Paarlberg et al., 2020) or backwater effects (Arkesteijn et al, 2019). These bed-level variations can affect river functions such as navigation. Insight into these bed-level variations and their relation to discharge fluctuations can help to predict and prevent the formation of local bottlenecks. In this paper, we use bi-weekly bed-level measurements of the river Waal to estimate the bed-level variations related to the river discharge, assuming that the river planform remains constant. We apply a wavelet transform to disentangle the relevant spatial scales from the measurements.

Method

The bed level in the navigation channel of the river Waal is measured bi-weekly from 2005 using multi-beam echo sounders. We average the bed level over the width of the navigation channel to estimate the bed-level variations over the river's longitudinal profile. After 2014, bed-level variations in the Waal are strongly affected by various 'Room for the River' interventions. Therefore, we focus on bed-level variations between 2005 and 2014 relative to the time-averaged bed level over this period.

Bed-level changes occur over various spatial scales. Large-scale (>4 km) changes are related to the long-term trends, i.e. bed degradation. Small-scale (<320 m) changes are related to dune-like bedforms and groynes. We apply a wavelet transform to isolate the bed-level variations over an intermediate (320 m–4 km) spatial scale. These variations are affected by a single discharge event.

We classify each bed-level measurement according to the maximum discharge between the measurement and the previous measurement using eight characteristic discharge categories (Paarlberg et al., 2020). The categories are chosen such that bankfull discharge (2,900 m^3/s), 2-year peak flow (4,000 m^3/s), and a 5-year peak flow (5,300 m^3/s) each fall into a different category. For each category, we will show the average deviation from the time-averaged bed-level profile.

Results

We present the bed-level variation as a function of the discharge for a segment in the lower part of the river Waal (rkm 933-940). Fig. 1A shows the time-averaged bed level and the time-averaged bed level after low and high discharge. The bed-level variation range is about 0.5 m and the largest deviation from the time-averaged profile occurs after high discharges. Fig. 1B shows the bed-level variation around the time-averaged bed level for the eight considered discharge categories. The red colour means that the bed level is higher than the time-averaged profile and blue means that the bed level is lower. Where deposition occurs during high discharges, scour occurs during low discharges and vice versa. These bed-level variations can, for example, result from fixed spatial gradients in the river's geometry. Just upstream of rkm 937, the right floodplain narrows, which means that at high discharge the fraction of the discharge conveyed by the main channel increases. This locally increases the sediment transport capacity and thereby causes local scour. The opposite occurs just downstream, where the floodplain widens. These gradients in sediment transport capacity only occur during high flow conditions, when the discharge is above bankfull and the floodplains convey water. During low flow conditions, the scour hole is filled and the sediment deposited at high flows is eroded.

We compare our results with so-called MGD (=Least Available Depth) locations to determine whether the local aggradation results in navigation bottlenecks. An MGD corresponds with the lowest navigable depth in a river trajectory. Fig. 1C shows three peaks at rkm 936, 936.6 and 937.4, where between 2005 and

* Corresponding author
Email address: r.p.vandenderen@utwente.nl (Pepijn van Denderen)

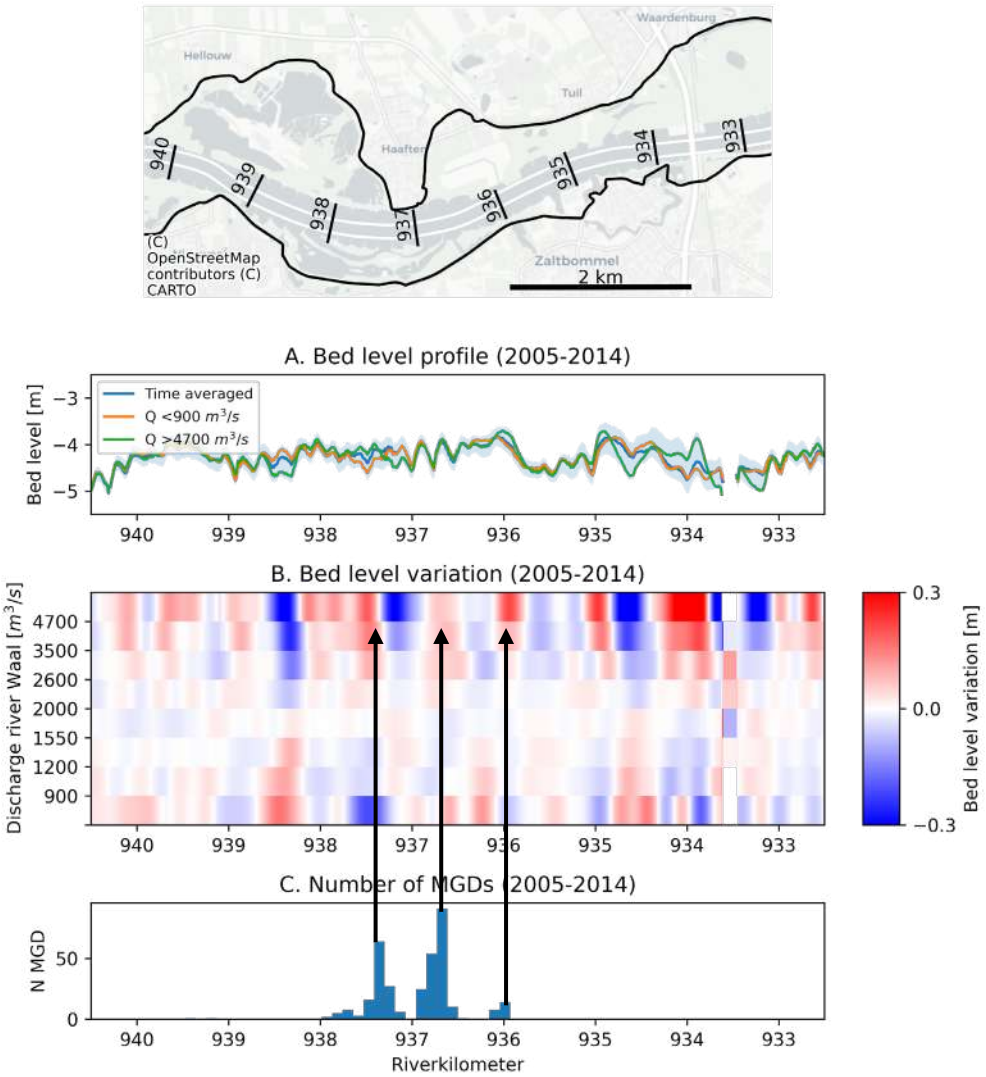

Figure 1. Considered river segment in the downstream part of the river Waal. (A) The time-averaged bed level, the average bed level during low and high discharges (filtered for wavelengths between 320 m and 4 km. The blue background gives the total range of the bed level between 2005 and 2014. (B) The bed-level variations around the time-averaged bed level for eight discharge categories. (C) The number of MGDs (Least Available Depth) in this segment, which shows where shipping bottlenecks occur.

2019 MGD occurred regularly. These peaks correspond with locations where, during high discharges, aggradation occurs. Note that we do not consider the migration of bed features such as bedforms, since we only include bed-level variations that occur over 320 m–4 km. These migrating features often determine the exact location of the MGDs.

Discussion

Insight into bed-level variations as a function of discharge fluctuations helps river managers to understand the river's dynamic behaviour. This can be used to determine the optimal type and location of river interventions such that existing bottlenecks disappear and new local bottlenecks are prevented. Fig. 1B can be used to optimize the location of, for example, a side channel. At the confluence of the side channel, scour is expected during peak flow and this scour could mitigate the deposition at rkm 934.

Here, we focus on a specific spatial scale (320 m–4 km) using a wavelet transform. This method can be used to distinguish between the spatial scales of bed-level changes. In rivers with less-frequent bed-level measurements, it is more difficult to relate these changes to the discharge. However, with fewer discharge categories a similar analysis could still be valuable in determining the trends and range of the river bed level dynamics.

References

Arkesteijn, L., A. Blom, M.J. Czapiga, V. Chavarrías, R.J. Labeur, 2019: The Quasi-Equilibrium Longitudinal Profile in Backwater Reaches of the Engineered Alluvial River: A Space-Marching Method. Journal of Geophysical Research: Earth Surface, 124, 2542-2560.

Bolla Pittaluga, M., R. Luchi, G. Seminara, 2014: On the equilibrium profile of river beds. Journal of Geophysical Research: Earth Surface, 119, 317-332.

Paarlberg, A., P. van Denderen, R. Schielen, D. Augustijn, 2020. Rivierbodemdynamiek meenemen in het ontwerp van maatregelen. Land + Water, 60(10), 30-31.

Session 3A
Small-scale river dynamics

The evolution of primary dunes during low flows on the Waal river

Lieke R. Lokin [a,b*], Jord J. Warmink [a], Anouk Bomers[a], Suzanne J.M.H. Hulscher[a]
[a]*University of Twente, Department Water Engineering and Management, Faculty of Engineering Technology, P.O. Box 217, 7500 AE, Enschede, The Netherlands*
[b]*HKV Consultants, Botter 29-11, 8232 JN, Lelystad, The Netherlands*

Keywords — River dunes, Wavelet analysis, Low flows, Dune height

Introduction

During low and extreme low flows in navigable rivers, dynamic bed forms such as river dunes influence the navigable depth. During extreme low flow, shippers depend on depth predictions to determine their maximum draft, and therefore the maximum load they can transport. Due to climate change extreme low flows are likely to occur more often in the future. Therefore, knowledge of dune evolution is key to model and predict water depths.

Most studies concerning river dunes focus on dune evolution during high flows for flood level predictions (eg. Wilbers and Ten Brinke, 2003), or dune shape statistics at specific moments in specific moments in time (eg. Cisneros et al., 2020). Also, most of the studies on river dunes are based on laboratory data. However, scaling of dunes from lab conditions to real rivers, gives inconsistencies in lee slope angles and the presence of higher order dunes. Therefore, knowledge of dune evolution in full scale rivers during low flows is lacking, while this is an important factor in determining minimum water depth.

Method

In this study, we investigate the dune evolution in a stretch of 2 km Waal river, the Netherlands, between the cities of Tiel and St. Andries, focussing on the low water period of 2018. The bed elevation profiles are based on Multibeam Echo Sounding (MBES) measurements of the fairway, measured on average once per two weeks. As we are interested in the dynamic part of the bed, the mean bed over the period 2017-2020 was determined and subtracted from the bed profiles of the individual measurements. Fig 1. shows the mean bed for this period at the study location.

The resulting bed profiles only contain the dynamic part of the bed, which are the dunes, higher order dunes and ripples. From these profiles the dune evolution has been studied, first based on a qualitative approach, then on a quantitative approach using wavelet analysis (Torrence and Compo, 1998).

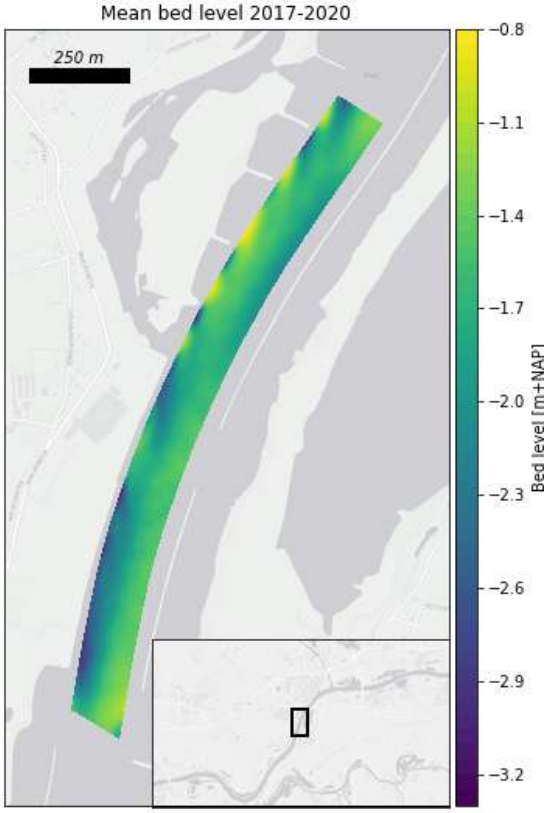

Figure 1. Mean bed level between 2017 and 2020 at the study location.

Based on the outcomes of the wavelet analysis, the signal of only the primary dunes was reconstructed. Next, the locations of the crests and troughs in the original signal were determined: these are needed to determine the dune heights. These, dune heights were then compared with the discharges, to derive a relation between these parameters.

Results

Fig 2. shows the evolution of the dune profiles in time in the middle of the fairway, combined with the discharges at Lobith (Rhine river) and at Tiel (Waal river) from April until December 2018. Fig 3. shows the dune height related to this discharge. The showed period can be divided in two discharge regimes. First the discharge between April and June with a value varying between 2000 and 3000 m^3/s at Lobith,

* Corresponding author
Email address: l.r.lokin@utwente.nl (L.R. Lokin)
URL: https://people.utwente.nl/l.r.lokin (L.R. Lokin)

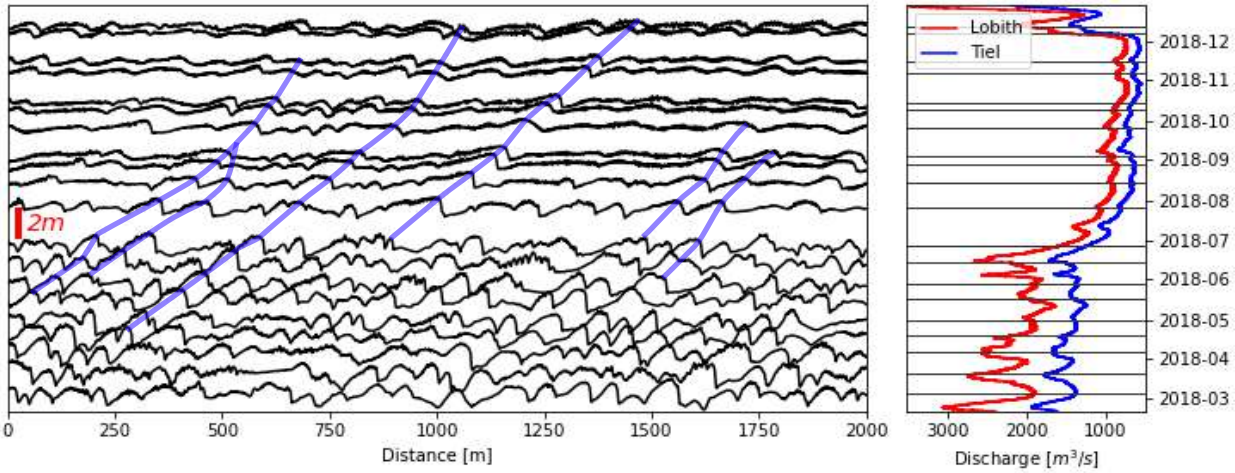

Figure 2. Left) Dune evolution from April until December 2018 in the middle of the fairway, each line represents one measurement. The length of the red bar indicates 2 m in the dune profile heights, blue lines indicate the propagation of the crests. Right) Discharge in the Rhine at Lobith (red line) and in the Waal at Tiel (blue line), the horizontal lines indicate the dates of the measurements. Discharge data: (www.waterinfo.nl)

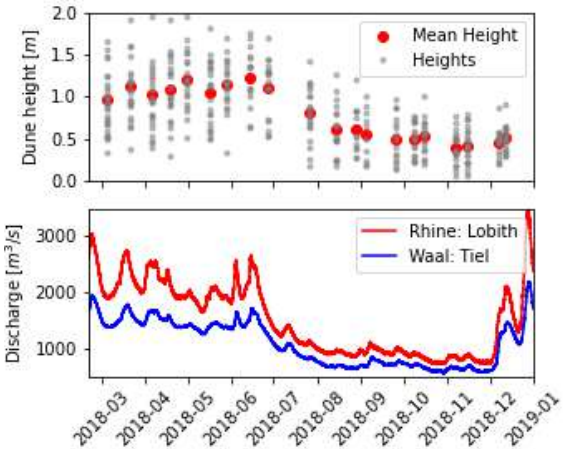

Figure 3. Top) The mean dune heights (red dots) with all found dune heights for each measured profile in the middle of the fairway. For the same dune profiles as shown in Fig 2. Bottom) Discharges of the Rhine and Waal.

which is around the median discharge for the Rhine river. Secondly, the discharge between July and December where the discharge varies between 800 and 1000 m^3/s at Lobith, which is extremely low. These two discharge regimes already show different dune evolution.

In the quantitative analysis, Fig 3., differences in dune height between the median and low discharge periods stand out. During the median flow, dune height varies around 1.1 m and the low flow results in dune heights around 0.6 m. In the transition from median flow towards low flow, the height adapts relatively fast to the new changed discharge.

These results can also be seen in the dune profiles in Fig 2: during the low discharges, the dunes are longer and slightly lower than during the period with the median discharge. During low flows dunes are still migrating, blue lines in Fig 2. These lines follow the dune crests during the low water period. While the dunes migrate, their shape is relatively constant compared to the median discharge period.

Here only the results for one line in the central part of the fairway are shown. However, this analysis can also be performed at any location in the cross-section of the river.

Preliminary conclusions and lookout

From these first results we conclude that during a period of low flow in the Waal river, dunes are mobile. The dune height decreases and eventually becomes relatively stable during the period of low discharge.

In the next phase of this research the method to determine the location, height and length of the primary dunes will be further developed. Also, a quantitative analysis of the dune lee slope will be related to the discharge. Future work will also include the spatial variety in streamwise direction and over the cross-section, to develop a relation between dune shape and flow characteristics.

Acknowledgements

This research is a part of the research program Rivers2Morrow (2018-2023). Rivers2Morrow is financed by the Dutch Ministry of Infrastructure and Water Management. All measurement data was made available by Rijkswaterstaat. Our words of gratitude for collecting and sharing this data go out to technical staff of Rijkswaterstaat.

References

Cisneros, J., Best, J., van Dijk, T., et al. (2020). Dunes in the world's big rivers are characterized by low-angle lee-side slopes and a complex shape. Nature Geoscience, 13(2), 156–162. https://doi.org/10.1038/S41561-019-0511-7

Torrence, C., & Compo, G. P. (1998). A Practical Guide to Wavelet Analysis. In Bulletin of the American Meteorological Society (Vol. 79, Issue 1). American Meteorological Society. https://doi.org/10.1175/1520-0477(1998)079

Wilbers, A. W. E., & Ten Brinke, W. B. M. (2003). The response of subaqueous dunes to floods in sand and gravel bed reaches of the Dutch Rhine. Sedimentology, 50(6), 1013–1034. https://doi.org/10.1046/j.1365-3091.2003.00585.x

Quantifying hydraulic roughness from field data: can bed morphology tell the whole story?

S.I. de Lange[a*], Suleyman Naqshband, Ton Hoitink
[a] *Wageningen University, Department of Environmental Sciences, Hydrology and Quantitative Water Management, Wageningen, the Netherlands*

Keywords — river dunes, hydraulic roughness, field data

Introduction

Bedforms are thought to be a major cause of hydraulic roughness in channels. The geometry of the river bed, shaped by bars, dunes, and ripples, and the spatial and temporal distribution of these, influence the resulting roughness variations. Roughness is a fundamental parameter for understanding river flow behaviour by influencing sediment transport and water level.

Quantification of roughness is challenging since it is not directly measurable in the field. It is therefore inferred from hydrological characteristics, -including water depth, water surface slope, flow velocity, discharge-, as well as morphological characteristics, -such as bedform height-, or derived from calibration of a hydraulic model.

In this research, we will use an extensive dataset from a well-researched simple river system, with dune covered bed, unimodal grainsize distribution and an unidirectional flow: river Waal, the Netherlands (Fig. 1). Three methods will be explored, to quantify the spatial distribution of hydraulic roughness in the field. A We aim to state the importance of bed morphology for hydraulic roughness and we pursue the auxiliary aim to explore the spatial distribution of bedforms and roughness in our case study area river Waal, the Netherlands.

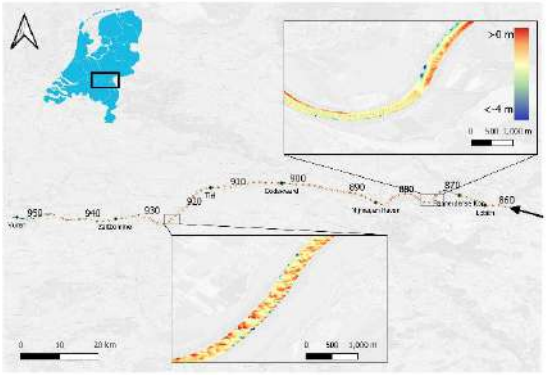

Figure 1. Study area.

Methods (Fig. 2)

Method 1 uses the St. Vernant equations (equation 1) (better known as the Chezy equations) to quantify roughness (f), with as input among others flow velocity, bed slope and water surface slope. This value is seen as the 'true' roughness of the river system.

$$C = \frac{u}{d(S0 - Sp - \frac{dQu}{dx} * \frac{1}{A\,g})} \qquad (1)$$

With u = flow velocity (m/s), d = width averaged river depth (m), S0 = bed slope (-), Sp = pressure slope (-), Q = discharge (m^3/s), x = along river distance (m), A = cross-sectional area (m^2) and g = gravitational constant.

Method 2 is a traditionally often used method (e.g. Bartholdy et al., 2010; Lefebvre & Winter, 2016; Soulsby, 1997; van Rijn, 1984), where form roughness (f_{dune}) is obtained from dune characteristics such as height and length via empirical predictors. Together with skin roughness (f_{grain}) this is believed to be equal to the hydraulic roughness (van Rijn, 1984).

Method 3 makes use of characteristics of the bed itself, not strictly related to 2D bedform geometry, specifically the inclination of the streamwise local elevation profile, i.e. leeside grid angle (γ(°)). Doing so eliminates the necessity of defining dune characteristics, and therefore taking one, often arbitrary, step out of the procedure to quantify roughness.

* Corresponding author
Email address: sjoukje.delange@wur.nl, S.I. de Lange

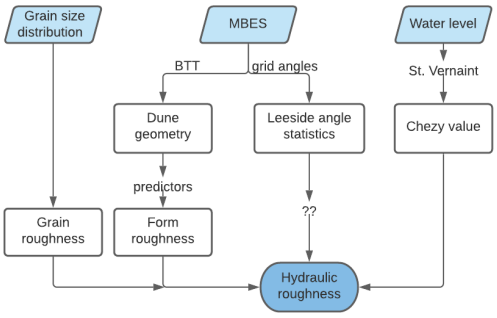

Figure 2. Summary of methodology.

Results

The three methodologies show the same general trend and order of magnitude of roughness (C=30-70 $m^{0.5}/s$, mean 42 $m^{0.5}/s$) however kilometer-scale variations show contrasting patterns (Fig. 3). Nor dune geometry neither leeside grid angle manage to fully explain the variations in the roughness as obtain from the st. Vernant equations. From this we conclude that bed morphology does not seem to be the only explaining factor for roughness variations.

Discussion and look-out

Possible explanations include the low leeside angle of dunes (mean <10°), the influence of man-made structures such as groynes and longitudinal training dams, the influence of fixed gravel layers in sharp bends, river curvature, and cross-sectional variation in river depth (bars) and flow velocity.

This study contributes to the elucidation of factors influencing hydraulic roughness, and its quantification from field data. Proper quantification of roughness and its spatiotemporal behavior will increase our knowledge in river behavior and will lead to improvement of river management strategies and operational models.

Acknowledgements

This research was funded by the Netherlands Organisation for Scientific Research (NWO), within Vici project “Deltas out of shape: regime changes of sediment dynamics in tide-influenced deltas” (Grant NWO-TTW 17062).

We would like to thank Rijkswaterstaat, the Dutch Ministry for Infrastructure and Environment, for providing the data. Furthermore Arjan Sieben and Denes Beyer from Rijkwaterstaat provided helpful feedback on the data analysis and interpretation.

References

Bartholdy, J., Flemming, B. W., Ernstsen, V. B., Winter, C., & Bartholomä, A. (2010). Hydraulic roughness over simple subaqueous dunes. *Geo-Marine Letters*, *30*(1), 63–76. https://doi.org/10.1007/s00367-009-0153-7

Lefebvre, A., & Winter, C. (2016). Predicting bed form roughness: the influence of lee side angle. *Geo-Marine Letters*, *36*(2), 121–133. https://doi.org/10.1007/s00367-016-0436-8

Soulsby, R. (1997). *Dynamics of marine sands*. London, Thomas Telford, 249p.

van Rijn, L. C. (1984). Sediment transport, part III: Bedforms. *Journal of Hydraulic Engineering*, *110*(12), 1733–1754.

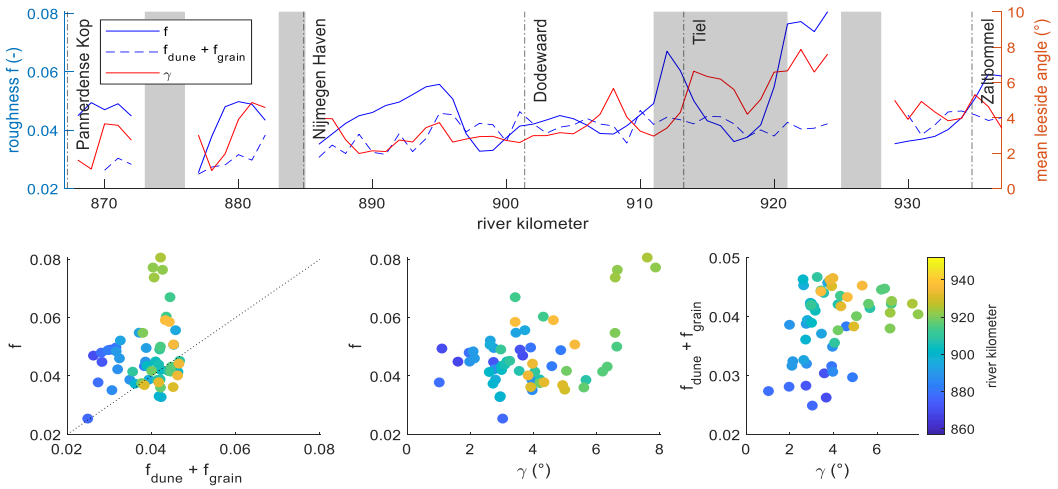

Figure 3. A. Hydraulic roughness over distance from field data, quantified with the St. Vernant equations (f), emphirical dune predictor (f_{dune}) and skin friction equation (f_{grain}) (van Rijn, 1984) and the leeside grid angle (γ). Grey blocks indicate fixed layers in the river bed, or other man-made structures such as Longitudinal Training Dams at Tiel. B, C, D) relation between the three methods.

Sand-bed river response to drier and wetter climate: the case of Pilcomayo

Alessandra Crosato[a], Francesco Bregoli[b*], Alberto Grissetti-Vázquez[a], Mário J. Franca [a],
[a] *IHE Delft Institute for Water Education, Delft, the Netherlands*
[b] *Department of Environmental Science, Radboud University Nijmegen, Nijmegen, the Netherlands*

Keywords —alluvial rivers, climate change, river morphodynamics

Introduction

Climate changes alter precipitation and river discharge which have direct effects on rivers morphology and their riparian and floodplains vegetation (Gurnell 2014; Vargas-Luna et al. 2019). The morphodynamic response of rivers to climate change is complex and the triggered effects of non-linear interactions between altered water, sediment fluxes and vegetation remain incompletely understood. We investigate here the cross-sectional response of sand-bed rivers to drier and wetter climate focusing on river width and depth adaptation.

Method

The Pilcomayo River flows for 1,100 km from the Bolivian side of the Andes through Paraguay and Argentina before entering the Parana River (Fig. 1). At the border between Argentina and Paraguay, the river presents an extremely dynamic behaviour, due to its strongly variable discharge and bed made of fine sand. Exceptional long time-series of daily discharge and bed topography measurements (Martín-Vide et al. 2014, 2019) make this river the perfect living lab for this investigation.

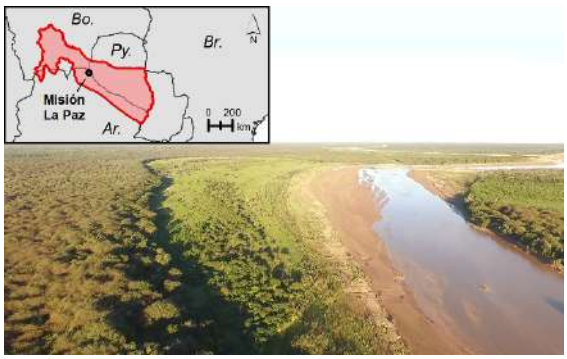

Figure 1. The Pilcomayo River in the study area: the upper left panel shows the geographical context of the basin (in red shade) and the background photo shows the river at dry condition close to Misión La Paz looking downstream (photo taken in June 2017, Courtesy of Kenny Goossen).

We constructed a two-dimensional model of the river using the open-source Delft3D code (oss.deltares.nl/web/delft3d). The fast dynamics of the Pilcomayo and its uniform sediment, allowed to considerably speed up of the computations. Calibration and validation were performed against historical measured data (1960-2018) of daily discharges, water levels and cross-sectional profiles available at a bridge location in Misión la Paz, Argentina, from The National Hydrological Network of Argentina. The distribution of floodplain vegetation was derived from satellite images. Vegetation characteristics were derived by simple observations.

We used the model to simulate plausible climate scenarios representing present (BC scenario), dryer (Dry scenario) and wetter (Wet scenario) situations reflected in discharge and vegetation alterations. The Dry scenario is based on the forecasts for the study area showing decreasing precipitation and increasing temperature. Sperna Weiland et al. (2012) estimated a 25% discharge reduction in December, January and February, a 30% reduction in March to August and a 20% reduction in September to November for the SRES A1B climate change scenario for the year 2100 (Stocker et al. 2013). We considered also a wetter climate, presenting the same percentages of discharge variations of the projected scenario, but in the opposite direction.

Results

Calibration and validation show remarkable results for selected time periods (Fig.2).

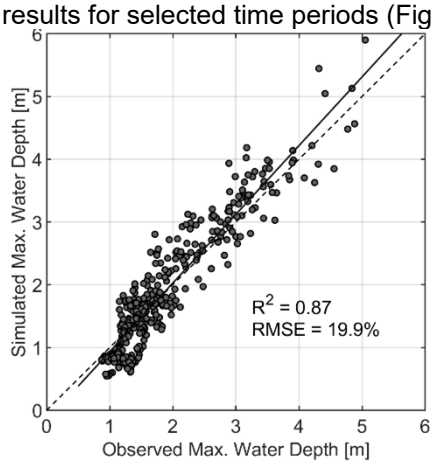

Figure 2. Results of model calibration: observed vs. simulated maximum water depth at Mision la Paz for the period 1st September 1972 to 1st September 1973 (RMSE is the root mean square error).

The calibrated model was then validated on an independent dataset, with good results. The outcome of the application of climate scenarios show that a dryer climate will reduce the river

channel width and depth, while a wetter climate will increase the channel depth, but produce negligible widening. Vegetation, which will be sparser with a drier climate and denser with a wetter climate, plays a major role on the channel width modifications (Fig. 3).

Conclusions

The analysis of the results permitted to unveil which alterations can be expected in alluvial sand-bed rivers with natural vegetated banks under climate change scenarios. Moreover, the presented method can guide further investigation on different river systems response to climate change forcing.

References

Gurnell A (2014) Plants as river system engineers. Earth Surf Process Landforms 39:4–25. https://doi.org/10.1002/esp.3397

Martín-Vide JP, Amarilla M, Zárate FJ (2014) Collapse of the Pilcomayo River. Geomorphology. https://doi.org/10.1016/j.geomorph.2012.12.007

Martín-Vide JP, Capape S, Ferrer-Boix C (2019) Transient scour and fill. The case of the Pilcomayo River. J Hydrol. https://doi.org/10.1016/j.jhydrol.2019.06.041

Sperna Weiland FC, Van Beek LPH, Kwadijk JCJ, Bierkens MFP (2012) Global patterns of change in discharge regimes for 2100. Hydrol Earth Syst Sci. https://doi.org/10.5194/hess-16-1047-2012

Stocker TF, Qin D, Plattner GK, et al (2013) Climate change 2013 the physical science basis: Working Group I contribution to the fifth assessment report of the intergovernmental panel on climate change

Vargas-Luna A, Duró G, Crosato A, Uijttewaal W (2019) Morphological Adaptation of River Channels to Vegetation Establishment: A Laboratory Study. J Geophys Res Earth Surf. https://doi.org/10.1029/2018jf004878

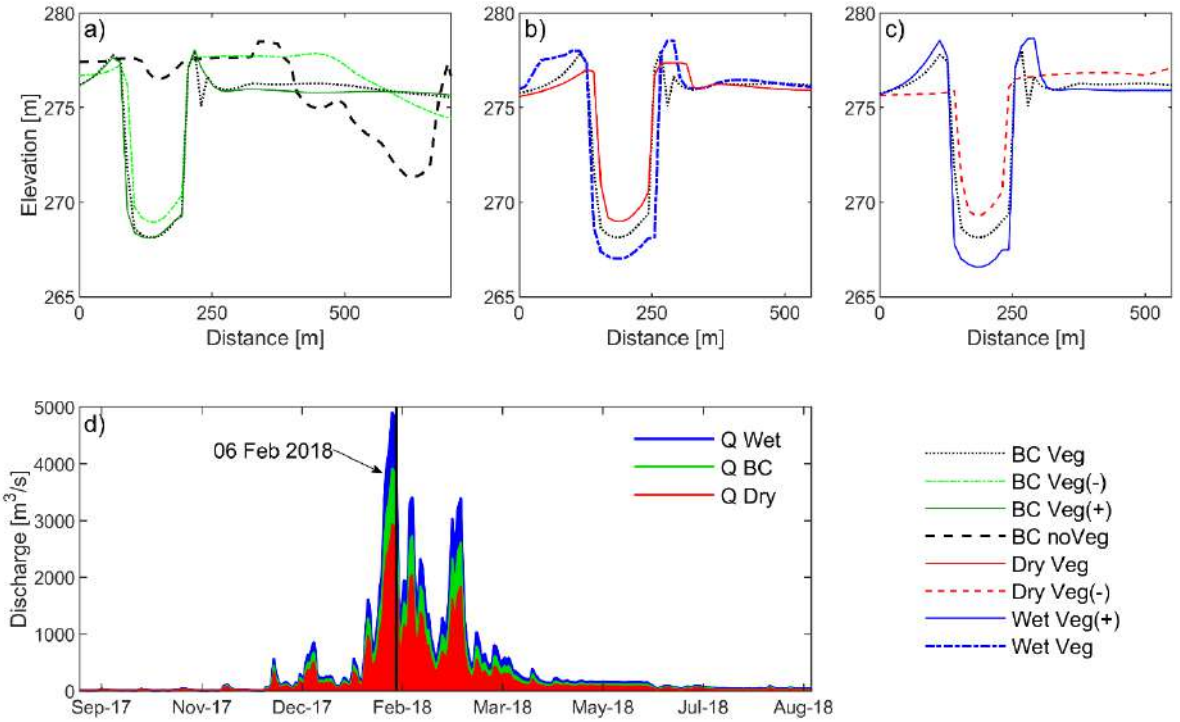

Figure 3 Predicted cross-section profiles at the measuring station of Misión la Paz on 06 Feb 2018 under different scenarios of hydrograph (BC is current scenario, Dry is the dryer scenario and Wet is wetter scenario. Legend acronyms: BC_Veg is current discharge and present vegetation (current climate); BC_Veg(-) is current discharge and reduced vegetation; BC_Veg(+) is current discharge and increased vegetation; BC_noVeg(-) is current discharge without vegetation; Dry_Veg is reduced discharge and current vegetation; Dry_Veg(-) is reduced discharge and reduced vegetation (drier climate); Wet_Veg is increased discharge and current vegetation; Wet_Veg(+) is increased discharge and richer vegetation (wetter climate).

* Corresponding author
Email address: f.bregoli@science.ru.nl (F. Bregoli)
URL: www.ru.nl/english/people/bregoli-f/ (F. Bregoli)

Session 3B
Long-term river behaviour and morphology

Scenarios for Controls of River Response to Climate Change in the Lower Rhine River

Clàudia Ylla Arbós[a,*], Astrid Blom[a], Ralph M.J. Schielen[a,b]

[a] *Delft University of Technology, Department of Hydraulic Engineering, Faculty of Civil Engineering and Geosciences, PO Box 5048, 2600 GA Delft, the Netherlands*

[b] *Ministry of Infrastructure and Water Management - DG Rijkswaterstaat, Utrecht, the Netherlands*

Keywords — Climate Change, River Controls, Lower Rhine River

Introduction

The majority of the world's large rivers are heavily engineered. In such heavily engineered rivers, channel response (i.e., changes in bed elevation, channel slope, and bed surface grain size) is predominantly determined by human intervention [e.g., Surian and Rinaldi (2003); Ylla Arbós et al. (2020)]. The relative influence of climate on channel response may, however, increase in the upcoming decades, as climate change alters the river controls. Specifically, climate change affects (1) the characteristics of the flow rate, through changes in precipitation patterns; (2) the downstream base level, through sea level rise, or lake base level drop; and (3) the sediment flux, due to changes in water discharge.

It is increasingly necessary to anticipate future channel response to climate-related changes in the river controls. This can be done using numerical models, by changing their boundary conditions. A required step is determining climate change scenarios for the river controls and translating them into suitable boundary conditions for numerical models, taking into account different sources of uncertainty.

Here we consider the Lower Rhine River, from Bonn (Germany) to Gorinchem (Netherlands). We discuss the projected changes of the hydrodynamic river controls over the 21st century, and how they can be transformed into suitable boundary conditions for a schematized model.

Changes in water discharge

Several studies have attempted to predict water discharge in the Rhine basin until 2100 using a model chain [e.g., Gorgen (2010); Hegnauer (2017)]. First, the different emission scenarios or representative concentration pathways (RCP's) defined by IPCC are used as input to climate models. The output is then used to obtain future precipitation time series. Finally, the precipitation time series are input to a hydrological model that transforms daily precipitation into daily river discharge. Numerous models and techniques are used in this process, and the results are sensitive to these choices, in particular to that of the climate model (Gorgen, 2010; Hegnauer, 2017).

In general terms, the different studies predict similar future trends in water discharge along the Rhine basin (Hegnauer, 2017). In upstream, snowmelt-dominated locations (e.g., Basel), higher temperatures lead to earlier snowmelt, which slightly shifts the annual discharge peak to earlier in the year, the magnitude of the peak not changing significantly. In the downstream, rainfall-controlled tributaries (e.g. Trier, Raunheim), higher peak flow rates and lower base flow rates are expected, without shifts in the timing of the peaks. In the Lower Rhine River, a combined behavior is expected, with a rainfall-peak in the winter, a smaller snowmelt-peak in summer, and higher peak flow rates and lower base flow rates. At Bonn, the winter mean monthly discharge may increase 15-50%, while summer mean monthly discharge may decrease 0-40% (Gorgen, 2010; Hegnauer, 2017).

A river tends to equilibrium channel characteristics, eventually attained if the controls do not change, or do so at low rates (Blom et al., 2017). The equilibrium bed profile can be decomposed in a mean bed profile, and fluctuations about it. The mean bed profile depends on the combination magnitude-frequency of flow events (the flow duration curve), while the order of flow events determines the fluctuations (Arkesteijn et al., 2019). Channel response is inseparable from discharge variability, and more information on discharge variability than mean monthly discharge is needed as an upstream flow boundary condition.

Gorgen (2010) provides an ensemble of synthetic daily discharge time series covering the period 1951-2100, and Hegnauer (2017) provides 50-year synthetic daily discharge time series representative of the period 1951-2006, 2050, and 2085. We propose to use these data to create create simplified hydrographs, which sufficiently preserve discharge variability, while ensuring that the only difference between sce-

*Corresponding author

Email address: c.yllaarbos@tudelft.nl (Clàudia Ylla Arbós)

URL: www.tudelft.nl (Clàudia Ylla Arbós)

narios is the climate signal, facilitating comparison between scenarios. A base-case, cycled 10-year hydrograph with similar statistical properties as the long-term historic time series, can be modified for each climate scenario, such that the future hydrographs have the same statistical properties as the synthetic hydrographs provided by Gorgen (2010); Hegnauer (2017), but keep the the order of flow events unchanged. From the synthetic hydrographs, the probability density function of water discharge for each scenario S_i can be obtained, providing the discharge associated to a certain probability of occurrence p, that is, $Q_{S_i}(p)$ (Figure 1a). The same exercise can be done with the base-case hydrograph, so as to obtain $Q_0(p)$. Each flow event in the base-case hydrograph can then be related to a probability of occurrence p, and further multiplied by the factor $F_{S_i}(p)$=$Q_{S_i}(p)/Q_0(p)$ (Figure 1b). The effect of the hydrograph cycled period can then be assessed. Further research is needed to validate this method.

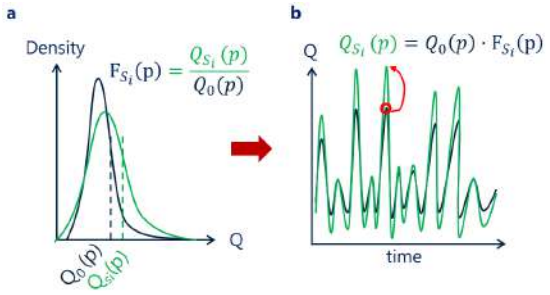

Figure 1: (a) Statistics of water discharge in the base case, and scenario S_i; (b) simplified hydrograph in the base case and in scenario S_i.

Changes in sea level

Climate scenarios foresee an increase of sea level between 0.2 and 3 m by the end of the century (Haasnoot et al., 2018). In all scenarios, sea level rise accelerates with time (up to 7 cm/a) when compared to the current rates of 0.2 cm/a. The increase in sea level has to be translated into the corresponding increase of water surface elevation at Gorinchem, the downstream boundary of our domain of interest. As an indication, an increase of sea level of 3 m at Hoek van Holland, would result into a water level increase of 2.75 m at Gorinchem, considering a water discharge of 2200 m^3/s, and based on hydrodynamic computations only (Haasnoot et al., 2018).

An increase in base level is expected to trigger a morphodynamic response towards a new equilibrium state, which consists of an increase of bed level equal to the total rise of sea level. Due to the sand deficit in the Lower Rhine-Meuse Delta (Cox et al., 2020), bed level cannot keep pace with sea level rise. Further analysis will provide insight on how the water level at Gorinchem will be affected by sea level rise.

Discussion and conclusions

Climate change affects the boundary conditions of the Lower Rhine River, which may affect future channel response. We have discussed foreseen changes in the hydrodynamic river controls. In addition, scenarios for changes in the sediment flux are required, based on changes in the hydrograph, and land-use changes. The high degree of uncertainty related to climate projections calls for a statistical or a scenario approach.

Changes in future intervention policy may have a greater effect on channel response than climate change. Modeling of channel response must consider intervention scenarios. A comparison between climate-triggered response and intervention-triggred response will shed light on the relative importance of natural versus human controls on channel response.

References

Arkesteijn, L., Blom, A., Czapiga, M. J., Chavarrías, V., and Labeur, R. J. (2019). The Quasi-Equilibrium Longitudinal Profile in Backwater Reaches of the Engineered Alluvial River: A Space-Marching Method. *JGR:ES*, 124(11):2542–2560.

Blom, A., Arkesteijn, L., Chavarrías, V., and Viparelli, E. (2017). The equilibrium alluvial river under variable flow and its channel-forming discharge. *JGR:ES*, 122(10):1924–1948.

Cox, J., Kleinhans, M. G., and Huismans, Y. (2020). An estuary out of equilibrium: The importance of dredging in determining the net sediment flux in the Rhine-Meuse Estuary. *River Flow 2020*, Delft.

Görgen, K. (2010). Assessment of climate change impacts on discharge in the Rhine River Basin : results of the RheinBlick2050 project.

Haasnoot, M., Bouwer, L., Diermanse, F., Kwadijk, J., van der Spek, A., (...) Huismans, Y., Sloff, K., and Mosselman, E. (2018). Mogelijke gevolgen van versnelde zeespiegelstijging voor het Deltaprogramma. Een verkenning.

Hegnauer, M. (2017). Analysis GRADE results for different locations in the Rhine Basin. Deltares.

Surian, N. and Rinaldi, M. (2003). Morphological response to river engineering and management in alluvial channels in Italy. *Geomorphology*, 50(4):307–326.

Ylla Arbós, C., Blom, A., Viparelli, E., Reneerkens, M., Frings, R. M., and Schielen, R.M.J. (2020). River Response to Anthropogenic Modification: Channel Steepening and Gravel Front Fading in an Incising River. *GRL*. doi:10.1029/2020GL091338

Efficient long-term one-dimensional morphodynamic modelling in alluvial rivers using simplified models – theory and validation

Hermjan Barneveld[a,b*], Ton Hoitink[a], Erik Mosselman[c,d], Victor Chavarrías[c]
[a] *Wageningen University and Research, Hydrology and Quantitative Water Management Group, Department of Environmental Sciences, Droevendaalsesteeg 3, 6708 PB Wageningen, the Netherlands*
[b] *HKV lijn in water, Botter 11-29, 8232 JN Lelystad, the Netherlands*
[c] *Deltares, P.O. Box 177, 2600 MH Delft, the Netherlands*
[d] *Delft University of Technology, P.O. Box 5, 2600 AA Delft, the Netherlands*

Keywords — river morphology, analytical approach, numerical modelling

Introduction

Morphodynamic numerical simulations can be time consuming, especially in a stochastic approach when multiple long-term simulations are required to address parameter uncertainty. To improved efficiency the flow and sediment dynamics can be decoupled when Froude numbers are below 0.8 (e.g. de Vries, 1965; Lyn, 1987; Lyn & Altinakar, 2002). A morphological acceleration factor can further speed up simulations. Another approach is to simplify models by neglecting terms in the governing equations. The quasi-steady approach may for example reduce simulation times to less than 25%.
The scope of this research is to assess how and when model simplifications are possible, without jeopardizing the predictive capacity in terms of sediment transport and riverbed development.

This work is part of a PhD research at Wageningen University & Research as part of the Rivers2Morrow programme (2018-2023). The PhD research is supported by the Dutch Ministry of Infrastructure and Water Management, HKV and Deltares.

Methododolgy

Theoretical analysis

Grijsen & Vreugdenhil (1976) performed a theoretical analysis, to assess the impact of simplification of 1-dimensional flow models on the propagation and damping of water waves. We extend their analysis to morphology. Basis are the St. Venant equations for water motion, the sediment mass balance equation and a closure relation for sediment transport.
The flag coefficients α_i (i = 1 … 4) can be 0 and 1 only. Values of 0 indicate model simplification.

$$\alpha_1 \frac{\partial u}{\partial t} + \alpha_2 u \frac{\partial u}{\partial x} + \alpha_3 g \frac{\partial h}{\partial x} + g \frac{\partial z}{\partial x} = -g \frac{u^2}{C^2 h}$$

$$\alpha_4 \frac{\partial h}{\partial t} + h \frac{\partial u}{\partial x} + u \frac{\partial h}{\partial x} = 0$$

$$\frac{\partial z}{\partial t} + \frac{\partial s}{\partial x} = 0$$

$$s = f(u, parameters)$$

with: t=time, x=longitudinal co-ordinate, u=flow velocity, h=water depth, z=bed level, C=Chézy coefficient, s=sediment transport per unit width, g=acceleration due to gravity.

We consider 2 simplified models:
1. Quasi-steady approach, neglecting time-derivatives: $\alpha_1 = \alpha_4 = 0$
2. Diffusive wave, neglecting inertia: $\alpha_1 = \alpha_2 = 0$

To assess the performance of these models, analytical solutions for the set of non-linear equations are derived through:
1. linearization
2. combination to one linear equation in the water depth h'
3. assuming a harmonic perturbation of flow and bed to get a solution for propagation and damping of water and sediment waves.

The ratio of solutions of the full dynamic model and simplified models determines how well simplified models perform. Three dimensionless parameters are important:

Froude number $Fr = \frac{u}{\sqrt{gh}}$

Water wave parameter $E = \sqrt{\frac{g^3 T^2}{C^4 h_o}}$

Transport parameter (uniform material) $\Psi = n \frac{s_o}{q_o}$

with: T = period of flood wave, n = power in sediment transport relation $s = mu^n$, q = discharge per unit width. Index $_o$ means undisturbed value.

* Corresponding author
Email address: hermjan.barneveld@wur.nl (Hermjan Barneveld)

Validation with numerical model

To check whether the results of the theoretical analysis are valid in practical, non-linear, cases, numerical simulations were performed. ELV is a one-dimensional numerical morphological modelling system (Chavarrías et al, 2019). ELV simulates the full set of equations, the quasi-steady model and the diffusive-wave model. Simulations were done with infinitesimal perturbations as well as with flood waves and larger bed disturbances in a quasi-equilibrium river reach. Flood wave characteristics, bed slope and grain sizes were varied within ranges realistic for lowland rivers. Figure 1 shows a sample result.

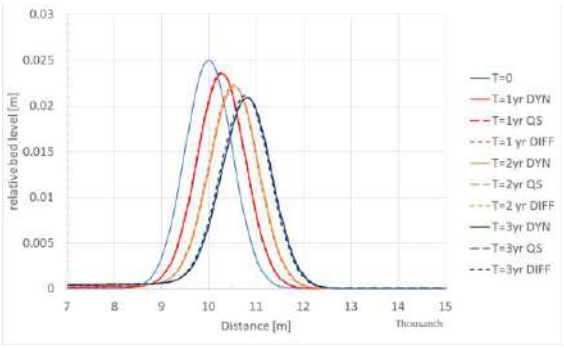

Figure 1. Propagation of small bed perturbation during 3 years with full dynamic (DYN), quasi-steady (QS) and diffusive-wave model (Diff). Vertical axis: bed level relative to mean bed slope. Fr=0.2, E=12,500 and Ψ=5.15e-5.

Results

Figure 2 shows the relative celerity of bed perturbations (*c/u*) according to theory (lines) and ELV (markers). The agreement is good for Froude numbers up to 0.3. For higher Froude numbers deviations occur.

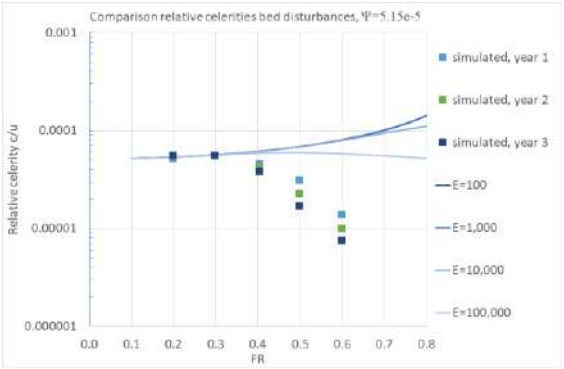

Figure 2. Relative celerity of full dynamic model: theory and simulated (ELV, average over three years).

In Figure 3 the full dynamic model (DYN) and simplified models are compared. The Figure shows the ratios of celerity of bed disturbances from theory (lines) and ELV (markers).

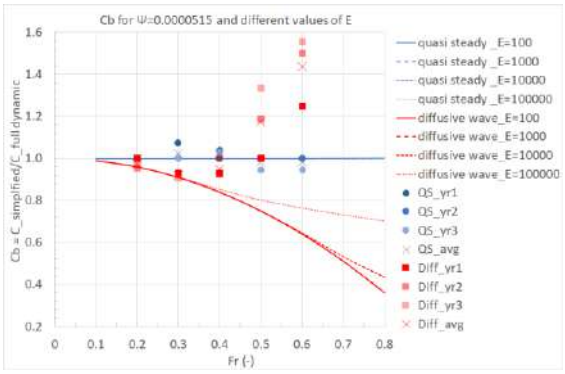

Figure 3. Ratio of celerities (c_b) from theory and ELV.

ELV results in Figure 3 are based on small perturbations for flow and bed. Simulations with large bed disturbances (aggradation 0.5 m over 1 km river length) and flood waves show similar trends.

Discussion

For Froude numbers up to 0.3, celerities of bed disturbances from theory and simulations agree. For larger Froude numbers the theoretical celerities are larger than according to numerical simulations. Nonetheless, for the quasi-steady model the theoretical error prediction for propagation (and damping) of bed disturbances is confirmed by numerical simulations. The quasi-steady model may be applied over a large range of hydrodynamic and morphological conditions. This model does not include flood wave damping. This aspect should be included alternatively.

The diffusive-wave model does describe flood wave damping, but the error prediction deviates from numerical results for $Fr \geq 0.4$. Up to $Fr=0.3$ the error in morphological changes with the diffusive-wave model is restricted to 10%.

Deviations between theory and numerical modelling require further research.

References

Chavarrías, V., Stecca, G., Siviglia, A., & Blom, A. (2019). A regularization strategy for modeling mixed-sediment river morphodynamics. Advances in Water Resources, 127, 291–309.

Grijsen J.G. and G.B. Vreugdenhil (1976). Numerical representation of flood waves in rivers; In: Proc. Int. Symp. Unsteady flow in open channels, Newcastle-upon-Tyne, BHRA Fluid Eng., Cranfield, paper K1, pp. K1.1-K1.16;

Lyn, D. A. (1987). Unsteady sediment transport modeling. Journal of Hydraulic Engineering, 113(1), 1–15.

Lyn, D. A., & Altinakar, M. (2002). St. Venant-Exner equations for near-critical and transcritical flows. Journal of Hydraulic Engineering, 128(6), 579–587.

Vries M. de (1965). Considerations about non-steady bedload transport in open channels. Proc. 11th IAHR-Congr., Leningrad.

Laying bare systemic river bed changes in the river Rhine

Freek Huthoff[a,b*], Pepijn van Denderen[a,b], Andries Paarlberg[a]
[a] *HKV Lijn In Water, Botter 11-29, 8232 JN Lelystad, The Netherlands*
[b] *University of Twente, Department of Water Engineering and Management, Faculty of Engineering Technology, P.O. Box 217, 7500 AE, Enschede, the Netherlands*

Keywords — River morphology, wavelet analysis, bed incision, large-scale processes

Introduction

Sandy or gravel river beds are continuously evolving in response to flow conditions and to the sediment supply coming from upstream. These morphodynamic forcing mechanisms can be affected by river engineering measures such as channel widenings, placements or adjustments of navigation or flood-protection structures, dredging activities or rehabilitation measures such as re-meandering or side-channel connections. To be able to anticipate and appropriately act on morphological changes in rivers, it is important to link cause-and-effect relations between bed response and their dominating triggers. This is particularly important in highly-engineered navigable rivers, where multiple influences from close-by and further away can obscure the dominating causes of local bed level changes, and thereby possibly point in the wrong direction when it comes to sustainable river management practices.

In recent years, such aspects have become increasingly important for the river Rhine in the Netherlands, as it is now recognized that there may be severe implications for river navigation, ecology, drought risk and flood risk if existing large-scale morphological trends continue in the way as they are now. Specifically, an apparent systemic trend of bed incision within the Rhine branches may lead to bottlenecks for river navigation and flood plains may dry out under lowering of mean water levels (e.g. Hiemstra et al, 2020). Also, a possible shift in the discharge distribution at bifurcation points may create a new hydrodynamic equilibrium in the system, and distort various water management practices.

A key objective of the recent national Dutch Delta Programme on Integrated River Management is to get bed level incision under control while addressing river functions such as navigation, flood management and ecology. The challenge is to separate systemic large-scale morphodynamic trends in the river from more localized effects that are caused by specific river interventions and may only be of temporary nature (Paarlberg et al. 2020). Only if the rate and the spatial distribution of systemic river bed incision are known, appropriate countermeasures can be designed. For this purpose, we compare methodologies to study systemic bed level trends, and show that different methods can lead to different results. The different outcomes show that interpretation of morphodynamic trends should be done with great care, for the river Rhine, but also for other rivers around the world.

Large-scale bed changes according to different methods

The traditional approach to study large-scale bed level changes is to spatially-average river bed levels and to see how these progress over time. Fig. 1 gives an example of this approach for a location in the river Rhine near river-km 870. The blue points show how the bed locally moves up and down within a range of +/- 20 cm during a period of about 12 years. The orange points show the bed level changes if an average bed level of a reach of 5 km is considered (see also Ylla Arbos et al. 2019). A clear downward trend of about 1.4 cm/year then reveals itself. When applying the wavelet methodology as done in Van Denderen et al. (2020, 2021) for bed signals >30 km, the downward trend becomes only half as strong (green line).

This result from the wavelet-methodology suggests that the 5-km-average trendline is still affected by bed level changes that act on scales of 10-20 km. Changes that originate from such spatial scales can hardly be considered systemic for a river as the Rhine, and may be associated with time scales of “only” several years to one or two decades. Indeed, trends in spatially-averaged bed levels that change on such time scales can clearly be seen in Fig. 2 for the IJssel branch of the River Rhine (compare blue and yellow line).

Fig. 2 uses the same methods as in Fig. 1. Only now it is shown for a river reach of around 100 km in the IJssel branch of the river Rhine, depicting only the fitted bed-level trends. It can be seen that the trends of the 5-km-averaged bed level still vary significantly over the past 20 years: in the past 5 years the bed along the entire river IJssel mostly went up by 0.5 to 1 cm/year (blue line), while over the past 10 to 20

* Corresponding author
Email address: huthoff@hkv.nl (Freek Huthoff)

years the bed was in some places stable and upstream of river-km 950 even went down by up to 1 cm/year (yellow and red line). The result from the wavelet analysis for signals >30 km (green line) shows a much smoother spatial distribution of bed level trends. The result is mostly consistent with the red and yellow lines in Fig. 2, but still some clear differences are found. For example, at river-km 960 a clear pronounced peak in bed level rise follows from the spatially-averaged methods, giving twice as large bed level change-rates compared to the wavelet result. Around river-km 900 the opposite is found: here, the wavelet method gives a downward trend of nearly 1 cm/year while the spatially-averaged methods produce a nearly stable to rising bed.

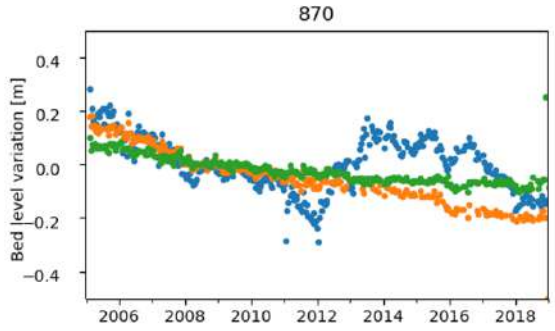

Figure 1. Bed level changes at location rkm870 in the river Waal just downstream of the Pannerdensche Kop when considering the raw local bed measurements (blue), when taking the raw data averaged over a reach of 5km (orange) and when using filtered wavelet analysis for signals >30km (green). Data as in Van Denderen et al. (2021).

Conclusions

The wavelet methodology allows to study morphological changes in a river associated with specific spatial scales. Here we filtered out smaller-scale effects to reveal systemic large scale trends. In a traditional spatially-averaged approach, smaller-scale processes remain present in the results. For the case of the river Rhine, where bed level incision has become a major concern in river management, it is important to identify exactly which trends are truly systemic, and how they will continue if no action is taken. It shows that traditional methods to estimate such trends can easily be off by a factor of two or more and can mistakenly interpret local temporary changes for longer-term systemic trends. It is recommended that the wavelet methodology as applied here becomes a standard tool for long-term river management, at the very least to provide complementary information to bed level trends derived from traditional spatially-averaged methods. Finally, also for rivers elsewhere around the world, the wavelet methodology is recommended to help identify systemic bed level trends.

References

Ylla Arbós, C., Blom, A., Van Vuren, S., & Schielen, R.M.J. 2019. Bed level change in the upper Rhine Delta since 1926 and rough extrapolation to 2050. Research report, Delft University of Technology, Delft.

Hiemstra, K.S., van Vuren, S., Vinke, F.S.R., Jorissen, R.E., & Kok, M. 2020. Assessment of the functional performance of lowland river systems subjected to climate change and large-scale morphological trends. International Journal of River Basin Management, 1-22.

Paarlberg, A., P. van Denderen, R. Schielen, D. Augustijn, 2020. Rivierbodemdynamiek meenemen in het ontwerp van maatregelen. Land + Water, 60(10), 30-31.

Van Denderen, R. P., Kater, E., Jans, L. & Schielen, R.M.J. 2020. The initial morphological impact of the longitudinal dams. NCR Days 2020, Nijmegen, Book of abstracts.

Van Denderen, R. P., Paarlberg, A.J., Augustijn, D.C.M., & Schielen, R.M.J. 2021. Insight into the local bed-level dynamics to assist management of multi-functional rivers. NCR Days 2021, University of Twente, Book of abstracts.

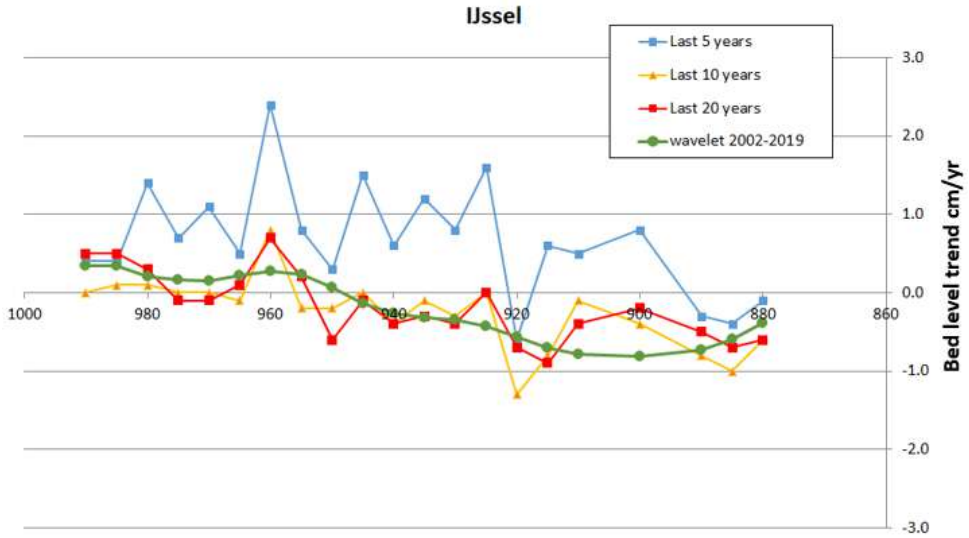

Figure 2. Yearly bed level changes in the river IJssel as derived from raw 5-km averaged data for the past 5, 10 and 20 years, together with results from the filtered wavelet analysis using 17 years of data for spatial scales >30 km.

Poster session I

A multi-criteria analysis for sediment management strategies

Eline Sieben[a,*], Jana R. Cox[a] , Jaap H. Nienhuis[a]
[a]*Faculty of Geosciences, Utrecht University, Utrecht, The Netherlands*

Keywords — Sediment management, Multi-criteria analysis, Global Deltas

Introduction

Delta systems are confronted with subsiding land and reduced sediment fluxes, a problematic scenario particularly when combined with a rising sea level (Syvitski et al., 2009). To prevent drowning and to maintain the morphological functioning of the delta, sufficient sediment and effective sediment management are crucial (Giosan et al., 2014; Paola et al., 2011).

Sedimentation enhancing strategies (SESs) are measures aimed to enhance natural sedimentation processes in deltas in a suitable manner. SESs can encompass >100 km^2, such as the proposed Mid-Barataria Sediment Diversion in the Mississippi(Bomer et al., 2019) SESs can also be applied on a smaller scale. In northern Vietnam, reforestation of mangroves covered an area of 11 km^2 (Marchand, 2020).

Many SESs are designed for local use and case specific. Best practices, including guidelines that would help to export designs to other areas, are lacking. The broad need for SESs globally inspired us to think of a multi-criteria tool to compare different sediment management strategies. Here, we report on our assessment on the applicability of existing SESs for use in different deltas. This will highlight environmental, social, and governmental criteria that affect the applicability of SESs.

Gathering data & case studies

A literature review on different SES case-studies took place. The result is a collection of data concerning various criteria on SESs. Together with insights from discussions with experts, the criteria are processed into a tool to assess the applicability of the different strategies. The applicability concerns global deltas, under current and future scenarios of change. Furthermore, trends and patterns in the various criteria which determine applicability, effectiveness and sustainability are assessed.

Data collection

Different case-studies from the Danube, Ganges-Brahmaputra, Mississippi and Rhine-Meuse delta were analysed. We focused on soft engineering strategies that build with nature and aim to increase sedimentation on the delta plain. Example SESs include; Tidal River Management (Gain et al., 2017), Sediment River Diversions (CPRA, 2014), wetland restoration (Hein et al., 2016) and depoldering (van der Deijl et al., 2018) .Further possible strategies we consider includes vegetation planting such as salt marshes and mangroves. We neglect restoration efforts outside of the delta itself, such as e.g. dam removal or reservoir flushing. We also exclude SESs that do not build with nature such as dredging and dumping of sediments.

The different criteria

We rate SES case studies in different delta and collect parameters in different categories;

1. Delta characteristics: delta features that influence the implementation or results of the sediment management strategies. i.e. dams, levees, sea level rise, land use type etc.
2. Project settings: characteristics of sediment management strategy. i.e. timing and/or duration of the strategy, costs, etc.
3. Biophysical settings: biophysical parameters. i.e. tidal range, vegetation type, discharge etc.
4. Environmental impact: influence of the sediment strategy on the local environment. i.e. land use change, salinity etc.
5. Stakeholder influence: stakeholder involvement during and after implementation of the strategy. i.e. number of stakeholders, main interests of stakeholders etc.
6. Governance and legal structures: governmental aspects influencing the implementation or execution of the strategy. i.e. governmental mode.
7. Results: General outcome of the sediment strategy. i.e. amount of sediment added to the system, etc.

Building a multi-criteria tool

The insights gained and the criteria considered relevant are processed into a multi-criteria tool. We provide an overview for decision makers that will highlight benefits and drawbacks of existing strategies, in relation to new areas of application.

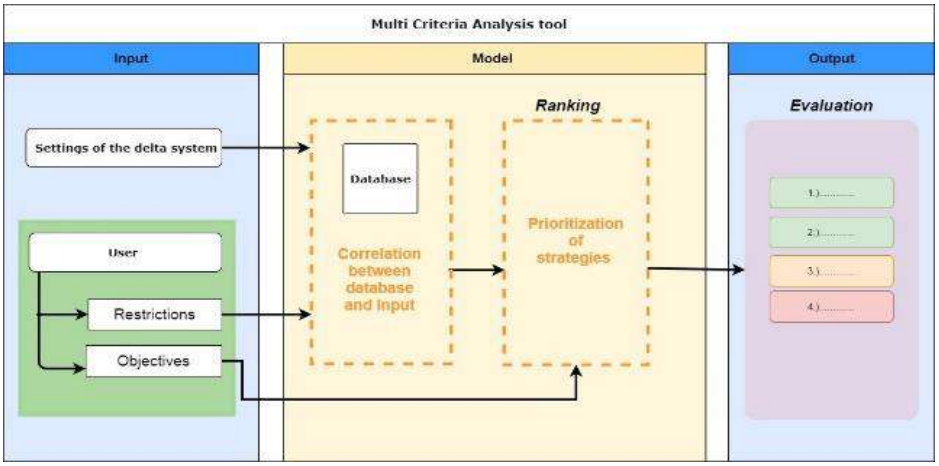

Figure 1 Visualisation of the multi-criteria tool

In Fig.1 a concise visualisation of the tool is given. The main input of the tool consists of delta features and user specific criteria or restrictions. A correlation takes place between the input given and the database that consists of criteria and data extracted from the case studies. With the objectives from the user, given as input, an evaluation of the strategies takes place. Outcomes of the tool are based on the practical experiences that have been gained from existing and planned sedimentation projects globally and expert views. The main outcome of the tool will consist of a generic template for implementing sediment strategies.

Some preliminary notes:

Balancing system specific characteristics with global applicability

- While each case study has local characteristics which determine their effectiveness, some trends can be observed
- Physical setting and selecting an appropriate location are key for a strategy to be implemented, this requires a lot of high quality and specific data (land use, tidal range, discharge, sedimentation maps etc.)
- Governance mode determines both the likelihood and speed of implementation
- Stakeholder engagement plays a key role: strategies which encourage stakeholder cooperation are more likely to be successful and sustainable

* Corresponding author
Email address: e.sieben@students.uu.nl

References

Bomer, E. J., Bentley, S. J., Hughes, J. E. T., Wilson, C. A., Crawford, F., & Xu, K. (2019). Deltaic morphodynamics and stratigraphic evolution of Middle Barataria Bay and Middle Breton Sound regions, Louisiana, USA: Implications for river-sediment diversions. *Estuarine, Coastal and Shelf Science*, *224*.

CPRA. (2014). *2017 Coastal Master Plan*. Coastal Protection And Restoration Authority. https://coastal.la.gov/our-plan/2017-coastal-master-plan/.

Gain, A. K., Benson, D., Rahman, R., Datta, D. K., & Rouillard, J. J. (2017). Tidal river management in the south west Ganges-Brahmaputra delta in Bangladesh: Moving towards a transdisciplinary approach? *Environmental Science & Policy*, *75*, 111–120.

Giosan, L., Syvitski, J., Constantinescu, S., & Day, J. (2014). Climate change: Protect the world's deltas. *Nature*, *516*(7529), 31–33.

Hein, T., Schwarz, U., Habersack, H., Nichersu, I., Preiner, S., Willby, N., & Weigelhofer, G. (2016). Current status and restoration options for floodplains along the Danube River. *Science of The Total Environment*, *543*, 778–790.

Marchand, M. (2020). *Mangrove restoration in Vietnam: Key considerations and a practical guide*.

Paola, C., Twilley, R. R., Edmonds, D. A., Kim, W., Mohrig, D., Parker, G., Viparelli, E., & Voller, V. R. (2011). Natural Processes in Delta Restoration: Application to the Mississippi Delta. *Annual Review of Marine Science*, *3*(1), 67–91.

Syvitski, J. P. M., Kettner, A. J., Overeem, I., Hutton, E. W. H., Hannon, M. T., Brakenridge, G. R., Day, J., Vörösmarty, C., Saito, Y., Giosan, L., & Nicholls, R. J. (2009). Sinking deltas due to human activities. *Nature Geoscience*, *2*(10), 681–686. 9

van der Deijl, E. C., van der Perk, M., & Middelkoop, H. (2018). Establishing a sediment budget in the newly created "Kleine Noordwaard" wetland area in the\hack\break Rhine–Meuse delta. *Earth Surface Dynamics*, *6*(1), 187–201.

Numerical study on the transition between river bar regimes due to varying discharge

Roline Montijn[a,b,*], Kees Sloff[a], Erik Mosselman[a]
[a] Deltares, P.O. Box 177, 2600 MH, Delft, The Netherlands
[b] Delft University of Technology, Department of Hydraulic Engineering, Faculty of Civil Engineering and Geosciences, P.O. Box 5048, 2600 GA, Delft, The Netherlands

Keywords — River morphodynamics, River bars, Morphological timescales, Discharge variability, Numerical modelling

Introduction

River bars are large-scale bedforms, formed by the local deposition of sediments. They create suitable habitats for aquatic fauna and riparian vegetation, which makes them valuable in river restoration projects. Understanding the dynamics of river bars is required for a proper design of the restoration project and for the development of a sustainable management scheme.

The channel width-to-depth ratio is the key controlling parameter for the formation of bars. Based on early described stability analyses, a resonance point and critical width-to-depth ratio have been defined, which mark the transition between different types of bar regimes (Colombini et al., 1987). By widening a river section to a width-to-depth ratio above its critical value, migrating bars develop. When they are fixed to a local perturbation, the bars show a pattern subcritically damped in downstream direction. By further increasing the width-to-depth ratio towards its resonance point, the celerity of the migrating bars becomes zero. This results in a pattern of steady bars, which are referred to as an unstable bar regime.

Due to the natural variability of river discharge, the width-to-depth ratio varies over time. The objective of this research is to give insights into the transition between river bar regimes due to a varying discharge. Therefore, insight in the timescale of adaptation to new flow conditions is necessary.

Methodology

A straight river channel is modelled in Delft3D, with non-erodible banks, starting with a flat bed. The geometry and the discharge hydrograph are roughly based on the Dutch river 'Grensmaas'. A fixed perturbation by means of a groyne is applied, which obstructs 20% of the channel width. A relatively small sediment size is applied to model morphological changes in the total discharge regime.

In the uniform analysis, the upstream boundary condition is a steady discharge, with magnitudes between 50 and 1250 m^3/s. The damping length and wavelength of the river bars are compared with theoretically obtained values to validate the numerical model and to determine the resonance point of the river model. Furthermore, the time to develop the river bars from a flat bed is assessed. This value is compared to existing morphodynamic timescales.

The transition between the river bar regimes around the resonance point (unstable to subcritically damped and vice versa) is modelled by means of a steady increasing and decreasing discharge, starting with a fully developed bed. The response of the river bars to the varying discharge is coupled to the timescale of development based on the uniform analysis.

Results

Three types of river bars are shown in Figure 1, being a. Unstable, b. Subcritically damped, and c. Supercritically damped. The corresponding discharge is 100, 150, and 1000 m^3/s, equivalent to width-to-depth ratios of 42, 32 and 9 respectively. The damping length and wavelength show good agreement with the values determined by the theory of Crosato and Mosselman (2009), which is based on the theory developed by Struiksma et al. (1985). The resonance point is at a width-to-depth ratio of 37-38.

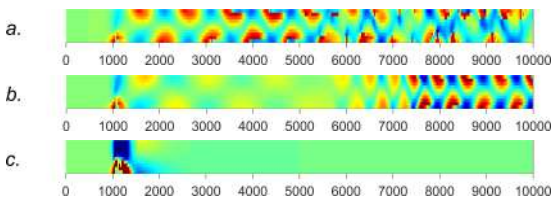

Figure 1: Unstable (a), subcritically damped (b), and supercritically damped (c) river bar regimes.

From the numerical simulations, two timescales have been defined. First, the development of migrating bars towards their final amplitude (Figure 2a). Secondly, the time

*Corresponding author
Email address: roline.montijn@deltares.nl (Roline Montijn)

to reach the final bed topography, which is in the unstable and subcritically damped bar regime a pattern of steady bars. The timescale of the development of migrating bars shows good agreement to the timescale defined by Taal (1989), which is inversely proportional to the sediment transport rate. The timescale to the final bed topography is 4-6 times greater.

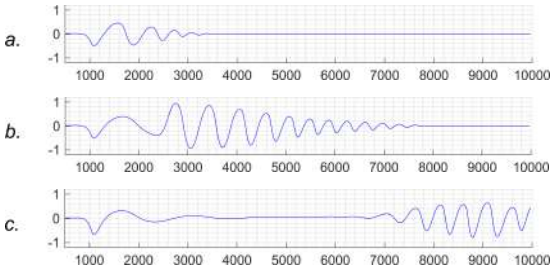

Figure 2: Bed levels along river bank, starting from a flat bed. a. Migrating bars develop from the fixed perturbation (t = 20 days). b. & c. A pattern of steady bars, damped in downstream direction, develops (t = 2 & 8 months).

The transition between an unstable to a subcritically damped bar regime is shown in Figure 3; vice versa in Figure 4. In both figures, bed levels are plotted for the width-to-depth ratios between 35 to 41, which captures the resonance point of the river. The same colour in the two figures corresponds to the same width-to-depth ratio. A qualitative description of the transition is given.

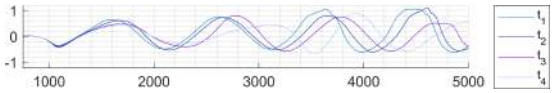

Figure 3: Bed levels along river bank, in the transition from an unstable to a subcritically damped bar regime.

From unstable to subcritically damped (Figure 3): The amplitude of the bars decreases towards a constant amplitude in downstream direction, and in this process the river bars are slowly migrating. Starting from the fixed perturbation, a new pattern of steady bars with a damped character develops (t_4). The bars migrate faster than the development of steady bars starting from the perturbation. Therefore, new migrating bars develop at the tail of the steady bars.

From subcritically damped towards unstable (Figure 4): At the tail of the subcritically damped steady bars, migrating bars develop. This bed instability slowly moves upstream. The pattern of steady bars becomes steeper with shorter wavelengths.

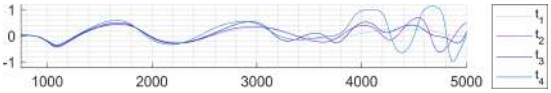

Figure 4: Bed levels along river bank, in the transition from a subcritically damped to an unstable bar regime.

Conclusion and recommendations

Based on the uniform analysis, a distinction in timescales of development of migrating and steady bars is made, with a shorter (4-6 times) timescale of development for migrating bars. This results in a different response of migrating and steady bars to a varying discharge. When the bed becomes unstable due to an increasing width-to-depth ratio, migrating bars develop. A pattern of steady bars follows, developing in downstream direction from the fixed perturbation.

The development of migrating bars in the idealized case of a straight river limits the validity of the results for real rivers, as their migration can be limited by other local perturbations, like a local widening or curvature.

Recommendations for further research are towards the effect of varying sediment sizes on the timescale of development and response of river bars to varying discharge.

Acknowledgements

Astrid Blom (Delft University of Technology), Ralph Schielen (RWS and Delft University of Technology) and Robert Jan Labeur (Delft University of Technology) contributed by valuable remarks. The full MSc thesis is accessible at the online repository of the TU Delft.

References

Struiksma, N., Olesen, K., Flokstra, C., de Vriend, H., 1985. Bed deformation in curved alluvial channels. Journal of Hydraulic Research 23, 57–79.

Crosato, A., Mosselman, E., 2009. Simple physics-based predictor for the number of river bars and the transition between meandering and braiding. Water Resources Research 45

Taal, M.C., 1989. Time-dependent near-bank bed-deformation in meandering rivers. (MSc Thesis). Delft University of Technology

Colombini, M., Seminara, G., Tubino, M., 1987. Finiamplitude alternate bars. Journal of Fluid Mechanics 181, 213-232.

Numerical and physical modelling of the effect of groynes lowering

Johan Harms[a*], Victor Chavarrias[b], Mohamed Yossef[b], Jeremy Bricker[a], Wim Uijttewaal[a], Burhan Yildiz[a,b,c]

[a] *Dept. of Hydraulic Engineering, Faculty of Civil Engineering and Geosciences, Delft University of Technology, P.O. Box 5048, 2600 GA, Delft, the Netherlands*

[b] *Deltares, Boussinesqweg 1, 2629 HV Delft, the Netherlands*

[c] *Mugla Sitki Kocman University, Department of Civil Engineering, 48000, Mugla, Turkey*

Keywords — Groynes, Groyne lowering, Physical modelling, Numerical modelling

Introduction

Groynes are a common sight in Dutch rivers, giving multiple advantages. They decrease the conveyance flow area, increasing the flow velocity in the main channel, inhibiting the formation of ice dams and deepening the main channel, which allows larges vessels to travel the river. They furthermore decrease the flow velocity at the bank, which protects the dikes. Groynes have some drawbacks however. One of those drawbacks is that during high-flow events, groynes hinder the river flow, increasing the overall friction and the water levels during flood events.

To increase safety against flooding *Rijkswaterstaat* is considering the lowering or streamlining of groynes. As a legal requirement the impact of such groyne adaptions have to be studied using WAQUA, a two-dimensional river model. In that model the groynes are modelled as fixed weirs, causing energy loss due to the constriction and subsequent expansion of the flow passing over the groynes. In contrast to weirs, groynes only obstruct part of the river however, allowing bypassing of water around a groyne. Furthermore there are mixing layers between the main channel, groyne fields and floodplains, which induce an extra momentum exchange in the river. The magnitude of this interaction depends on the difference in flow velocity in the different parts of the river and depends thus on the proper modelling of the groynes (Ambagts, 2019).

Current practice to compensate for these differences in flow physics is by calibration with measured water levels, applying a friction factor on the weir formulas. With such a method one cannot be certain about the effects of changing the groyne geometry (Yossef & Visser, 2018).

Therefore a numerical and a physical model are set up to determine modelling coefficients for groyne schematization. The numerical modelling includes 3D modelling with the groynes included in the bathymetry, as well as 2D sub-grid modelling with groynes included as (a combination of) weirs (Chavarrias, 2020).

These numerical simulations are calibrated on the results of physical modelling of groynes. The physical model is a 1:30 scale model of a representative section of the Waal. For this model different water levels with different discharges are modelled in the physical model, as well as the numerical model. The modelled situation includes the situation of emerged groynes, submerged groynes with emerged floodplain and high water conditions with submerged groynes and floodplain.

The measured quantities in the physical model are water levels and flow velocities. From these quantities the friction in the flume with and without groynes can be determined.

Physical groyne modelling

The physical model consists of a 36 m long, 5 m wide straight flume consisting of a main channel, groyne field and floodplain. For these dimensions 6 groynes fit in the experiment. Water levels and velocity profiles are measured up- and downstream of each groyne and within the third groyne field, in which also the surface velocities are measured using particle tracking velocimetry. Current physical modelling results without the groynes as reference case are preliminary and show a large influence of the upstream inflow boundary (Fig. 1).

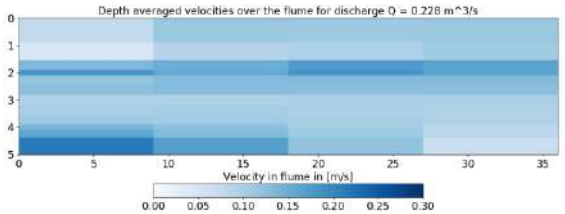

Figure 1. Mean flow velocity in the physical model, with the main channel at Y=0. The mean flow velocity increases in the main channel and decreases in the floodplain over the whole domain.

* Corresponding author
Email address: j.m.harms-1@student.tudelft.nl (J.M. Harms)

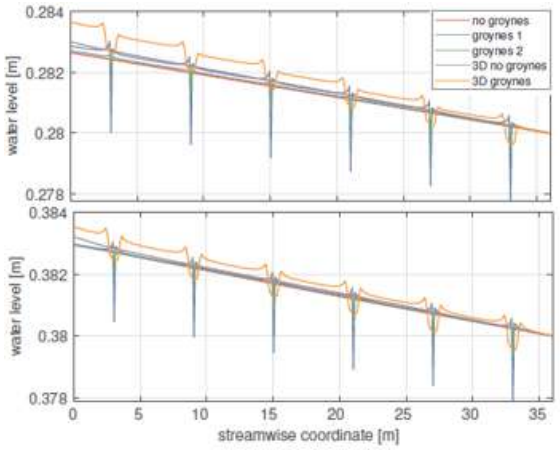

Figure 2. Water levels for different submergence levels of the groynes. On top the water levels for the case with submerged groynes. Below the case with submerged groynes and inundated floodplain. Case without groynes in 2D and 3D is modelled, as well as 2D groyne schematizations as 1 or 2 weirs and 3D modelling of groynes.

Groyne resistance modelling

Current results from numerical modelling are also preliminary. But comparing 2D and 3D modelling results shows that under high flow conditions the effect of groynes is negligible in 2D, while not in 3D (Fig. 2).

Emerged groyne modelling

For low water levels, with emerged groynes, the sub-grid modelling of weirs does produce eddies in the groyne fields (Fig. 3), and gives results which correspond well to the 3D simulation. A double gyre pattern is expected in the physical model in the groyne fields in contrast to the single gyre in the numerical models, otherwise the model correctly reproduces essential features, such as: flow unsteadiness, eddy periodicity, the role of wall friction in eddy periodicity and secondary circulation in 3D modelling (Chavarrias, 2020).

Discussion

The aim of the current research is to verify numerical models with a large flume, with few uncertainty in translating the results to the full scale. The scale (1:30) is large compared to most physical models of groynes currently build. The chosen scale does have a large drawback that the flume is relatively short, and only models 6 groynes. The influence of the inflow conditions can be large therefor, with only a few groyne fields actually representing flow conditions independent of the boundary conditions. Furthermore the accuracy of measurements is limited. The measured water level differences in the flume are in the order of

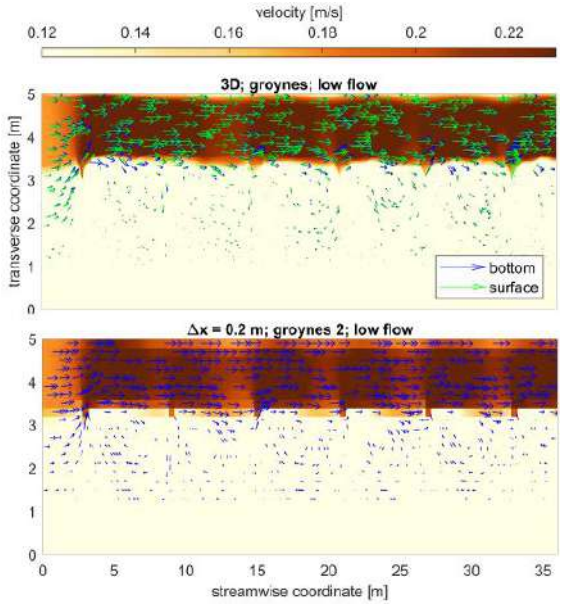

Figure 3. Flow velocities in flume for (Top) 3D modelling of groynes and (Bottom) 2D sub-grid modelling of groynes as two weirs

millimetres, where the additions of groynes and adaptations of the groyne geometry will result in water level changes of the order of 0.1 mm, which is difficult to measure in even a controlled environment.

The current report only shows preliminary results. Future research will also include the modelling of more combinations of water levels and discharges, and of different groyne geometries, with the main goal of the overall research to find a proper modelling practice for adapted groyne geometries.

Conclusion

A research project is started to improve the modelling of groynes. A physical model is set up, together with a numerical model. At the moment the 2D modelling of groynes correspond well to the 3D situation, whereas for submerged groynes the 2D sub-grid modelling of groynes does give satisfactory results.

Acknowledgment

The sixth author of this study (B.Y.) is granted a scholarship for his Post Doc study funded by TUBITAK from Turkey.

References

Ambagts, L. (2019). *Flow over and around submerged groynes - Nuerical modelling and analysis of a groyne flume experiment.* Thesis, Delft.

Chavarrias, V. (2020). *Modelling laboratory groynes: set-up of a DELFT3D-FM model.* Memo, Deltares, Delft.

Yossef, M. F., & Visser, T. (2018). *Effect of groyne schematization on WAQUA model results.* Technical report, Deltares.

Determining the wind drag coefficient for shallow, fetch-limited water systems:

A case study in Fryslân, The Netherlands

Stijn E. Overmeen[a*], Anouk Bomers [a], Nicolette D. Volp [b], Thomas Berends [b], Nynke E. Vellinga [c] & Jord J. Warmink [a],

[a] *University of Twente, Department of Water Engineering and Management, Faculty of Engineering Technology, P.O. Box 217, 7500 AE, Enschede, The Netherlands*

[b] *Nelen & Schuurmans, Zakkendragershof 34-44, 3511AE Utrecht, The Netherlands*

[c] *Wetterskip Fryslân, P.O. Box 36, 8900 AA Leeuwarden, The Netherlands*

Keywords — Wind set-up, wind drag coefficient, shallow waters, fetch-limited systems, wind direction

Introduction

A well-known effect of high sustained winds from one direction is wind set-up (see Figure 1). Water managers strongly benefit from an accurate prediction of the wind set-up from hydrodynamic models to plan adequate measures and ensure safety. Possbile measures are closing barriers or pumping water out of the system. Nevertheless, modelling the wind effect accurately is difficult, especially in fetch-limited water systems, such as the lake system in Fryslân. There is limited information available for practical applications under these circumstances. This study investigates how to determine the wind drag coefficient for these systems to obtain better model predictions.

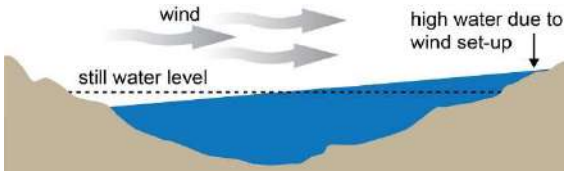

Figure 1. Wind set-up illustration (Watershed Council, 2019)

Theoretical background

The transmission of m omentum between wind and water is a complex and partly unknown process. The momentum transmission is generally formulated as a shear stress term, depending on the relative wind velocity with respect to the water velocity $u_w\,[m/s]$, the density of air $\rho_{air}\,[kg/m^3]$ and a drag coefficient $C_d\,[-]$ (Nelen & Schuurmans, 2020):

$$\tau_w = \rho_{air} C_d |u_w| u_w \qquad (1)$$

It is widely accepted that the transmission of momentum is scaled with a C_d that depends on the mean wind speed at 10 m above the water surface and on the wave state (Grachev et al., 1998). For open seas and oceans, the C_d at high wind speeds is based on an empirical relation that includes merely the wind speed (KNMI, 2017). Meanwhile, in previous modeling studies of large shallow lakes the C_d in the wind stress formulation is defined based on empirical reference values or is calibrated using field data (Cheng et al., 2020).

However, knowledge on drag coefficients for fetch-limited, shallow water systems is scarce. In fetch-limited, shallow water systems the actual wind at the water surface is strongly affected by local characteristics. Therefore, it might deviate strongly from the assumed wind at 10 m height. The local shear stress is affected by the roughness of adjacent terrains, the shielding by obstacles and/ or shores and the effective fetch (see Figure 2 for an illustration). It is hypothesized that these effects need be taken into account to obtain optimal model results. Hence, the objective of this study is to investigate to what extend the drag coefficient varies with three components: not only with wind speed, but also spatially and with wind direction.

Figure 2. Wind shielding on Holland Lake, illustrated by reflection of visible light on waves (Markfort et al., 2010)

Method & Case Study

To investigate the importance of the three described components of C_d, the Frisian bosom will serve as a case study. The Frisian bosom is an enormous system, consisting of openly connected lakes through a dense system of canals (see Figure 4). The impact of strong winds on local water levels can be substantial. A large accumulation of water can develop at one side of the bosom, as water can flow freely through the system. Water level measurements of twenty locations, scattered over the bosom, were used to evaluate the wind set-up. These measurements stations are located within lakes

* Corresponding author
Email address: s.e.overmeen@student.utwente.nl (Stijn Overmeen)

or canals. A 2D hydrodynamical model was set up with the 3Di hydrodynamic software (Nelen & Schuurmans, 2020). This 2D model can integrate the directional effect of the wind. Wind events taken place between 2015 and 2019, categorized based on wind force and direction, served as input for this model.

The wind drag coefficient was calibrated, such that the model output of the water level matched the observations as closely as possible. The Kling-Gupta Efficiency (KGE) objective function was used to assess the simulation results. The calibration was implemented as a progressive Monte-Carlo with parameters values chosen within an interval. After the calibration phase, the optimized drag coefficients were validated using an independent data set per categorized wind event. For each event, an optimal C_d was obtained for the whole domain, as well as for each measurement location separately. Based on these drag coefficients, the variation in space and per wind velocity was determined.

Preliminary results

In total, 23 wind events were simulated. Figure 3 shows an example of the water level at Stavoren, a location in the southwest of the bosom (see Figure 4), during a southwestern wind event with wind forces reaching up to 8 Bft. For this specific event a domain-wide optimal C_d was determined of 1.1×10^{-3} $[-]$, while the variation in optimal C_d per location was approximately 1×10^{-3} $[-]$. The optimal domain-wide drag coefficients show an increasing trend for increasing wind speeds. Furthermore, a small directional dependence is perceived. It seems that these drag coefficients tend to be higher for southwestern and western winds, in comparison to northwestern winds. This could be explained by the larger fetch lengths of the lakes, due to their geometry in line with the wind direction. However, local circumstances seem to affect the results strongly. This is observed in deviations in these trends and is underlined by the variation in optimal drag coefficients per location.

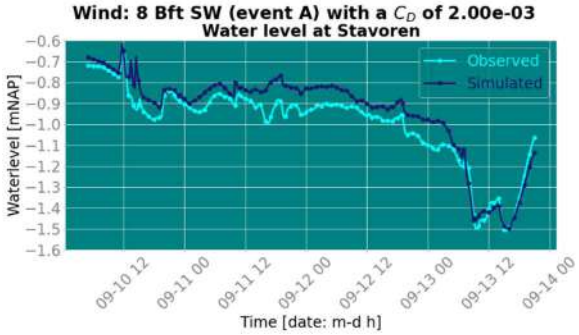

Figure 3. Simulated and observed water levels at Stavoren

References

Cheng, F., Zang, C., Brett, M. T., & Nielsen, J. M. (2020). The importance of the wind-drag coefficient parameterization for hydrodynamic modeling of a large shallow lake. Ecological Informatics, 59

Grachev, A. A., Fairall, C. V., & Larsen, S. E. (1998). On the determination of the neutral drag coefficient in the convective boundary layer. Boundary-Layer Meteorology, 86, 257–278.

KNMI. (2017). Drag at high wind velocities - a review (Tech. Rep.). RWS-VWL.

Markfort, C. D., Perez, A. L. S., Thill, J. W., Jaster, D. A., Porté-Agel, F., & Stefan, H. G. (2010, March). Wind sheltering of a lake by a tree canopy or bluff topography. Water ResourcesResearch,46(3)

Nelen & Schuurmans. (2020). 5. wind effects. Retrieved from https://docs.3di.lizard.net/b_wind.html

Watershed council. (2019). Seiches. Retrieved from https://www.watershedcouncil.org/seiches.html#

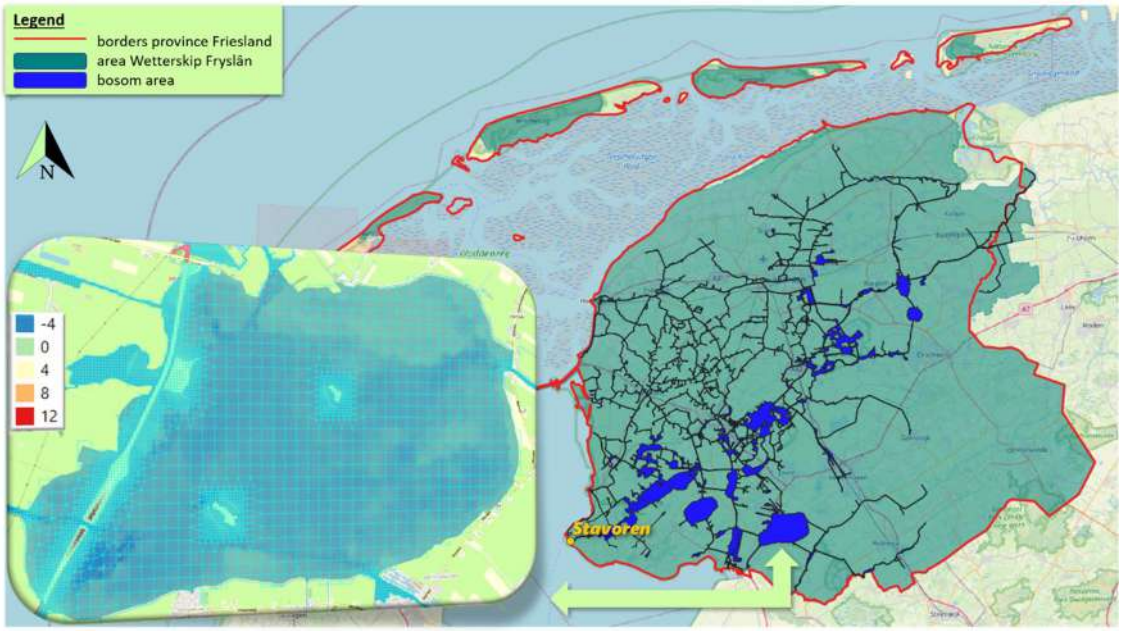

Figure 4. An overview of the Frisian bosom/ model domain (in blue), measurement station Stavoren and a snapshot of the Digital Elevation Model (legend in m+NAP) with the computational grid cells of Tjeukemeer, one of the Frisian lakes (see arrow).

Short-term morphological effects of the pilot 'Xstream-bloc groynes' in the IJssel

Anna Kosters[a*], Frans Buschman[a]
[a]*Deltares, Boussinesqweg 1, 2629 HV Delft*

Keywords — Groynes, local scour, IJssel

Introduction

In the context of the program *Self Supporting River System*, Rijkswaterstaat, BAM/Van den Herik and Deltares are conducting a pilot with an innovative type of groyne, referred to as 'Xstream-bloc groyne' in the remainder of this abstract.

This type of groyne is constructed by dumping Xstream blocs on the river bed. Xstream blocs are concrete elements with a weight of about 27 kg, that are shaped such that they have the ability to interlock. The resulting construction can have several advantages with respect to a traditional groyne construction. One of these advantages is that the concrete elements can easily be removed, added or replaced. Maintenance costs could therefore be reduced compared to traditional groynes, which are difficult to adjust due to their complex construction.

In November 2019, three Xstream-bloc groynes were realised in the IJssel near Kampen, see Fig. 1.

Figure 1. Location of the pilot Xstream-bloc groynes. Image source: Google, 09/05/2020.

In the period between November 2019 and November 2020, the stability and permeability of the groynes, as well as morphological changes in the pilot area were monitored in order to study the functioning of the groynes. In this abstract we describe and analyse the local changes in the river bed level that were observed within the first 6 months after realisation of the groynes.

Method

The river bed level was measured 0, 1, 3 and 6 months after realisation, over a length of approximately 2 km along the river axis (river km 991 – 993). Measurements were carried out with a multibeam echosounder mounted on a small, remotely controlled vessel.

The measurement data was post-processed and interpolated to create images of the river bed level in the pilot area. By subtracting the measured bed levels at two moments in time, the bed level change in the period between the measurements is determined.

Results and discussion

Fig. 2 shows the bed level around river km 992 that was measured 6 months after realisation of the pilot.

On the right bank, both upstream and downstream of Xstream-bloc groyne 1, we clearly see the scour holes downstream of the tip of the traditional groynes in this area. These scour holes result from the local flow pattern near the groyne tips and the generation of macro-turbulence (Yossef, 2002).

For Xstream-bloc groynes, a similar pattern is expected to occur. However, as they have a steeper slope and a more irregular surface than traditional groynes and are somewhat permeable, the dimensions of the resulting scour holes are expected to differ. Furthermore, within 6 months the equilibrium scour depth has most likely not yet been reached.

Fig. 2 shows that only at Xstream-bloc groyne 2 a pronounced scour hole has developed.

* Corresponding author
Email address: anna.kosters@deltares.nl (A. Kosters)

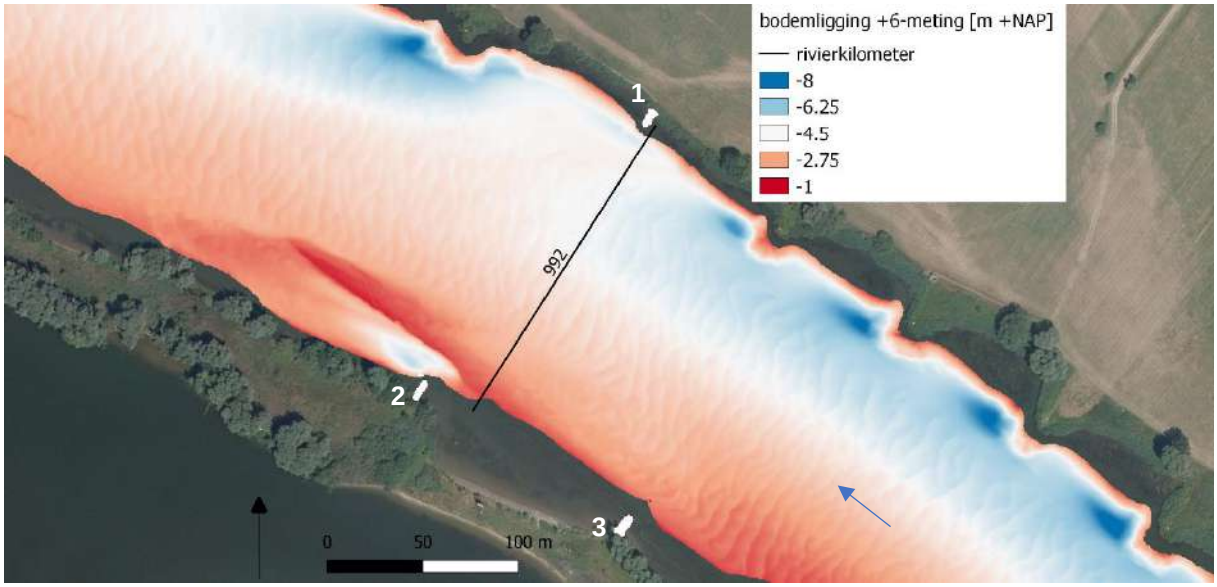

Figure 2. Measured bed level 6 months after realisation of the groynes. The location of the three groynes is indicated in white. The blue arrow indicates the flow direction.

In Fig. 3, showing net bed level change in the first 6 months after realisation, only minor bed level differences are visible near Xstream-bloc groyne 1 and 3.

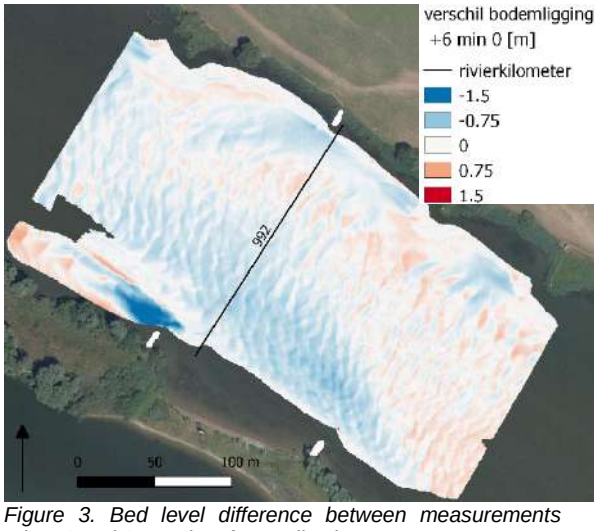

Figure 3. Bed level difference between measurements taken 0 and 6 months after realisation.

For Xstream-bloc groyne 1, this may be explained by the fact that this groyne is much shorter than the surrounding traditional groynes. The groyne is therefore protected from the main flow, such that a pronounced scour hole has not (yet) developed.

For groyne 3, its location in a relatively shallow area plays a role in the resulting morphological effect. Flow velocities are smaller here, thus leading to less scour around the groyne tip. Furthermore, from on-site inspection a layer of cohesive sediment appears to be present parallel to the left bank, extending along groyne 2 and 3 and further up- and downstream (Buschman and Kosters, 2020). Xstream-bloc groyne 3 seems to be located on top of this layer, which is harder to erode than the non-cohesive sediment that is present elsewhere.

Xstream-bloc groyne 2 on the other hand, appears to lie between the cohesive strip and the bank. Hence, erosion occurs within this narrow area, but does not extend in the direction of the main channel due to the presence of the cohesive layer.

Conclusion and recommendations

Three groynes made of concrete elements were constructed in the IJssel near Kampen. Only one of these groynes led to a pronounced scour hole within 6 months after realisation. The other two groynes did not have a significant morphological effect within this period, due to the specific flow and sediment characteristics at their location.

To further investigate the local morphological effects of Xstream-bloc groynes, we recommend to extend groyne 1 toward the main channel and to keep monitoring the bed level at the pilot location.

References

Yossef, M. F. (2002). The effect of groynes on rivers: literature review. Delft Cluster project no. 03.03.04, Delft University of Technology.

Buschman, F. and Kosters, A. (2020). Pilot flexibele kribben in de IJssel. Analyse waarnemingen tot een jaar na aanleg. Deltares rapport 11202372-001-ZWS-0002.

Salt accumulation at floodgates and salt-water intrusion in rivers

Fateme Ebrahimierami[a*], Vasileios Kitsikoudis[a], Bart Vermeulen[b], Suzanne J. M. H. Hulscher[a]
[a] *University of Twente, Department of Marine and Fluvial Systems, Faculty of Engineering Technology P.O. Box 217, 7500 AE, Enschede, the Netherlands*
[b] *Wageningen University, Hydrology & Quantitative Water Management, PO Box 47, 6700 AA, Wageningen, the Netherlands*

Keywords — Salt intrusion, Salt accumulation, Floodgate

Introduction

Salt-water intrusion widely occurs in estuarine areas and can be very problematic to local communities. Worldwide, there is an urgent need for accurate models for salt intrusion predictions since it is one of the most challenging and widespread environmental problems that threaten the quality and sustainability of freshwater resources.
This phenomenon can be aggravated by long-term alterations in weather patterns. On top of this, human activities increased significantly due to heavy urbanization with structural changes to the coastal areas such as deepening of estuaries or construction of gates and locks. Therefore, the understanding of the role of anthropogenic changes on the severity and frequency of salt intrusion events is of high importance in order to get accurate predictions. For example, in Haringvliet inlet in the Rhine-Meuse Delta, the study area of this study, salt intrusion occurs during periods of low flow in the rivers and salt accumulation at floodgates can potentially exacerbate the salinization of freshwater in coastal environments. Hence it is important to understand and quantify how much salt enters freshwater resources through gray-green infrastructures.

Literature review and existing models

Several studies have investigated saltwater intrusion in estuaries. Extensive field data and 3D-hydrostatic (HS) models have been used to study the advection of the salt wedge in the Rotterdam Waterway by De Nijs et al. (2011) and the stratification in the Rhine region of freshwater influence, by Rijnsburger et al. (2016). Schloen et al. (2017) indicated that predictive capabilities of 3D HS models depend on the coupled delta-coastal ocean system, and particularly on the wind and wave forcing and stratification at the mouth of estuaries.

Certain man-made structures such as floodgates that can restrict this free exchange of salt-water and freshwater in an estuary must be managed. Salt can be accumulated in scour pits behind the Haringvliet floodgates and released during every lock cycle towards the inland, resulting in contaminating the freshwater. Flow in a scour hole can be non-hydrostatic (NHS) as Vermeulen et al. (2015) showed for a scour pit in a river bend. NHS models have been used for idealized studies of resonant trapped internal waves generated by sand waves (Labeur and Pietrzak, 2005).

Objective

The final goal of this study is to develop a sophisticated 3D-HS model which will be parameterized by using NHS-3D models and field data from the Haringvliet inlet in the Rhine-Meuse Delta in order to model salt exchange through low dynamic systems such as floodgates.
The model will be able to establish under which conditions salt accumulates in scour pits and under which conditions the salt is released again into the inland freshwater systems. To reach the ultimate objective, a better understanding of the trapping and releasing processes is needed. This insight will be obtained by extensive field measurements to mitigate and control freshwater salinization.

Methodology

Vermeulen et al. (2015) showed that the hydrostatic pressure distribution of flow turns to non-hydrostatic into the scour pits. In order to explore whether the same transition happens to the flow in the scour pits near the floodgates of the Haringvliet system, intensive field data collection will be carried out by using CTD casts and ADCPs (Acoustic Doppler Current Profilers) in the study site which is shown on Fig. 1. Same instrumentation will be used to monitor the inland propagation of the salt wedge.

* Corresponding author
Email address: f.ebrahimierami@utwente.nl (Fateme Ebrahimierami)

Figure 1. Top view of the study site at Haringvliet and the location in the Netherlands. Retrieved from Google Maps

For a better understanding and quantification of the NHS flow, the novel and available measurement techniques developed by Vermeulen et al. (2014) will be adapted and modified accordingly. Additional instruments will be deployed to complement the existing data.
By parameterizing non-hydrostatic effects in scour holes, a 3D-HS model will be developed to simulate the trapping and release process of salt.

Expected result and application

This research strives to deliver an advanced 3D-HS salt intrusion model which is validated and parameterized for the NHS physical processes that occur at floodgates by data retrieved from field measurements.
This model can be applied in estuaries to simulate the salt exchange through low dynamic systems, such as floodgates.

Acknowledgment

This work is part of the Perspective Program, project Saltisolutions, which is financed by NWO Domain Applied and Engineering Sciences, in collaboration with private and public partners.

References

De Nijs, M.A.J., Pietrzak, J.D., Winterwerp, J.C., (2011). Advection of the salt wedge and evolution of the internal flow structure in the Rotterdam Waterway. Journal of Physical Oceanography, 41, 3-27.

Labeur, R.J., Pietrzak, J.D. (2005). A fully three dimensional unstructured grid non-hydrostatic finite element coastal model, Ocean Modelling, 10, 51-67.

Rijnsburger, S, Hout, C.M. van der, Tongeren, O. van, Boer, G.J. de, Prooijen, B.C. van, Borst W.G., Pietrzak, J.D. (2016). Simultaneous measurements of tidal straining and advection at two parallel transects far downstream in the Rhine ROFI. Ocean Dynamics, 66(5), 719-736.

Schloen, J., Stanev, E.V., Grashorn, S. (2017). Wave current interactions in the southern North Sea, Ocean Modelling, 111, 19-37.

Vermeulen, B., Hoitink, A.J.F., Labeur, R.J. (2015). Flow structure caused by a local cross-sectional area increase and curvature in a sharp river bend. Journal of Geophysical Research, 120(9), 1771-1783.

Vermeulen, B., Sassi, M.G., Hoitink, A.J.F. (2014). Improved flow velocity estimates from moving-boat ADCP measurements. Water Resources Research., 50(5), 4186-4196.

Approaches to predict bedform states, associated flow resistance and depth: Physics-based to machine learning

Amin Shakya[a], Sanjay Giri[b], David C. Froehlich[c], Toshiki Iwasaki[d], Satomi Yamaguchi[d], Mohamed Nabi[b], Suleyman Naqshband[e], Pravash Mool[f], Biswa Bhattacharya[a], Yasuyuki Shimizu[d]
[a]*IHE Delft, Department of Hydroinformatics and Socio-Technical Innovation, 2601 DA, Delft, the Netherlands*
[b]*Deltares, 2600 MH, Delft, the Netherlands*
[c]*303 Frenchmans Bluff Drive, Cary, North Carolina 27513, USA*
[d]*Hokkaido University, Sapporo, Japan*
[e]*Wageningen University, Department of Environmental Sciences, Wageningen, The Netherlands*
[f]*Hydroconsult, Kathmandu, Nepal*

Keywords – Lowland River, Bedforms, Flow Resistance, Hysteresis, Numerical Model, Machine Learning (ML)

Introduction

Lowland rivers are an essential component of fluvial and coastal deltas. It is important to understand and assess their behaviour to manage and adapt to various phenomena such as floods, drought, groundwater, ecology, erosion and sedimentation that are directly associated with the livelihood, safety and security. Evolution of fluvial bedforms in lowland rivers is a micro-scale morphological process that influences river management decisions, for example, high-flow (for flood management), and low-flow (for navigation and other water use) prediction. Numerical models are widely used to predict flow levels and morphological changes in various studies and implementation projects such as 'Room for the River' and 'Sustainable Navigation at Rhine Branches' in The Netherlands. This work builds upon our past efforts that include physics-based modelling, physical experiments and the machine learning techniques to predict bedform features, states, associated flow resistance and depth.

State-of-the-art

We revisit our works on developing and applying numerical models that are simple to sophisticate, such as Delft3D model with an attempt to consider roughness variation under varying flow considering bedform height and lag (Giri et al., 2008). There are some CFD models, capable of simulating bedform evolution (Giri and Shimizu, 2006; Paarlberg et al.,2009; Niemann et al., 2011; Nabi, 2012). However, only a few of them are capable to simulate bedform transition, associated flow resistance and depth in a physics-based manner under steady and varying flow conditions (e.g. Giri and Shimizu, 2006). Most of these models can only be applied for small-scale high-resolution modelling to capture the underlying physical processes (an example of a simulated result is depicted in Fig.1). Giri et al. (2015) applied the model for the Waal River. Nelson et al. (2010) coupled the models, in which the flow resistance was computed using the CFD model and used as an input to a large-scale model. However, such an approach is not very efficient for extensive application in real-world problems. Recently, Froehlich and Giri (2019) applied a machine learning (Artificial Neural Network) to classify bedform states – ripples, dunes, plane beds, and anti-dunes. They used field and laboratory data to develop the approach. It should be noted that there is not much data available related to dune evolution and transition processes. It is rather difficult to measure them during a flood wave.

Findings and a way forward

Despite an extensive application of numerical models in river engineering and management efforts, there are noticeable inaccuracies and uncertainties in their prediction. There are various physical and non-physical reasons (numerical artefacts, discretization, imprecise inputs) for such inaccuracies and uncertainties. A major problem is related to the prediction of micro-scale morphological changes and associated flow resistance (form drag) in alluvial rivers. These morphological changes are associated with the evolution and transition of micro-scale bedforms (e.g., ripples, dunes, anti-dunes, flatbed transitions) under varying flow. Such micro-scale features are typical for many alluvial rivers regardless of their differences in spatial and temporal dynamics, such as largely engineered and less dynamic Rhine branches (in The Netherlands) and mostly natural and highly dynamic Lower Brahmaputra (in Bangladesh). In such rivers, the evolution and transition of river bedforms during the rising and falling stages of a flood wave have a noticeable impact on morphology and flow levels. The interactions between flow and micro-scale bedforms cannot be considered in a physics-based manner in large-scale

* Corresponding author
Email address: sanjay.giri@deltares.nl (Sanjay Giri)

numerical models due to the incompatibility between the resolution of the models and the scale of morphological changes. The dynamic changes in bedforms and the corresponding changes in flow resistance are not captured. Instead, flow resistance in most of the large-scale models is parameterized as a roughness coefficient. It is used as a tuning parameter for model calibration that cannot always be physically justified. Some modelling tools allow using a discharge-dependent roughness coefficient. In contrast, others incorporate semi-empirical/empirical formulations to consider changes in flow resistance under varying flow (e.g. depth-dependent or bedform height-dependent roughness). However, there is no generic relationship for roughness variation under varying flow conditions considering bedform evolution and transition processes.

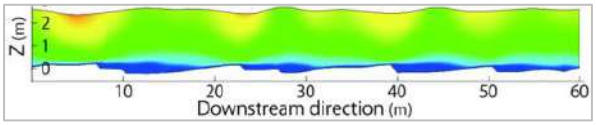

Figure 1 Simulated result of bedforms, velocity and flow depth by the model (Yamaguchi et.al, 2019; Giri & Shimizu, 2006)

In this research, it is proposed to apply a state-of-the-art CFD model, field and laboratory observations to generate a large amount of data, analyse them and develop a ML model. The CFD model, developed at Hokkaido University (Giri and Shimizu, 2006; Shimizu et al., 2009; Yamaguchi et al., 2019), which can replicate bedform evolution and transition processes as well as associated flow resistance and its effect on flow level variation under steady and varying flow conditions. The model can simulate the hysteresis effect (an example is shown in Fig.2). Proposed steps can be outlined as follows: (i) carry out a wide range of scenario simulations and analysis of bedform evolution, transition, and associated flow resistance under a range of steady and varying flow conditions to generate a sufficient amount of data by making use of proposed model; (ii) conduct sensitivity analysis of the model results to evaluate the quality and reliability of simulated data (e.g., using observed data and statistical/spectral analysis of numerical results); (iii) collect and analyse the data from field and laboratory observations; (iv) develop a generic model based on generated data using machine learning to predict bedform characteristics, states and associated flow resistance under steady and varying flow conditions.

Concluding remarks

The review reveals that the research is needed to address one of the major sources of uncertainty that large-scale numerical models cannot resolve appropriately due to large spatial and temporal scales of solution domains as well as solution schemes. The hybrid approach of using CFD and ML models can offer better prediction of flow resistance that can be coupled with large-scale numerical models to improve their performance. The ML model can also be used to predict bedform characteristics, states and flow depth (useful for assessing inland navigability and optimal improvement measures). The research is in progress.

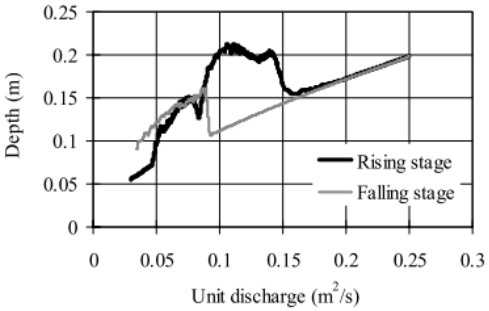

Figure 2 Stage-discharge relation showing hysteresis effect under varying flow, simulated by the model (Shimizu et al., 2009)

References

Froehlich, D. C., and Giri, S. (2019). Teaching a Machine to Predict Alluvial Stream Bedforms, 14th International Symposium on River Sedimentation, Chengdu, China

Giri, S., and Shimizu, Y. (2006). Numerical computation of sand dune migration with free surface flow, Water Resour. Res., 42 (10), W10422.

Giri, S., S. van Vuren, W. Ottevanger, K. Sloff, and A. Sieben (2008). A preliminary analysis of bedform evolution in the Waal during 2002-2003 flood event using Delft3D. Proceedings of MARID, Leads, UK

Giri, S., Yamaguchi, S., Nabi, M., Nelson, J. M., and Shimizu, Y. (2015). Numerical modeling of river dunes in the Waal under extreme flood, Proceedings of the 36th IAHR World Congress, June 28 – July 3, The Hague, The Netherlands

Niemann, S. L., Fredsoe, J., and Jacobsen, N. G. (2011), Sand Dunes in Steady Flow at Low Froude Numbers: Dune Height Evolution and Flow Resistance, J. Hydraul. Eng, ASCE, Vol. 137, No. 1, 5-14

Nabi, M. (2012). Computational modelling of small-scale river morphodynamics, Ph.D. thesis, Delft Univ. of Technol., Delft, Netherlands.

Nelson, J.M., Shimizu, Y., Giri, S., McDonald, R. R. (2010). Computational Modelling of Bedform Evolution in Rivers with Implications for Predictions of Flood Stage and Bed Evolution, 2nd Joint Federal Interagency Conference, Las Vegas, NV, June 27 - July 1, 2010

Paarlberg, A. J., Dohmen-Janssen, C. M., Hulscher, SJMH, and Termes, P. (2009). Modeling river dune evolution using a parameterization of flow separation, J. of Geophys. Res., Pt. F: Earth surface, 114 (F01014). ISSN 0148-0227

Shimizu, Y., Giri, S., Yamaguchi, S., and Nelson, J. (2009). Numerical simulation of dune–flatbed transition and stage-discharge relationship with hysteresis effect, Water Resour. Res., 45, W04429, doi:10.1029/2008WR006830

Yamaguchi, S., Giri S., Shimizu Y., Nelson J. M. (2019). Morphological Computation of Dune Evolution with Equilibrium and Non-Equilibrium Sediment-Transport Models, Water Resources Research 55-11, https://doi.org/10.1029/2018WR024166

Poster session II

The influence of mesh structure on simulated water levels and flow velocities in meander rivers

E. Bilgili[a,b,*], A. Bomers[a], J. van Lente[b], F. Huthoff[a,b], S. J. M. H. Hulscher[a]
[a] *University of Twente, Enschede, the Netherlands*
[b] *HKV lijn in water, Lelystad, the Netherlands*

Keywords — Mesh resolution, Mesh shape, Numerical diffusion, False diffusion, Two-dimensional depth-averaged model

Introduction

A detailed insight in flow patterns in rivers is essential to evaluate the efficacy and impact of river interventions. To investigate such processes, a common approach is by making use of hydrodynamic simulations, which solve the (depth-averaged) shallow water equations. Fully triangular and fully curvilinear meshes are commonly applied in these models to discretise study areas. It is also possible to combine curvilinear and triangular mesh cells, which is known as a hybrid mesh (see Fig. 3). In *Bomers et al.* (2019), it is shown that the accuracy and computation time of depth-averaged models are substantially influenced by the mesh structure.

In *Caviedes-Voullième et al.* (2012) and *Bomers et al.* (2019), it is highlighted that in river models, poor alignment between mesh and the direction of the flow and mesh coarsening cause a smoothed hydrograph, resulting in a lower depth-averaged flow velocities and hence higher water levels. These numerical errors by a mesh are known as respectively false diffusion and numerical diffusion. Nonetheless, in *Caviedes-Voullième et al.* (2012) and *Bomers et al.* (2019), the numerical errors are interrelated with how well the bathymetry is captured by a mesh. Therefore, it is unclear to what extent numerical errors affect hydraulic river modelling outcomes, especially in river bends. Therefore, the objective of this study is to understand under which conditions numerical errors influence the outcomes of a hydraulic model in schematised meander bends with a flat bed.

Method

The characteristics of the Grensmaas river, which is a section of the Meuse River in the Netherlands, is used to set up the schematised rivers. In the Grensmaas river, both mild and sharp bends are present, with local variations in floodplain width. In order to capture the extremes of these geometrical characteristics in the Grensmaas river, four idealised river schematisations are set up which can be differentiated by a mild or sharp bend and the presence or absence of floodplains (Fig. 1 and 2).

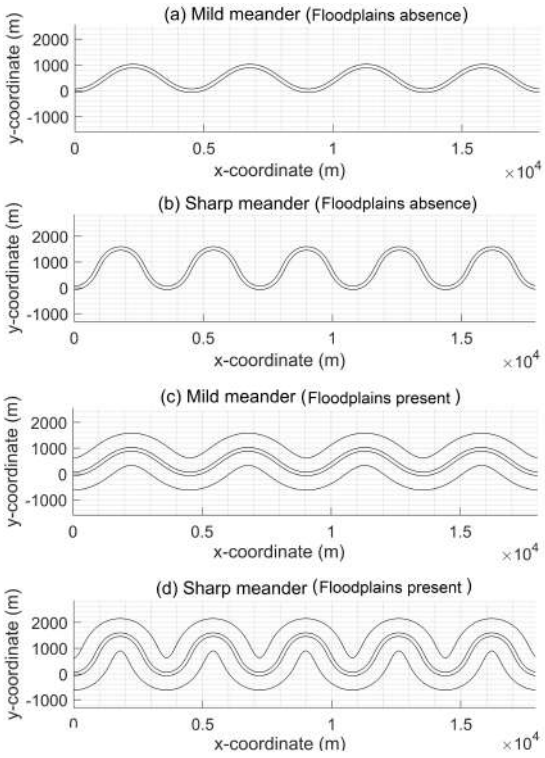

Figure 1: In (a-d) a top-view of a section of the four schematised rivers.

A floodplain height of 6 m is considered with respect to the bed level of the main channel for the cases with floodplains (Fig. 2). A valley slope of 4.49×10^{-4} m/m is applied for all idealised models, which is the slope along a straight line through the meanders bends. A constant bed level in transverse flow direction is used, except for the transition between main channel and floodplains. At $x = 0$, all four rivers are forced with a constant discharge until similar water levels are obtained between the cases. Three flow scenarios are simulated with each lasting 10 days: (i) low; (ii) mid and (iii) high discharge range. The downstream boundary conditions are set by predefined rat-

*Corresponding author
Email address: eray.bilgili10@gmail.com (E. Bilgili)

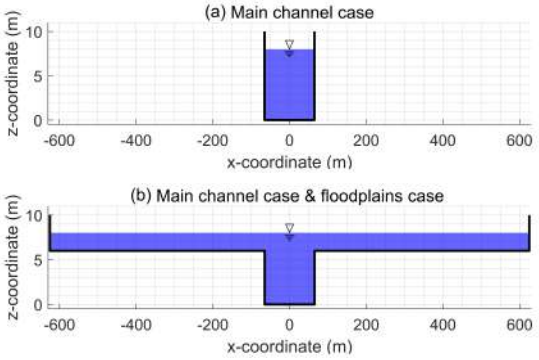

Figure 2: In (a-b) the applied cross-sections in the absence/presence of floodplains respectively.

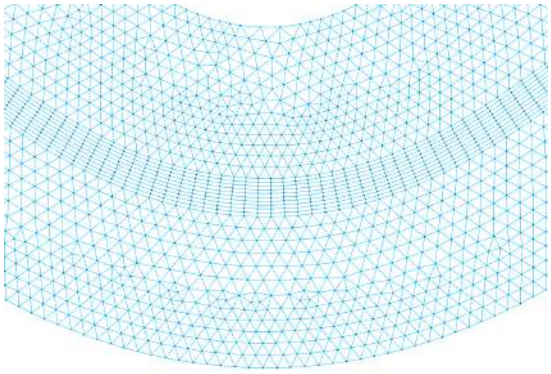

Figure 3: Medium resolution hybrid mesh for the schematised mild river meander with floodplains.

ing curves based on steady uniform flow considerations.

In cases a and b (Fig. 1), triangular and curvilinear meshes are considered with three different mesh resolutions (low, medium and high). In terms of the resolution in the main channel of the triangular meshes, 3, 4 and 8 cells are placed in the transverse flow direction for respectively the low, medium and high resolution. For the curvilinear meshes, 5, 10 and 20 mesh cells are placed in the transverse flow direction for respectively the low, medium and high resolution. In cases c and d (Fig. 1), curvilinear and triangular meshes, as well as hybrid meshes are used with only a medium and high mesh resolution (Fig. 3). To perform the computations, D-Flow FM is used as the modelling software.

Results

The analysis showed that in the schematised river meanders in the absence of floodplains, lower depth-averaged flow velocities and hence higher water depths are obtained with coarser meshes. In the sharper bend larger deviations are simulated since rapid flow changes have to be captured by the meshes, which eventually leads to a greater numerical diffusion. At higher discharges, these differences become more evident. Regarding the differences between mesh shapes, a lower false diffusion is obtained with triangular meshes at lower resolutions than curvilinear meshes. In contrast to the former, the low resolution curvilinear meshes are less capable of capturing the flow changes in the river bends due to their highly stretched cells. For the highest resolution of both meshes, the opposite is observed.

In terms of the water level in cases c and d (Fig. 1), negligible deviations are obtained, which is in contrast to the cases without floodplains. This is a consequence of relatively less deviations in depth-averaged flow velocity differences in the floodplains even though considerable differences are observed in the main channel.

Conclusion

The results showed that the generated false diffusion and numerical diffusion become larger in the case of higher discharges and hence higher depth-averaged flow velocities, and under circumstances in which rapid flow changes occur (i.e. for cases with sharp river bends). The influence of the generated numerical diffusion and false diffusion is dampened by the presence of floodplains. This suggest that the numerical errors are proportional to the discharge per unit width.

References

Bomers A., Schielen R., Hulscher S. (2019, 2). The influence of grid shape and grid size on hydraulic river modelling performance. *Environmental fluid mechanics 19*(5), 1273–1294. Springer. doi:10.1007/s10652-019-09670-4.

Caviedes-Voullieme D., Garcia-Navarro P., Murillo J. (2012, 07). Influence of mesh structure on 2d full shallow water equations and scs curve number simulation of rainfall/runoff events. *Journal of Hydrology s 448–449,* (39-59). doi:10.1016/j.jhydrol.2012.04.006.

Modelling morphodynamic changes over fixed layers

Victor Chavarrias[a,*], Willem Ottevanger[a], Kees Sloff[a,b], Erik Mosselman[a,b]
[a] *Deltares, Delft, the Netherlands.*
[b] *Faculty of Civil and Environmental Engineering, Delft University of Technology, Delft, the Netherlands.*

Keywords — Morphodynamics, mixed-size sediment, fixed layers

Introduction

A physical process relevant for accurately predicting morphodynamic development in some areas in the Dutch river system such as the bifurcation areas of the Rhine and in the Meuse, is the formation and break-up of immobile sediment layers (a.k.a. fixed layers). Immobile sediment layers develop by vertical sorting processes in the top layer of the bed. Under low-flow conditions, only the finest sediment-size fractions at the bed surface are mobile. Winnowing and transport of fine sediment causes the formation of a layer of coarse sediment over which fine sediment is transported. During high-flow events, these coarse layers can break up, suddenly entraining sediment from below.

Several modelling approaches exist for predicting morphodynamic development under the presence of immobile sediment. However, they present several limitations which limit their applicability range. Here we review the modelling approaches, show the limitations, and develop two possible modelling alternatives that are tested against laboratory measurements.

Existing modelling approaches

Struiksma (1999) modified the Exner equation used for modelling bed level changes under alluvial conditions. He prescribed an alluvial thickness and reduced the sediment transport if the actual sediment thickness above the fixed layer became smaller than the alluvial thickness. This reduction depended on the ratio of actual thickness to alluvial thickness.

Struiksma (1999) conducted flume experiments for testing his approach. A fixed layer of limited length composed of coarse sediment was installed in a fine-sediment bed. A trench was dug upstream. It exposed the fixed layer as it travelled downstream. We modelled the experiments using Elv (Chavarrías et al., 2019). Figures 1, 2, and 3 show the initial condition, an intermediate situation, and the final state using Struiksma's model. Sediment size-fractions 1 and 2 correspond to fine and coarse sediment, respectively.

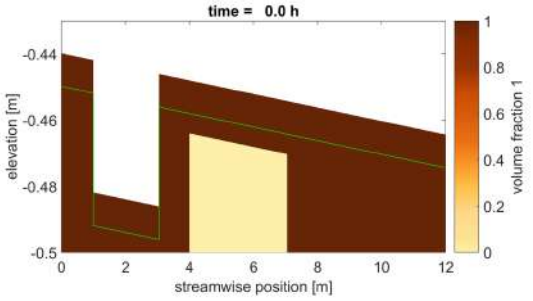

Figure 1: Initial condition.

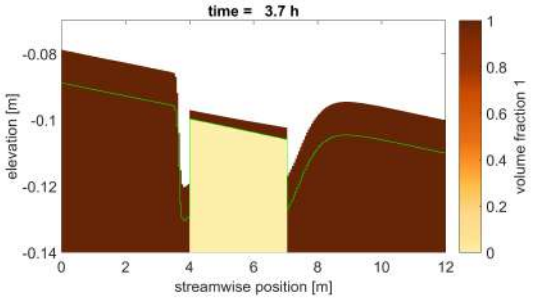

Figure 2: Intermediate state using Struiksma's model.

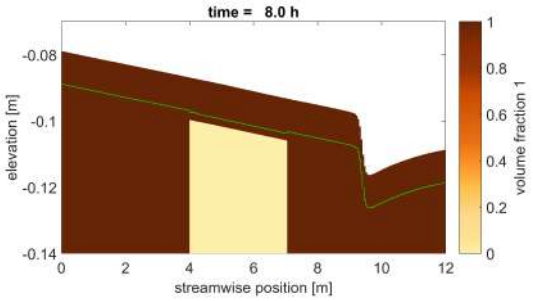

Figure 3: Final state using Struiksma's model.

Struiksma's model can only be used when the sediment forming the fixed layer is never mobile. In order to consider cases in which sediment may become mobile, one can consider using the active-layer model. In this case, as the bed degrades, immobile sediment enters the active layer (Figure 4). Immobile sediment in the active layer reduces the sediment transport rate of fine sediment not only because of

*Corresponding author
Email address: victor.chavarrias@deltares.nl (Victor Chavarrias)

its presence (i.e., a smaller amount of fine sediment is present at the bed surface) but also due to the hiding-exposure effect. Unfortunately, under aggradational conditions a physically unrealistic process occurs. Sediment in the active layer is equally transferred to the substrate, which causes immobile sediment to be transported upwards (Figure 5).

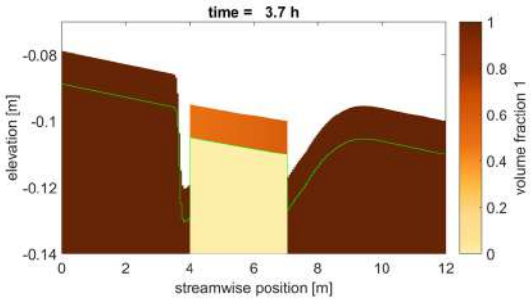

Figure 4: Intermediate state using the active-layer model.

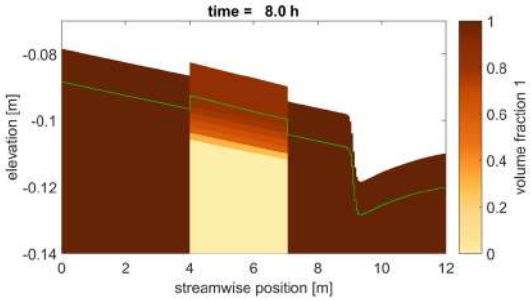

Figure 5: Final state using the active-layer model.

Tuijnder and Ribberink (2010) developed a model for predicting the formation and breakup of immobile sediment layers adding a "coarse layer" below the active layer. The essence of the model is that immobile sediment in the active layer is transferred to the coarse layer. The model, featuring a large number of closure relations and complex fluxes, presents certain limitations and modelling of the same experiment in Delft3D does not fully solve the issue of the active-layer model (Chavarrias et al., 2020).

Model development

We developed two alternatives for modelling morphodynamic development under the presence of sediment that may be immobile. The first one consisted of a modification of the active-layer model in which, under aggradational condition, immobile sediment in the active layer (if any) is preferentially transferred to the substrate. This prevents unrealistic upward transport of immobile sediment. The intermediate state of the experiment is the same as when using the active-layer model and the final state is the same as when using the model by Struiksma (1999).

The second alternative, implemented in Delft3D, is a simplification of the model by Tuijnder et al. rethinking the sediment fluxes. The model behaves as Struiksma's model when modelling the laboratory experiment and allows transport of coarse sediment if this becomes mobile.

Conclusions and future development

Two models have been developed for predicting morphodynamic changes under conditions in which sediment may be immobile. The main difference is that in one of them immobile sediment is allowed to be in the active layer while in the second one it does not enter. Both models correctly reproduce the laboratory experiment by Struiksma. The first one has the benefit that mobile sediment is affected by hiding-exposure. This is also an inconvenience if the difference in grain size is larger than the range of applicability of the usual relations. The second model presents some limitations when, for instance, all sediment becomes immobile.

Probably the first alternative is more realistic and robust, although an improved hiding-exposure relation must be developed for modelling cases in which immobile sediment is significantly larger than the mobile one. Laboratory experiment would be necessary for this development. The models need to be applied to other situations (especially field cases) for clarifying the applicability.

Acknowledgements

This project is part of KPP Rivierkunde funded by Rijkswaterstaat thanks to Arjan Sieben and Rien van Zetten.

References

Chavarrias, V., Ottevanger, W., Mosselman, E., 2020. Morphodynamic modelling over alluvial and non-alluvial layers. Literature review, update to Tuijnder concept. Technical Report 11205235-016-ZWS-0006_v0.1. Deltares.

Chavarrías, V., Stecca, G., Siviglia, A., Blom, A., 2019. A regularization strategy for modeling mixed-sediment river morphodynamics. Adv. Water Resour. 127, 291–309.

Struiksma, N., 1999. Mathematical modelling of bedload transport over non-erodible layers, in: Proc. RCEM, Genova, Italy, pp. 89–98.

Tuijnder, A., Ribberink, J., 2010. A morphological concept for semi-fixed layers. Technical Report 2011R-003/WEM-003. Twente University.

Impact of *Chelicorophium curvispinum* on the concentration-discharge response of suspended sediment in the Rhine River

Marcel van der Perk[a]
[a]*Utrecht University, Department of Physical Geography, P.O. Box 80.115, 3508 TC Utrecht, The Netherlands*

Keywords — suspended sediment, Rhine River, sediment rating curve, invasive species

Introduction

In an ongoing study to the decline in suspended sediment concentrations and loads in the Rhine river at the Lobith monitoring station, the Netherlands, since the mid-1950s (Fig. 1; Van der Perk et al., 2019), the temporal changes in the power-law sediment rating curve parameters were examined. This exploratory study revealed that the rating exponent b of the rating curve increased substantially between the early and late 1980s. This period coincided with the period that the Ponto-Caspian *Chelicorophium curvispinum* (Caspian mud shrimp) invaded the Rhine river basin. *Chelicorophium curvispinum* is a suspension feeder, filtering suspended particles from the water column (Van den Brink et al., 1993) and so forms dense colonies of muddy tubes on stony substrates. The filtering of suspended solids results in a removal of suspended solids from the water and hence in a reduction of the suspended sediment concentration. This invasive species could explosively populate the Rhine river following the Sandoz chemical accident in Basel, Switzerland, in November 1986. This accident caused massive fish kills in the Rhine river and so created opportunities for new aquatic settlers to fill the empty niches (Den Hartog et al., 1992).

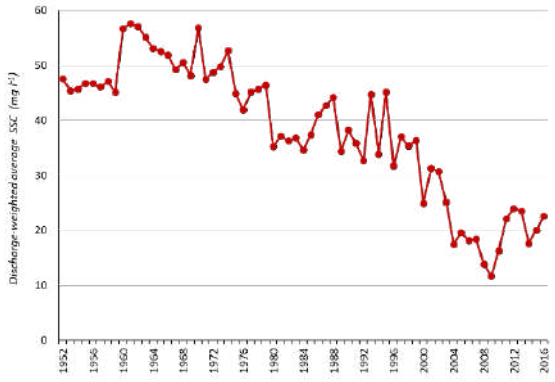

Figure 1. Decline of the discharge-weighted average suspended sediment concentrations (SSC) in the Rhine river at the Lobith monitoring statopn between 1952 and 2016(Van der Perk et al., 2019)

* Corresponding author
Email address: m.vanderperk@uu.nl (Marcel van der Perk)

Tilting of the sediment rating curve

The power-law sediment rating curve takes the form

$$SSC = a\,Q^b \quad (1)$$

where *SSC* = suspended sediment concentration (mg l^{-1}), *Q* = discharge (m^3 s^{-1}), and *a* and *b* are the rating curve parameters. Fig. 2 shows the 5-year rating curves for the River Rhine at the Lobith monitoring station since the mid-1950s. In general, the vertical position of the rating curves decreased over the years, which is in line with the above long-term declining trend in suspended sediment concentrations.

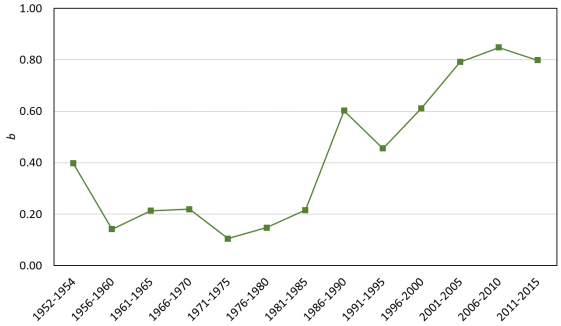

Figure 2. Temporal variation of the rating exponent b for the 5-year periods between 1952 and 2016 (Van der Perk et al., 2019)

The relatively flat pre-mid-1980s rating curves indicate relatively small values of the rating exponent b. The values of parameter b generally varied around 0.2 (Fig. 3). For three 5-year periods, the value of b did even not differ significantly from 0. In the mid-1980s, parameter b increased suddenly to a value between 0.4 and 0.6 and since then has remained within this range. Accordingly, the rating curve tilted during the mid-1980s.

This tilting of the rating curves can primarily be attributed to a decrease in suspended sediment concentrations during low flow conditions, which was partly compensated by increased SSC during high discharges as observed in the rating

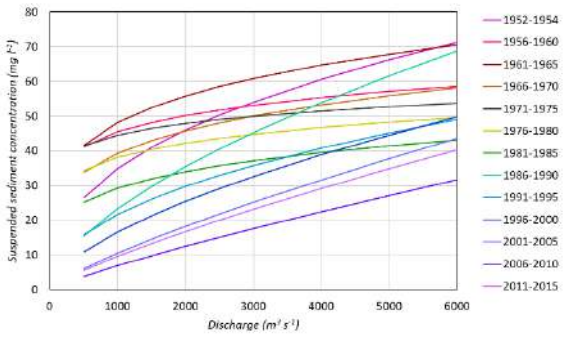

Figure 3. Fitted sediment rating curves for the 5-year periods between 1952 and 2016 (Van der Perk et al., 2019)

curve for the period 1986-1990. In the subsequent periods, the declining trend as reflected in the vertical position of the rating curves continued.

Interpretation and implications

The coincidence of the sudden increase in the rating curve exponent b during the mid-1980s and the invasion of *Chelicorophium curvispinum* leads to the hypothesis that this species bears the prime responsibility for this increase. However, this jumpwise increase in parameter b does not become manifest in the long-term gradual trend of declining suspended sediment concentrations and vice versa. Apparently, the sequestration of sediment by *Chelicorophium curvispinum* is only temporary and does not affect the annual average suspended sediment concentrations and loads. This sequestration has the largest effect on the suspended sediment concentrations during low flow conditions. The initial increase in SSC for high discharges in the period following the invasion *Chelicorophium curvispinum* indicates that the stored sediment is remobilised during periods high discharge. Therefore, the invasion of *Chelicorophium curvispinum* has not had a significant effect on long-term suspended sediment transport and thus has not played a significant role in the decline of suspended sediment concentrations. The precise reasons for this gradual decline in suspended sediment concentration remain yet unknown. The hypothesis that the invasion of *Chelicorophium curvispinum* is responsible sudden increase in the rating curve parameter b and associated tilting of the rating curve requires further study and independent evidence.

References

Den Hartog, C., Van den Brink, F. W. B., Van der Velde, G. (1992). Why was the invasion of the River Rhine by Corophium curvispinum and Corbicula species so successful?. Journal of Natural History, 26(6), 1121-1129.

Van den Brink, F. W. B., Van der Velde, G., & Bij de Vaate, A. (1993). Ecological aspects, explosive range extension and impact of a mass invader, Corophium curvispinum Sars, 1895 (Crustacea: Amphipoda), in the Lower Rhine (The Netherlands). Oecologia, 93(2): 224-232.

Van der Perk, M., C.A.T. Sutari, H. Middelkoop (2019) Examination of the declining trend in suspended sediment loads in the Rhine River in the period 1952-2016. In: E. Stouthamer, H. Middelkoop, M. Kleinhans, M. van der Perk, & M. Straatsma (Eds.) (2019) Land of Rivers: NCR DAYS 2019 Proceedings. Netherlands Centre for River Studies Publication 43-2019: 73-74.

Multiscale bedform migration and interaction in the Waal river, the Netherlands

Judith Y. Zomer[a,*], Suleyman Naqshband[a], A.J.F. (Ton) Hoitink[a]

[a] *Wageningen University & Research, Department of Environmental Sciences, Hydrology and Quantitative Water Management Group, P.O. 47, 6700 AA, Wageningen, the Netherlands*

Keywords — Bedform superimposition, Low-angle river dunes, Multibeam Echosounding

Introduction

Trains of secondary bedforms, superimposed on primary dunes, have been observed in rivers worldwide. To date, it has remained unclear how these secondary bedforms affect the hydraulics and sediment transport dynamics in a fluvial system. We have studied the dynamics and properties of secondary bedforms, superimposed on large fluvial river dunes and quantified the sediment transport rates associated with primary and secondary bedform migration. We further investigated the correlation between primary and secondary dune properties and determined when secondary bedforms persist on the primary dune's lee slope and thus form an additional bedload transport component.

Methods

A field campaign was conducted in the river Waal, near Ophemert. The river bed was scanned over a reach of 460 m, through MBES (Multibeam Echosounding). Within the same reach, 8 repeat measurements were done. The MBES data were interpolated on a 0.1 m equidistant grid. The secondary bedform morphology was separated from the underlying morphology, including primary dunes, following *Zomer et al.* (in review). Secondary bedform properties, and primary dune length and height were determined following *Van der Mark and Blom* (2007). The primary lee side angles were determined as the maximum lee side angle between the trough and upstream dune crest. Primary dune migration was determined based on complimentary MBES data, made available by Rijkswaterstaat.

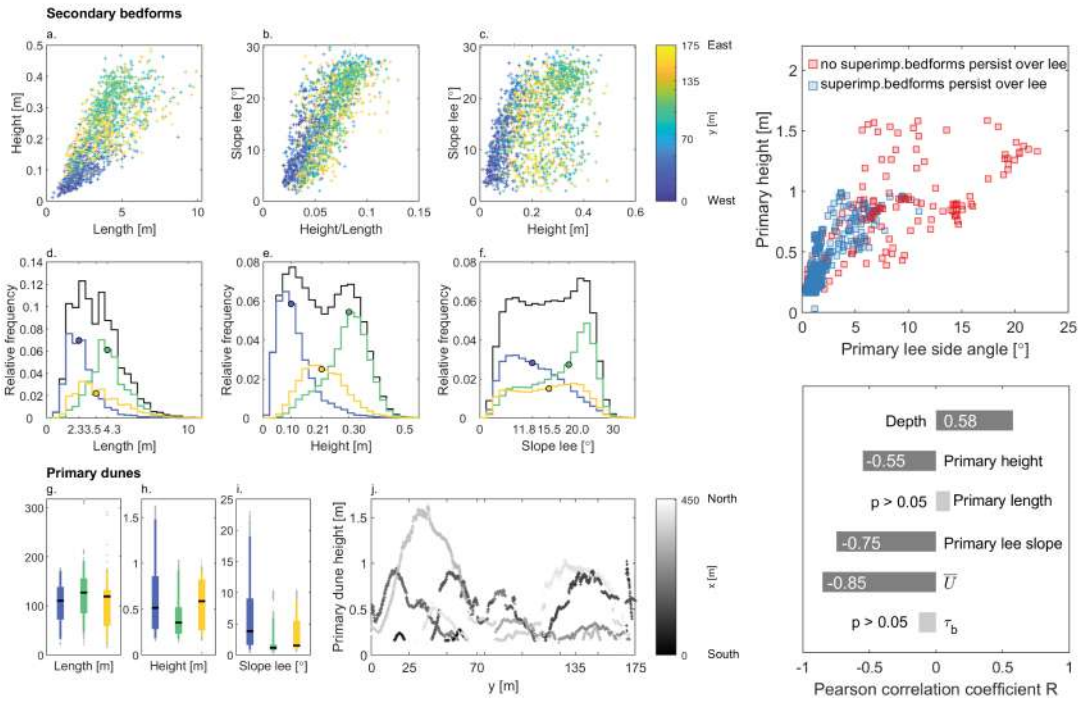

Figure 1: a-j: Properties of the primary and secondary bedforms. Plots d-f show the distribution of secondary bedform properties per section, as well as the median value per section. Plots g-i show the distribution ([5,25,50,75,95]th percentiles) of primary dune properties per section. The sections are indicated with blue ($y \leq 70$ m), green (70 m$< y \leq 135$ m), and yellow ($y > 135$ m). k: Heights and maximum lee side slopes of primary dunes. l: Pearson correlation coefficients indicating the correlation between secondary bedform height on the one hand, and depth, primary dune properties, and flow properties ($\overline{U}$, τ_b) on the other hand.

*Corresponding author
Email address: judith.zomer@wur.nl (Judith Y. Zomer)

Results and discussion

Fig. 1 shows the cross-channel variation in primary and secondary bedform properties. Secondary bedforms are larger and more developed in the central section, where they persist over low-angle primary lee slopes. In the western section, primary dune have largest heights and lee side slopes, whereas superimposed secondary bedforms are small. Fig. 1-k indicates that secondary bedforms can only persist over primary lee slopes with angles below 11°. Fig. 1-l further indicates that secondary bedform height inversely correlates with primary height and lee side slope.

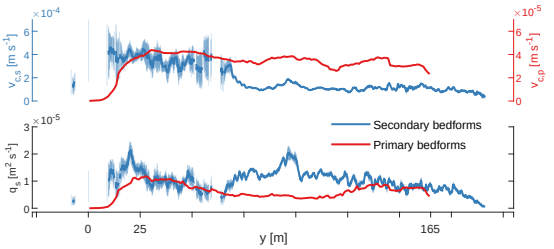

Figure 2: Top: The migration celerity of secondary bedforms $V_{c,s}$ and of primary dunes $V_{c,p}$; Bottom: Sediment transport associated with primary and secondary bedform migration, determined through dune tracking.

Secondary bedforms reaching primary lee slopes near or at the angle of repose, disintegrate because of sediment avalanching. A second mechanism through which the primary lee side slope determines whether secondary bedforms persist or disintegrate at the primary lee might be the flow structure over the primary dunes. The internal boundary layer over the dune stoss, in which secondary bedforms develop (*Venditti et al.*, 2005), does not persist over steeper lee side slopes. Flow separates over the steep lee side, along with high turbulence production (*Kwol et al.,*, 2016). Over low angle lee slopes, on the other hand, flow separation is not or only intermittently (*Kwol et al.,*, 2016), allowing superimposed bedforms to pass through the primary troughs.

Fig. 2 shows that the bedload sediment transport associated with secondary bedform migration is of the same order and even exceeds that associated with primary dune migration. Though the secondary bedforms are much smaller, their migration rate is an order of magnitude larger.

The overall impact of secondary bedform migration on the total transport of bed sediments depends on how the two scales interact. When superimposed bedforms travel over the stoss side and dissipate across the primary dune lee side, they fully contribute to the migration of the primary dune. Where superimposed bedforms uninterruptedly travel through the primary dune troughs, however, they transport additional bed sediment. In this case, at least a subtle interaction between the two scales is likely to occur. Secondary bedforms may cause the migration of a primary dune by causing net erosion of the primary stoss, which is when the secondary bedforms grow, and causing net deposit of sediment at the lee side, which is when the secondary bedforms shrink (Fig. 3).

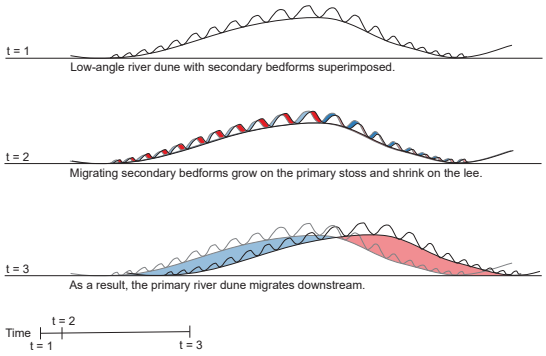

Figure 3: Schematic illustrating the hypothesis concerning the interaction and co-migration of two bedform scales.

Future research

Building upon the current study, we are analysing a large MBES dataset from the river Waal, aiming to understand how and when secondary bedforms develop in relation to hydraulic conditions, primary dune morphology and bed grain size distributions. We further question how secondary bedforms in turn affect primary dune dynamics and sediment transport in the system.

Acknowledgements

This study is part of the research program Rivers2Morrow. Funding for the field campaign was provided by Rijkswaterstaat Oost-Nederland, within the WaalSamen program.

References

Zomer, J.Y., S. Naqshband, B. Vermeulen, A.J.F. Hoitink (In review), Rapidly migrating secondary bedforms can persist on the lee of slowly migrating primary river dunes.

Van der Mark, C. & Blom, A. (2007). A new and widely applicable tool for determining the geometric properties of bedforms. *Civil Eng. & Man. Res. Reports. 2007R-003/WEM-002* (1568-4652).

Kwoll, E., Venditti, J., Bradley, R., & Winter, C. (2016). Flow structure and resistance over subaquaeous high-and low-angle dunes. *Journal of Geophysical Research: Earth Surface*, 121 (3), 545–564.

Venditti, J. G., Church, M., & Bennett, S. J. (2005b). Morphodynamics of small799 scale superimposed sand waves over migrating dune bed forms. *Water resources research*, 41 (10)

Dynamic morphology of the Sittaung estuary, Myanmar: A detailed investigation and modeling of rapid bank erosion

H. de Haas[a,*], Z.B. Wang, E. Mosselman, T.A. Bogaard, J. Cleveringa[a,**]

[a] *Technical University of Delft, Department of Water Management, Faculty of Civil engineering and Geosciences, Building 23, 2628CN, Delft, the Netherlands*

Keywords — Bank erosion, Numerical modelling, Sittaung estuary

Introduction

The Gulf of Mottama, located in the southwest of Myanmar, is home to morphologically interesting processes. The Sittaung estuary is subject to strong dynamic morphological activity, unique in the world, which is alleged to be driven by the large tidal energy and sediment inputs. Dynamics of the tidal channels in the Sittaung estuary result in severe bank erosion, at immense rates of up to 3 km/y, (see satellite imagery in Fig. 1). This is caused by an interplay of different processes and mechanisms, inherent to the estuary. The knowledge of these main processes and mechanisms enable in determining suitable and sustainable solutions to reduce erosion problems, but this knowledge is currently lacking. This research has made strides in demystifying the main contributors of the fundamental dynamic behaviour as well as clarifying the course towards sensible mitigation in the region. In the process, a grapple with the extent of application of numerical models in these particular dynamic contexts is evaluated till a certain extent.

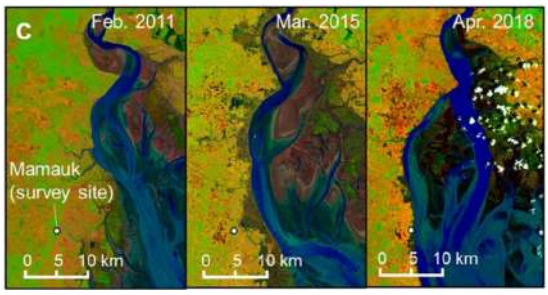

Figure 1: Rapid bank erosion of the last decade on west side and tidal channel evolution of Sittang estuary image from (Shimozono, 2019)

Method

A combination of literature analysis, data analysis from several sources and numerical simulations is performed. Previous research has provided preliminary insights into the processes that are responsible for the rapid bank erosion in the estuary. Several questions have risen which initial analysis of the problem have deemed interesting avenues of inquiry. Aspects such as the tidal bore related phenomena and channel migration characteristics are investigated in their relation to the dynamic morphological activity.

A depth-averaged 2-dimensional model is used to investigate the mechanisms behind these dynamic characteristics. Multiple cases are evaluated with an elaboration on the case specific physical and numerical parameters in the respective sections. Various simulations with altering conditions are performed. With the evolving computational capabilities and the continuing development of modelling tools it becomes possible to evaluate ever more complex problems. Previous studies have been important for the model set-up of this thesis. The modeled situation is further applied to investigate certain hypotheses and discrepancies that might unfortunately develop.

With the help of a satellite analysis the interesting phenomena were further investigated and data has been gathered. A focus is applied to morphological (large-scale) processes concerning the formulated hypotheses and to retrieve relevant and necessary recent data supplementing the information. The modeled situation is applied to investigate certain hypotheses and discrepancies might unfortunately develop. In a sense, the model is applied with an engineering approach to serve a prospective goal.

Results

It seems as if the flow channels cannot reach much deeper either due to a erosion resistant layer in the subsoil or chocking of the channels due to an overload of sediment. A field measurement campaign is designed and initiated to clarify these claims but has not yet been performed.

*Corresponding author
**Corresponding co-authors / supervisors
Email addresses: H.deHaas-1@student.tudelft.nl (H. de Haas), z.b.wang@tudelft.nl; e.mosselman@tudelft.nl; t.a.bogaard@tudelft.nl; jelmer.cleveringa@arcadis.nl (Z.B. Wang, E. Mosselman, T.A. Bogaard, J. Cleveringa)
URL: www.tudelft.nl (Z.B. Wang, E. Mosselman, T.A. Bogaard, J. Cleveringa)

It is evident is that the middle estuary region, where erosion is most rapid, experiences erosion at a similar rate throughout the year. This in contrast to the original hypothesis that the erosion would be related to the monsoon driven discharge increase. Which is a factor 10 difference with the dry season discharge. Furthermore, analysis of the recent cyclone arrival shows no additional implications to the morphological trends.

Simulations show that the large storm events, like cyclones, have a limited effect on the the dynamic morphology of the system, which is in accordance with the satellite analysis results. The investigated cross sections at different heights along the river and estuary show differentt profiles velocity profiles. According to these the expected erosion trend would be more severe in the upper parts, see Fig. 2. But the opposite is the case, indicating a stronger dependency on the tidal bore related phenomena. Zooming out and looking at the estuary wide sediment transport shows a discrepancy between the observed import behaviour of fines and the 2D modeled results. There is a strong indication that the 2D situation under represents large scale baroclinic sediment transport processes which are responsible for additional sediment streams.

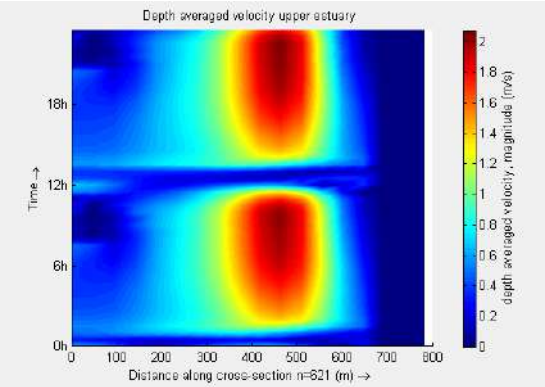

Figure 2: Upper estuary cross section plot of the velocity profile of the wet season discharge configuration.

Long term simulations with respect to the bank erosion result in several hindrances. The numerical difficulties with ascribing the bank erosion fluxes to the dry cells of the grid have shown to deserve extra attention. Channel incision occurs at levels which are much higher than observed or what would be expected, see Fig. 3. This is caused by a numerical instability of the advection scheme under certain conditions. Currently a workaround of increased transverse bed level factors is employed.

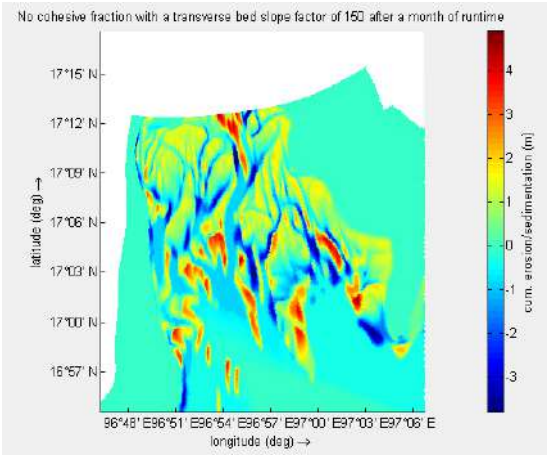

Figure 3: Plot of the high middle region of the estuary. Indicating the effect of a combination without cohesive sediment fractions but with a 100 times increased transverse bed slope factor.

Conclusion

- There is little to no correlation between the wet season and the bank erosion rates. This points to an added importance of the tidal bore specific induced erosion.
- Analysis of the recent cyclone arrival shows no additional implications to the dynamic morphology caused by large incidental storm events.
- Qualitative representations are not near the correct values and also the bank at wet/dry interface does not necessarily show an eroded behaviour. This is because the representation of bank erosion in the model is subject to some technical hindrances.
- The calculated residual transports point to large-scale and local redistribution of sediments. The presence of adjacent upstream and downstream directed zones in the estuary indicate sediment circulation at the scale of the entire estuary, resulting in redistribution of sediment along the entire estuary.

References

Shimozono, T. (2019), Large-scale Channel Migration in the sittang River estuary, in *Scientific reports*, edited by T. Shimozono and Y. Tajima and S. Akamatsu and Y. Matsuba and A. Kawasaki, Nature Publishing Group

Flow Structure at the Pannerdense Kop Bifurcation

Mohammad Kifayath Chowdhury[a,*], Astrid Blom[a], Ralph Schielen[a,b]
[a]*Faculty of Civil Engineering and Geosciences, Delft University of Technology, Netherlands*
[b]*Ministry of Infrastructure and Water Management-Rijkswaterstaat, Netherlands*

Keywords — Flow structure, River bifurcations, Long term morphological change

Introduction

The upper Dutch Rhine bifurcations- Pannerdense Kop and IJsselkop are of utmost importance for the river management authority for both flood mitigation and navigation in the Netherlands. The riverbed of the Rhine has been degrading as a result of narrowing and other interventions of the river channel (*Arbós et al.*, 2020), which often creates problems for navigation. Now climate change has added more concerns for the river managers as the rising sea level and changing rate of precipitation influence the stability and partitioning ratio of the bifurcations (*Edmonds*, 2012; *Wang et al.*, 1995) and current proportion of water and sediment received by the branches may change with them. How large that effect will be, is still an open question. There are several characteristics in the bifurcation neighborhood that control the partitioning, for example: transverse bed slope , variable width, backwater effect (*Edmonds*, 2012), secondary current, upstream meanders and downstream slope advantage, tides, width-depth ratio (*Kleinhans et al.*, 2012), and mixed size character of the sediment (*Schielen and Blom*, 2018). Flow structure provides useful information regarding these by detailing the three- dimensional features of flow. This abstract mainly focuses on some of the observations from the ADCP surveys performed between November 2019 and February 2020 at the Pannerdense Kop.

Method

Six surveys conducted from November 2019 to February 2020 by Rijkswaterstaat at several discharges were selected for this study with one transect at each branch. Selected transects are located 1700m upstream from the bifurcation at Lobith, 800m downstream of the bifurcation into the Pannerdensch Kanaal, and 920m downstream into the Waal river. All three transects have a thalweg close to the outer bank due to the meandering pattern. A $600kHz$ Rio Grande ADCP was used for these surveys with a bin size of 25cm. Each transect was repeated at least ten times. The Velocity Mapping Toolbox (VMT), a suite of Matlab routines, was used for the flow structure analysis.

Results

The Pannerdensch Kanaal (PK) in these surveys was observed to receive 20 to 31% of the flow at Lobith and the fraction percentage increased with higher discharge. However, the depth-averaged velocity at PK, follows a different approach. At lower values of water discharge ($< 2540m^3/s$), the depth-averaged velocity at the Kanaal is significantly lower than the Waal (Fig.1).

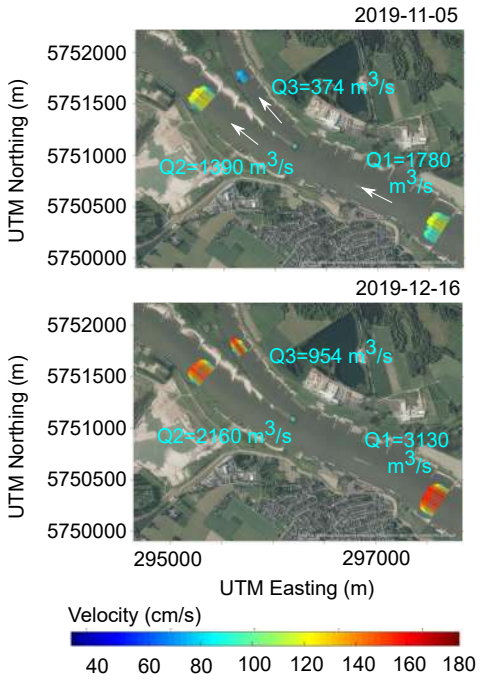

Figure 1: Depth-averaged velocity at Pannerdense Kop at two discharge conditions

However, the depth averaged velocity at PK gets almost as high as that in the Waal at water discharge values greater than $2540m^3/s$ (Fig.1). As the velocity, bed shear stress at PK also increases compared to low discharge conditions. Despite the fact that the water discharge partitioning into the branches remains below the agreed ratio, sediment discharge ratio would be influenced differently due to this velocity characteristics along with the sorting effect caused by the approach condition.

*Mohammad Kifayath Chowdhury
Email address: m.k.chowdhury@tudelft.nl
(Mohammad Kifayath Chowdhury)

Out of the six surveys at Lobith, five of them clearly show a large coherent clockwise circulation induced by the meandering pattern. Several other smaller cells were also found close to the left bank. At the Pannerdensch Kanaal transect (riverkm 868), the branch is narrower with a steeper transverse slope than Lobith. The typical helical flow direction due to meandering for this transect should be counterclockwise (looking downstream), and the hint of this circulation is apparent from the surveys (5 out of 6 times) (Fig.2b). The circulation velocity increases with the increasing value of water discharge, but the variation is small. The location of the cell along the width also varies with different discharge conditions. Apart from this cell, different other coherent cells of similar size were also observed at this transect that were not always fully developed. Further downstream (riverkm 870) (Fig.2a), well developed circulation cells were observed. We hypothesize that it occurred because the transect was located inside the separation zone downstream of the bifurcation point. Further away from this zone, the cells can develop fully.

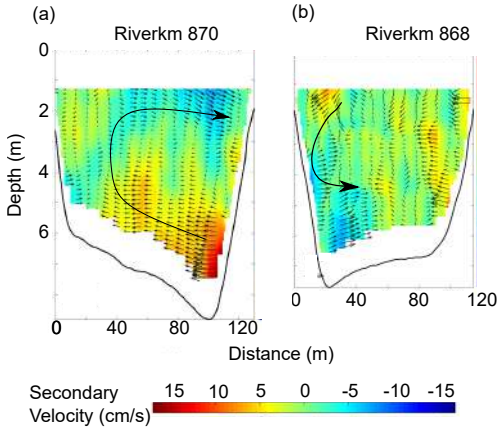

Figure 2: Flow structure at Pannerdensch Kanaal at different discharge, contour and vectors both indicate secondary velocity in Rozovskii frame of reference.

The transect at the Waal (riverkm 868) located 920m downstream of the bifurcation point, shows a coherent channel-wide counterclockwise circulation (Fig.3a) similar to the Pannerdensch Kanaal transect. It was most apparent at discharge 1610 to $1840 m^3/s$ and at higher discharge, more cells appear (Fig.3b). The same hypothesis may explain such occurrence. To confirm that, more ADCP surveys are required closer to the bifurcation point. The flow structure results discussed here show how flow behaves at these transects at a range of discharge conditions. The coherent structures induced by the meandering pattern is apparent from almost all the transects. However, the transects sometimes also show a number of coherent cells existing simultaneously. Why that occurs and how that may influence the partitioning of sediment requires further study.

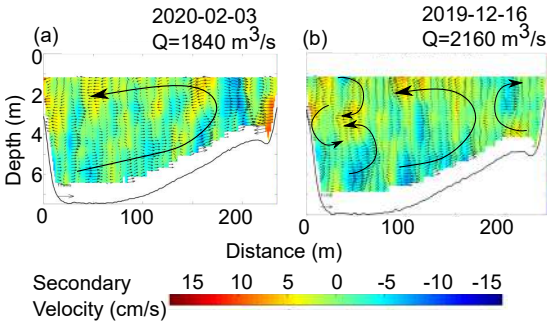

Figure 3: Flow structure at a transect at the Waal (riverkm 868) at different discharge, contour and vectors both indicate secondary velocity in Rozovskii frame of reference.

Future works and Acknowledgements

Future research will contain survey and analysis of flow structure closer to the bifurcation and incorporate them results into the bed surface grain size and bed elevation dataset to draw a more complete picture of the dynamics and long term morphological evolution of a bifurcation system. This study is part of the research program Rivers2Morrow, financed by the Dutch Ministry of Infrastructure and Water Management. We thank the technical staff of Rijkswaterstaat for collecting and sharing the data used in this study.

References

Arbós, C. Y., A. Blom, E. Viparelli, M. Reneerkens, R. Frings, and R. Schielen (2020), River response to anthropogenic modification: Channel steepening and gravel front fading in an incising river, *Geophysical Research Letters*.

Edmonds, D. A. (2012), Stability of backwater-influenced river bifurcations: A study of the mississippi-atchafalaya system, *Geophysical Research Letters*, *39*(8).

Kleinhans, M. G., R. I. Ferguson, S. N. Lane, and R. J. Hardy (2012), Splitting rivers at their seams: bifurcations and avulsion, *Earth Surface Processes and Landforms*, *38*(1).

Schielen, R. M., and A. Blom (2018), A reduced complexity model of a gravel-sand river bifurcation: Equilibrium states and their stability, *Advances in Water Resources*, *121*, 9–21.

Wang, Z., M. D. Vries, R. Fokkink, and A. Langerak (1995), Stability of river bifurcations in ID morphodynamic models, *Journal of Hydraulic Research*, *33*(6), 739–750.

Flow and sediment transport in a stratified estuary: first insights from field data

Niesten, I. (Iris)[a,*], A.J.F.Hoitink[a], B. Vermeulen[a], Y. Huismans[b]
[a]*Wageningen University & Research, Department of Environmental Sciences, Hydrology and Quantitative Water Management Group, P.O. 47, 6700 AA, Wageningen, the Netherlands*
[b]*Deltares, Delft, 2629 HV, The Netherland*

Keywords — Estuaries, sediment transport

Introduction

Many estuaries are characterized by a mixture of clay (D_{50}≤3 µm), silt (4≤D_{50}≤62 µm) and sand (D_{50}≥63 µm). The erosion, (re)suspension and transport of these sediments determine the bathymetry and stability of an estuary. Net estuarine sediment transport is the result of multiple processes. For example, Schindler et al. (2013) found that high suspended mud concentrations in the Tamar Estuary coincide with high bed shear stress, whereas high suspended sand concentrations are related to advection of marine sand during the flood deceleration phase, resulting in a bimodal suspended particle distribution. In more stratified estuaries, gravitational circulation (Hansen and Rattray. 1965) may lead to a net near-bed sediment transport which is directed opposite to the net sediment transport higher in the water column. Considering that coarse material is often transport near the bed, while suspended sediment usually consists of finer particles, gravitational circulation may cause a seaward flux of fine sediment and a landward flux of coarse sediment. It is therefore highly relevant to understand the contribution of sand and mud transport to the total estuarine sediment transport.

In this research, we propose a method which combines data analysis with numerical modelling, aiming to better understand and quantify sediment transport in stratified estuarine channels.

Research area

The New Waterway in the Southwest of the Netherlands (Figure 1), is the only remaining open connection between the Rhine-Meuse Estuary and the North Sea since the closure of the Southern branch of the estuary in 1970 (Vellinga et al., 2014). As such, the channel is continuously dredged to allow navigation to the Rotterdam Port area. (Cox et al., 2020).

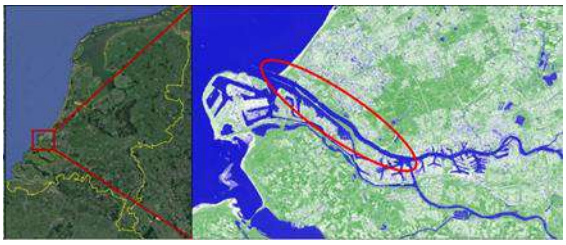

Figure 1. Location of the New Waterway in the Netherlands.

The increased fresh-water discharge combined with deepening of the channel have intensified stratification, resulting in a strong salt wedge-type of flow. De Nijs et al. (2010) have shown how turbulence suppression at the pycnocline leads to decoupling between the upper (mainly fresh) and lower (saline) layer, resulting in strongly different flow velocity as well as turbulence levels across the vertical.

Over the past decade, maintenance dredging volumes in the Rotterdam Port area have increased. The dredged material is composed of both fluvial and marine origin. However, the amount and composition of the material entering from sea are not yet well understood, nor is known which conditions contribute most to marine sediment import.

Data and methods

We propose both a field campaign and a numerical modelling approach to unravel the flow structure and sediment transport mechanisms in the New Waterway.

Field campaign

A field campaign is designed, which combines flow measurements with determination of suspended sediment characteristics in the New Waterway. A measurement frame is equipped with a Sequoia LISST-200x and an YSI EXO Turbidity meter. Suspended sediment characteristics are determined every hour at three depths, next to water temperature, salinity and turbidity. Water samples are taken simultaneously to determine suspended sediment concentration (SSC), and flow is monitored continuously using a vessel-mounted

* Corresponding author
Email address: iris.niesten@wur.nl

ADCP. The full campaign will include two 13-hour measurements and covers two locations in the New Waterway.

Numerical modelling

After analysis of the field data, a modelling study is carried out, to evaluate the effect of gravitational circulation on net sediment transport and to determine the sensitivity of net sediment transport to sediment composition. For this study, the hydrodynamic module of Delft3D-4 (Deltares, 2020) is used, in combination with an offline sediment transport calculation in MATLAB.

Results

A preliminary campaign reveals a decoupling between flow in the upper layer of the water column, and the saline layer below. Before the flood acceleration phase, the upper and lower layer show an opposite flow direction, corresponding to the findings of De Nijs et al (2010). The sediment LISST-measurements show that suspended sediment in the upper water layer has a relatively high amount of clay and silt, while the material close to the bed is predominantly sand (Figure 2). The SSC is significantly higher in the lower part of the water column.

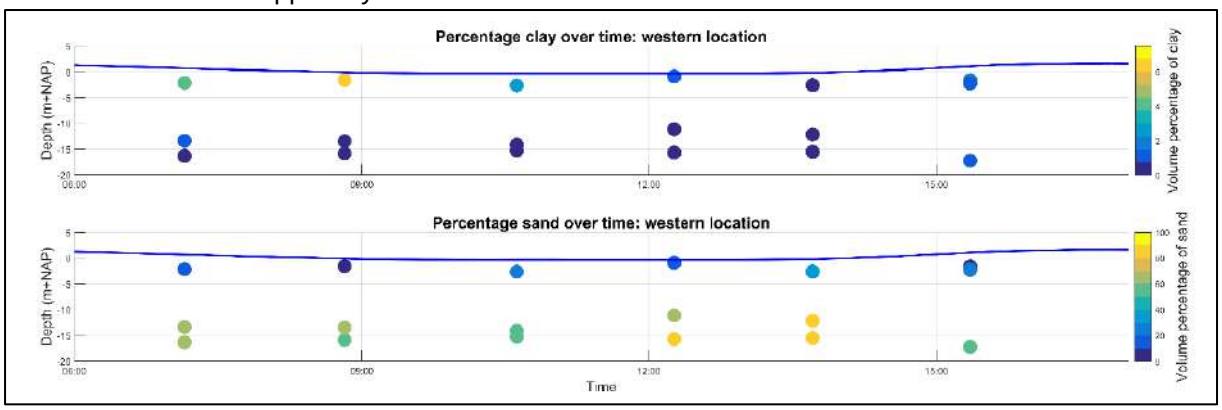

Figure 2. Clay and sand content in suspension during the preliminary measurements at 3 November, 2020. Colours indicate the clay volume content (upper panel) and sand volume content (lower panel) at three depths, measured over six hours. The blue line indicates the water level.

Discussion and preliminary conclusions

A preliminary measurement campaign illustrates the stratified flow character in the New Waterway. The found sediment distribution varies strongly in the vertical, and suggests a correlation between sediment type and net transport direction. It should be noted here that the major part of suspended sediment seems to be transported in the saline layer, and that near-bed processes and local sediment availability could play an important role in the net sediment transport.

Cox et al. (2020) have shown that the New Waterway would be gaining sediment in case of no dredging. The paper by Cox et al. (2020) states that the sediment import at the mouth is strongly dependent on the strength of the estuarine circulation, and that the deep mouth area combined with sea level rise will lead to further sediment import in the future. Our measurements will verify these statements, and provide insight in the type of sediment that is imported from sea. The modelling study will further reveal the sensitivity of the net sediment transport to sediment type, and provide insight in the effect of channel deepening works.

References

Cox, J.R., Y. Huismans, J.F.R.W. Leuven, N.E. Vellinga, M. Van der Vegt, A.J.F. Hoitink, and M.G. Kleinhans. “Anthropogenic e Ects on the Ontemporary Sediment Budget of the Lower Rhine-Meuse Delta Channel Network.” *Manuscript submitted to Earths Future*, 2020.

Deltares. “Delft3D-FLOW - User manual (version: 3.15).” Deltares, Rotterdamsweg 185, 2600 MH Delft, The Netherlands, 2020,

Hansen, D.V., and M. Rattray. “Gravitational Circulation in Straits and Estuaries.” Journal of Marine Research 23 (n.d.): 104–22.

Nijs, Michel A. J. de, Johan C. Winterwerp, and Julie D. Pietrzak. “The Effects of the Internal Flow Structure on SPM Entrapment in the Rotterdam Waterway.” Journal of Physical Oceanography 40, no. 11 (November 1, 2010): 2357–80. https://doi.org/10.1175/2010JPO4233.1.

Schindler, Rob, Sarah Bass, and Andy Manning. “Effects of Non-Cohesive Particles on Suspended Particle Characteristics in a Partially Flocculated Estuary during Spring Tides.” Journal of Coastal Research, July 2, 2013, 1206–11. https://doi.org/10.2112/SI65-204.1.

Vellinga, N. E., A. J. F. Hoitink, M. van der Vegt, W. Zhang, and P. Hoekstra. “Human Impacts on Tides Overwhelm the Effect of Sea Level Rise on Extreme Water Levels in the Rhine–Meuse Delta.” Coastal Engineering 90 (August 1, 2014): 40–50. https://doi.org/10.1016/j.coastaleng.2014.04.005. .

NCR Organisation

The Netherlands Centre for River studies (NCR) is the leading cooperative alliance between all major Dutch institutes for river studies. We integrate knowledge, facilitate discussion and promote excellent science. By linking the strongest expertise of its partners, NCR forms a true centre of excellence in river studies. The disciplines within NCR are contributed by its partners and include Hydrodynamics and Morphodynamics, Geomorphology and sedimentology, River ecology and water quality and River governance, serious gaming and spatial planning.

The NCR has three bodies: the program secretary, program committee and supervisory board. Their tasks are agreed upon in the cooperation agreement (samenwerkingsovereenkomst) 2012, which is an update from the original 1998 agreement.

Program committee

The program committee consists of representatives from each of the NCR partners. The program committee chooses the chair, which currently is drs. Matthijs Boersema of Rijkswaterstaat. The program committee is responsible for the (scientific) program of NCR. The committee initiates and stimulates research activities, proposals, and exchange of knowledge, ideas, experience, and results. The committee has regular meetings, with a frequency of about four times per year.

Supervisory board

The supervisory board consist of one senior member of each NCR partner. The member of the board choose their chair, which currently is prof. dr. Jaap Kwadijk of Deltares. The board supervises the implementation of the cooperation agreement, mediates in disputes and approves the annual program.

Program secretary

The program secretary is responsible for the continuity, day-to-day management, communication (e.g. website, mailing, social platforms) and reporting of the NCR. Additionally, the program secretary is part of the program committee and supervisory board in the role of secretary. The secretary is appointed by the Supervisory board. The current secretary is dr. ir. Koen Berends of Deltares.

Netherlands Centre for River studies NCR

Partners

TU Delft Delft University of Technology

WAGENINGEN UNIVERSITY & RESEARCH

UNESCO IHE DELFT

Rijkswaterstaat
Ministerie van Infrastructuur en Milieu

UNIVERSITY OF TWENTE.

Radboud University

Utrecht University

Deltares